A Life Cycle Analysis of Algal Biofuel- Treating Uncertainty and Variability

A Thesis

Presented to the Faculty of the Graduate School

of Cornell University

In Partial Fulfillment of the Requirements for the Degree of

Master of Science

By Vidia Paramita

January 2012

ABSTRACT

Although a number of life cycle analysis studies (LCAs) have been published, there is little consensus on the feasibility of producing algal biofuels sustainably. For example, the net energy ratio ($\frac{Energy\ of\ Algal\ Biofuel + Energy\ of\ By-products}{Non-renewable\ Energy\ Inputs}$) from the reported studies ranges from about 0.02 to 3.33. Our work attempted to understand these discrepancies by separating results dependent on subsystem choice or assumed performance from those caused by lack of process knowledge or its variability. Each of the life cycle stage: algae cultivation, dewatering, oil extraction, and fuel processing are analyzed independently of the other to consider various process options in them. In addition to the process choices made in each stage, the outcomes of any LCA are subject to uncertainty and variability within the model. This study couples LCA with Monte Carlo simulation to propagate the uncertainties from parameters through the modeled processes to the final output. Especially for algal biofuel, implementing uncertainty analysis improves the transparency of the results, considering that no industrial-scale plant is in operation and the algal biofuels industry is in a very early stage with unknown or unreported performance.

Thesis advisor: Prof. Jefferson Tester, Prof. Ruth Richardson

BIOGRAPHICAL SKETCH

Vidia Paramita was born on November 28, 1986, in Jakarta, Indonesia. She spent most of her childhood in Riau, Sumatra. At age 14, she received a scholarship from the Singapore Government and thus moved from Indonesia to pursue an education in Singapore. Vidia attended Raffles Girls' Secondary School and Victoria Junior College, where she spent 4 years growing up together with her best friends in a dormitory.

Vidia and her parents decided that pursuing a higher degree in the USA was a great option, since it would open up many more opportunities and exposed her to new experiences. Vidia went to the University of Texas at Austin and finished her degree in Chemical Engineering within 3 years in the Spring of 2009. With a strong interest in renewable energy and environmental management, she pursued a Master of Science degree straight after graduation with the hope of having more advanced understanding and skill sets. She joined Cornell University firstly in the Environmental Engineering department, and then switched back to Chemical and Biomolecular Engineering due to a more matching research interest. She defended her thesis on September 2011.

Vidia hopes to implement her work in sustainable energy systems and environmental management in the context of developing countries in the future. In her spare time, she can be found reading, writing, or playing tennis. Having moved around from one place to another has evoked in her the love for travelling and experiencing different cultures. She plans to keep on travelling as much as possible, while keeping Indonesia close to her heart as a true home.

Thank God for His grace and divine providence.

I dedicate this manuscript to the most loving parents anyone could ask for.
Thank you for raising me well and for always being there.

I love you.

ACKNOWLEDGEMENTS

First and foremost, I would like to acknowledge the guidance and support of my advisor, Prof. Jefferson Tester who provided the opportunity to pursue this research and lent his valuable assistance throughout the study. Prof. Tester has been an inspiring figure for me, a mentor who truly cares for the well being of his students and somebody with a contagious love for knowledge and learning. His encouragements for me have been a strong motivation in completing this work. I would also like to thank Prof. Ruth Richardson, my minor advisor, as well as Prof. Charles Greene for serving as a great source of knowledge, and their kind advice and support have been invaluable. Thank you to Cellana Inc., especially Mark Huntley and Ian Archibald for allowing me to visit their pilot plant in Kona, Hawaii, and for providing significant amount of data to use.

This study would not have been completed without the help of many great peers. I would firstly like to thank Jeremy Johnson, who helped me understand his thesis work that became a foundation for mine, and Michael Franke and Michael Johnson, both great collaborators of this work. Thank you to Justin Greenly, Jeremy Lutherbacher, Adam Carr, and Deborah Sills who helped me progress by giving ideas and feedbacks, engaging in discussions, and editing my writing materials.

Grad school was sometimes stressful for me, but I was very lucky to find joy in many friendships. I will remember all of them after leaving Cornell: Irma Amelia, Resya Kania, Davina Widjaja, Shanshan Zhang, Ntando Dhlamini, Jin Gi Hong, Raymond Kim, Prayut Bhamawat, and others in the Tester research group, Polly Marion, Andrea Aguirre, Koenraad Beckers, Elaina Shope, Tim Reber, George Stutz, Don Fox, Maciej Lukawski, Sean Hillson, and Andre Chabaneix.

Last but not least, I would like to thank my parents, Aswin Widjaja and Murniati Sudartha, my sister, Prita Puspasari, my grandparents, Opa Leo, Oma Eliza, Opa Wibowo, Oma Tien, my aunt, Titut Riani, and my boyfriend, Handi Chandra Putra. Thank you for the love with endless heartfelt prayers and for having faith in me. I love you very much.

Table of Contents

List of Tables

1 INTRODUCTION

1.1 Background and Motivation

The challenges of ensuring energy security, economic well-being, and the stability of global climate have motivated mankind to develop renewable energy systems that are efficient and sustainable. Liquid fuel, in particular, plays an important role in the energy sector as it has great properties as energy carriers: a high energy density and high combustion temperatures ranging from 1000 ˚C to 2500 ˚C. The transportation sector depends almost entirely on using liquid fuels. The liquid fuels consumption in 2009 was 38% of the total US primary energy consumption as depicted in Figure 1.1 below (EIA, 2011). Of the 38% of liquid fuel consumed, 74% was dedicated to the transportation sector.

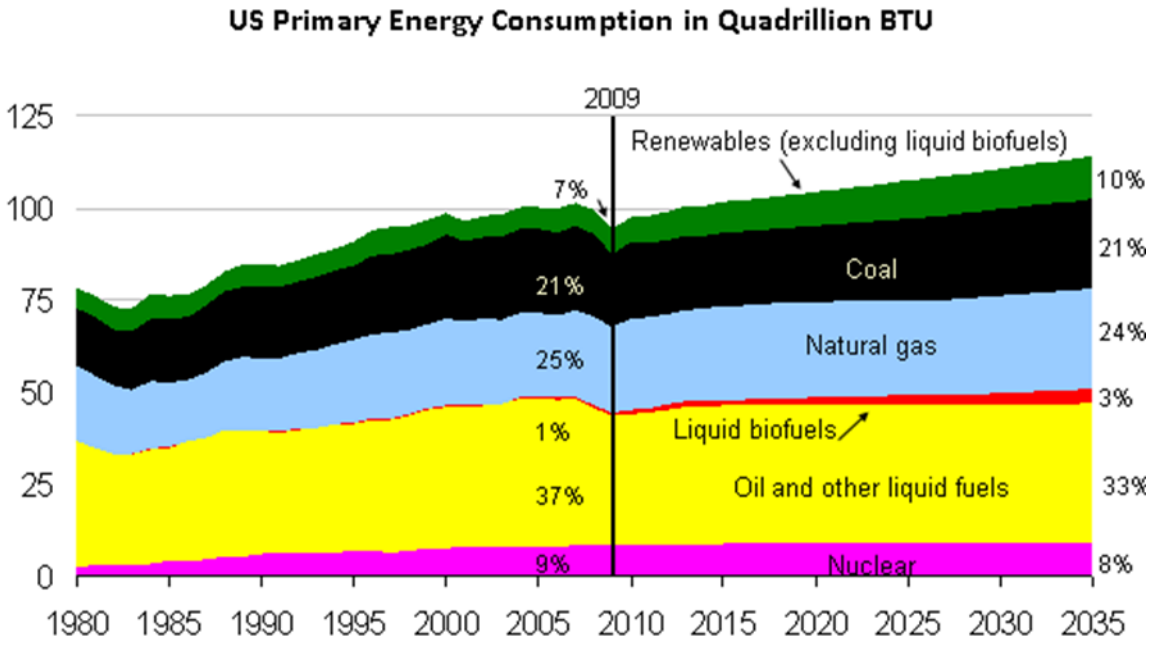

Figure 1.1: The US primary energy consumption from 1980 projected to 2035 (US EIA Annual Energy Outlook, 2011)

Amongst the portfolio of renewable energy system (wind, solar, geothermal, etc.), biofuel is the only viable alternative to liquid transportation fuel. The Energy Independence and Security Act of 2007 (EISA) established a mandatory Renewable Fuel Standard (RFS) requiring transportation fuel sold in the U.S. to contain a minimum of 36 billion gallons of renewable fuels, including advanced and cellulosic biofuels and biomass-based diesel, by 2022. Currently, biofuel use in the U.S. is dominated by bioethanol produced from corn starch. Although corn ethanol has generated debates on issues such as the food vs. fuel demand, land use, and fertilizer run-offs, corn is still expected to be the major biofuel feedstock in the future as the technology has matured and it has available supporting infrastructure. There is a tendency to shift towards cellulosic biofuels with higher crop yield and to avoid the fuel vs. food issue. However, a number of next generation biofuels show great potentials in aiding to reach the goal, one of them being algal biofuel.

Microalgae have attracted interest as a feedstock for biofuels for several reasons:

1. Microalgae are able to accumulate neutral lipids, analogous to seed oil triglycerides, some species greater than 50% of their dry biomass wright (Chisti, 2007).
2. It has the highest productivity of any known biofuel feedstock (Pienkos, 2007), as shown in Table 1.1. Microalgae are generally more efficient converters of solar energy because of their simple cellular structure. They are capable of producing many more times the amount of biomass per unit area of land, compared to terrestrial oilseed crops because the cells grow in aqueous suspension allowing for a more efficient access to water, CO_2, and other nutrients (Sheehan, 1998).

Table 1.1: Comparison of oil yield (gallons/acre) of the main oilseed plants (Pienkos, 2007)

Crop	Oil Yield Gallons/acre
Corn	18
Cotton	35
Soybean	48
Mustard seed	61
Sunflower	102
Rapeseed/Canola	127
Jatropha	202
Oil palm	635
Algae (10 g/m^2/day at 15% TAG)	1,200
Algae (50 g/m^2/day at 50% TAG)	10,000

3. Micro algae can be grown on non-arable land, so it does not have to compete for land with food feedstocks.
4. The potential to use of seawater, brackish water, or wastewater for its cultivation saves us from draining society's limited fresh water stock.
5. There is a potential to couple algae production with a power plant by routing the power plant's flue gas to the algae farm, which provides the algae an elevated carbon source and at the same time reusing CO_2 and reducing environmental impacts (Kadam, 1997).

However, the technology to produce fuel from microalgae is far from being mature. Obstacles such as choosing the right strain, optimizing growth systems, high energetic cost in dewatering, and reaching high efficiency in extraction of lipid, are key issues to be solved. With the current knowledge of production, algal biofuel is not able to compete in the market. Efforts to reduce both capital and operational costs have to be put in place for algal biofuel to reach its potential in the future (Lundquist, 2010). A representation of the algal biofuel production system showing material and energy inputs and the potential outputs is shown in Figure 1.2.

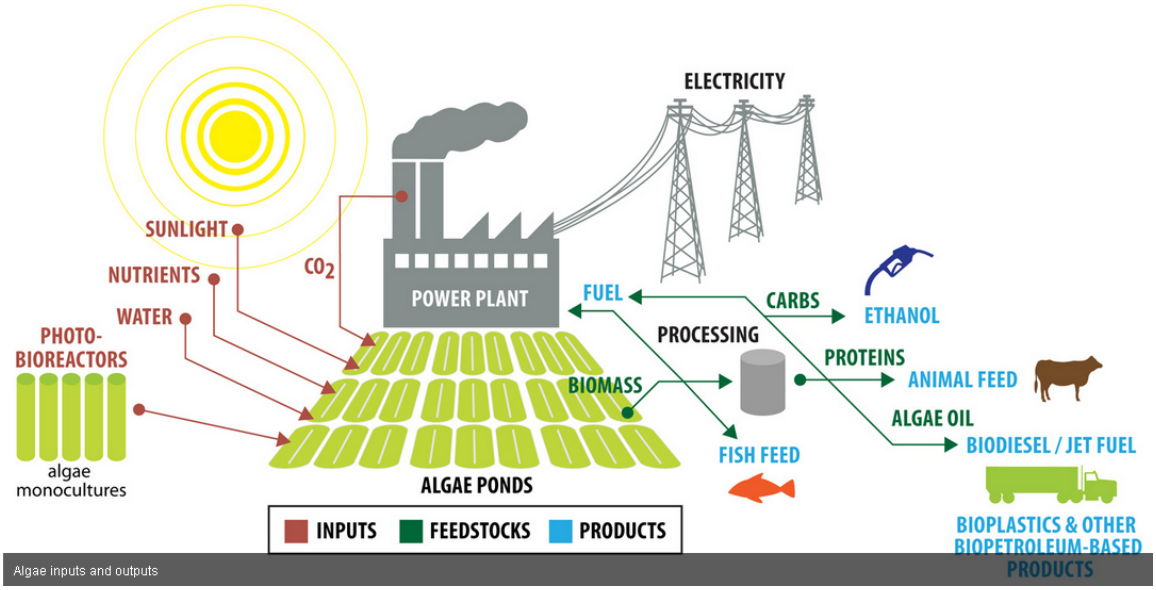

Figure 1.2: Algal biofuel production overview (taken from Cellana Inc. website)

Although the concept of using algae to produce energy has existed since the late 1950s, the idea to process its lipid content into usable liquid fuel only gained high attention in the early 1970s, during the oil embargo when the energy price increased significantly (US DOE, 2010). The embargo led US Department of Energy (DOE) to establish the Aquatic Species Program (ASP) which lasted from 1978 to 1996 and was supported largely by the National Renewable Energy Laboratory (NREL). Approximately $25 million was invested in ASP, with the following focus (Sheehan, 1998):

1. Screening, isolation, and characterization efforts resulting in a unique collection of oil-producing microalgae algal strain of 300 species, mostly green algae and diatoms.
2. Understanding of physiology and biochemistry of algae especially to increase lipid production.
3. Study of molecular biology and genetic engineering. The program was the first to isolate the enzyme Acetyl CoA Carboxylase (ACCase) from a diatom which was found to catalyze a key metabolic step in the synthesis of oils in algae.
4. Demonstration of open pond systems for mass production of microalgae to test the feasibility of long term growth in California, Hawaii, and New Mexico.

5. Conducting cost analyses for large-scale microalgae production. A major conclusion from these analyses is that there is little prospect for any alternatives to the open pond designs and that the factors that most influence cost are biological, and not engineering-related.
6. Conducting resource assessments, looking at climate, land, water, and CO2 availability to support this technology.

Due to revived interest in the last 5 years, the DOE's Office of Energy Efficiency and Renewable Energy prepared the National Algal Biofuels Technology Roadmap to identify critical challenges currently hindering the development of a domestic, commercial-scale algal biofuels industry. One of the proposed challenges was to produce a life cycle analysis (LCA) of algal biofuel systems to assess the environmental aspects and potential impacts associated with the industrial-scale production. This type of assessment is designed to aid researchers, industries, and the government in identifying bottlenecks as well as promising technologies to be implemented in the future. The difficulty in conducting such assessment is in obtaining data input for the model since many processes are proprietary and results of research could vary largely. Addressing the uncertainties in a systematic and integrated modeling and analysis framework becomes an important part of the analysis will help guide needed investments and speed the deployment of an algal biofuels industry (DOE, 2010). This thesis takes into account that issue by coupling LCA with uncertainty analysis methods.

1.2 Objectives

This report will present a life-cycle assessment (LCA) of algae biofuels. The key variables that will be measured are energy input to the growing, harvesting, oil extraction and fuel production processes as well as greenhouse gas output from these processes. An LCA tracking these parameters will give a measurement of how carbon neutral and renewable a biofuel really is, a metric that can be used to compare the sustainability merits of different feedstocks and technologies side-by-side. The main objectives to be fulfilled by this study are as follows:

1. Conduct a meta-analysis of published LCA studies on algal biofuel to determine causes of variation and build a new data inventory.

2. Complete an LCA of algal biofuel by analyzing several process options for each of the four production part: cultivation, harvesting and dewatering, oil extraction, and fuel production.
3. Calculate LCA results for two main environmental impact assessments: non-renewable energy input and greenhouse gas emission.
4. Conduct sensitivity analysis and incorporate Monte Carlo uncertainty analysis in LCA to obtain a 95% confidence limit on the results to show the result spread.

1.3 Thesis Organization

In Chapter 2, a literature review of the cultivation and other processes involved in the production is done as background information. In Chapter 3, the methodology of conducting the LCA coupled with uncertainty analysis is presented. Chapters 4 and 5 explain the results which include the meta-analysis of current published LCA work and the results of the LCA from this study. Lastly, a summary and conclusions that outline the significance of this work and suggestions for future research are included in Chapter 6.

REFERENCES

Chisti, Y. (2007). Biodiesel from Microalgae. *Biotechnology Advances, 25*, 294-306.

John Sheehan, T. D. (1998). *A Look Back at the U.S. Department of Energy's Aquatic Species Program - Biodiesel from Algae.* National Renewable Energy Laboratory.

Kadam, K. (2002). Environmental Implications of Power Generation Via Coal-microalgae Co-firing. *Energy, 27*, 905-922.

Pienkos, P. T. (2007). *The Potential for Biofuels from Algae.* San Fransisco: Presentation at Algae Biomass Summit .

T.J. Lundquist, L. W. (2010). A Realistic Technology and Engineering Assessment of Algae Biofuel Production. *Energy Biosciences Institute*, 1-178.

U.S. DOE. (2010). *National Algal Biofuels Technology Roadmap. U.S. Department of Energy, Office of Energy Efficiency and Renewable Energy, Biomass Program.*

U.S. Energy Information Administration. (2011). *Annual Energy Outlook 2011 With Projections to 2035.*

2 REVIEW OF ALGAL BIOFUEL PRODUCTION

2.1 **Microalgae Characteristic and Potential Products**

Microalgae are a diverse group of microscopic organisms that can grow suspended in either fresh water or seawater environment. Depending on the species, their size ranges from a few micrometers to a few hundred of micrometers. Biologists characterize microalgae mainly by distinguishing their pigmentation, life cycle and cellular structure. The four most abundant classes of microalgae are diatoms (Bacillariophyceae), green algae (Chlorophyceae), blue-green algae (Cyanophyceae), and golden algae (Chrysophyceae) (Carlsson, 2007). Diatoms and green algae are more promising for biodiesel production due to their relatively higher lipid contents (Sheehan, 1998). While the high number of microalgae species create challenges for screening and discovery of superior species, it also provides many species alternatives and potential for genetic engineering.

Algae are comprised of carbohydrates, lipids, proteins, and nucleic acids, though the composition varies across species. They are also commonly rich in antioxidants, vitamins, and carotenoids, which make them appropriate to be grown for human food, pharmaceutical, and neutraceutical products (de la Noue & de Pauw, 1988). Lipids and carbohydrate contents of algal biomass are the main concern when considering the production of liquid fuel. However, it is important to consider potential co-products that may be obtained from the remaining biomass components. Lipids that accumulate in microalgae are largely in the form of triglycerides which are esters of fatty acids. The length of the fatty acid chain may range from C_{14} to C_{22}, and they may be saturated or unsaturated (Hu, 2008). Based on several studies, the quality of the lipid resembles that of a fish oil or vegetable oil, suggesting that it could be used as a substitute for petroleum products. Algal lipid is not directly usable as fuel because just like other vegetable oils, it is more viscous than conventional fuel and it does not burn the same in the engine, making significant engine modification necessary (Altin, 2001). Table 2.1 gives a summary of the different liquid transportation fuels that could potentially be produced from microalgae.

Table 2.1: Potential types of liquid transportation fuel produced from microalga biomolecules

Fuel Type	Biomass Fraction	Description
Biodiesel	Lipid	A long-chain alkyl ester formed by transesterification which reacts the lipids with an alcohol in the presence of a base or acid catalyst. Glycerol is a by-product of this reaction. Biodiesel could be used directly or blended with petroleum diesel in engines without any modification.
Green diesel or biogasoline	Lipid	Green diesel is primarily made out of long hydrocarbon and considered as more superior than biodiesel because it is more deoxygenated and has higher energy content. It can be formed by hydrotreating and hydrothermal liquefaction in which the biomass is contacted with water at an elevated pressure and temperature to produce the organic oily liquid that phase separates in the end of reaction.
Crude oil blended feedstocks	Lipid	Algal oil might be blended with crude oil to be used as feedstock in a refinery where hydrocracking or hydrogenation can be used to produce conventional gasoline and diesel.
Bio-ethanol	Carbohydrate	It is a replacement or a blend for gasoline that is produced by fermentation of sugars or starches. Ethanol has a lower energy density than gasoline, but it has a higher octane rating.
Bio-butanol	Carbohydrate	Bio-butanol is a replacement for gasoline that is better than ethanol due to its longer carbon chain and higher energy density. It is produced by fermentation of sugars in the ABE (Acetone-Butanol-Ethanol) process using the bacterium *Clostridium acetobutylicum*.

This thesis focuses on converting the lipid content to liquid fuel; therefore, bio-ethanol and bio-butanol will be considered as co-products when they are produced. When they are not produced, the remainder of the biomass consists of largely carbohydrate and protein, which could be used for several purposes. The amino acid pattern of most algae species is comparable to that of other food protein; therefore, it can be used as protein source for humans or animals. However, the nutritive value of the protein and the degree of availability of amino acids should be completely characterized before using it. The carbohydrate fraction is mainly in the form of starch, glucose, sugars, and other polysaccharides, with a high overall digestibility. This provides an advantage of using the whole remaining dried biomass for foods or feeds (Spolaore, 2006).

Another alternative would be to utilize the biomass for energy production such as by co-firing it with coal for electricity (Kadam, 2001) or by producing bio-gas through anaerobic digestion. This will offset the energy input for the main biofuel production, thus improving the net energy ratio of the life cycle. Additionally, digesting the biomass provides an advantage of recycling the nutrients trapped in the digested by-product when the bio-gas has been produced, and will also reduce the life cycle burden (Sialve, 2009).

In the transesterification process, a significant by-product is glycerol. Glycerol is widely used in the food industry as a sugar substitute, food preservative, emulsifier, and shortening. Another big market for glycerol is for pharmaceutical and personal care products where it is used to produce soap, toothpaste, mouthwashes, skin care products, lubricants, cough syrups, and many more. In 2005, the estimated world demand for glycerol was 800,000 tons (Pagliaro, 2007). With roughly 1 ton of glycerol produced for every 10 tons of biodiesel, the market for glycerol could be easily saturated.

2.2 **Microalgae Growth Basics**

Many microalgae species are able to switch from phototrophic to heterotrophic growth. As heterotrophs, the algae use organic carbon sources, while as phototrophs they rely on inorganic carbon sources for metabolism and energy production (Carlsson, 2007). Heterotrophic growth has not been largely considered in algal biofuel production due to the expensive organic carbon input. However, it has been considered as the finishing step in the growth cycle to aid more lipid production (Bai, 2011)

In phototrophic growth, photosynthesis is the basic process in microalgae that leads to biomass production to be converted to biofuel. Photosynthetic organisms convert light to chemical energy which is in the form of biomass feedstock such as protons and electrons for biohydrogen, starch and sugars for bioethanol or biobutanol, fats for biodiesel, or the whole biomass for solid fuels, liquid fuels, and biomethane (Schenk, 2008). In photosynthesis, the main starting materials are CO_2 gas and water, which are converted in the presence of sunlight (as an energy source) to sugars and O_2 gas as a by-product. The overall photosynthesis equation is as below.

$$6\,CO_2 + 6\,H_2O \xrightarrow{\text{sunlight}} C_6H_{12}O_6 + 6\,O_2 \qquad \textit{(Equation 1)}$$

The photosynthetic efficiency is defined as the percentage of energy in the whole light spectrum that is converted into biomass. In theory this efficiency could be targeted to reach to 9%, while in current practice, it is much lower at less than 1% (Wijffells, 2007). This productivity of biomass ranges from species to species, the type of reactor used, and the environmental condition. The metabolism of microorganisms is also influenced by their surface-to-volume ratio. Approximating the shape of a microorganism as a sphere, the growth rate is inversely proportional to its cell diameter. Under a favorable environment, most microalgae is able to divide every 1 to 2 days and therefore can be harvested daily or every few days (Williams, 2010). Table 2.2 below shows some reported value of productivities, based on theoretical calculations to assess the absolute maximum and best case value that could thermodynamically be reached, followed by actual data.

Table 2.2: Productivity values based on theoretical calculations and actual data from outdoor pond experiments

Reference	Productivity		Notes
	g/m^2/day	ton/ha/yr	
Theoritical Calculation			
Weyer (2009) - Absolute Maximum	196	715	
Weyer (2009) - Best Case	33-42	120-153	Solar irradiation of 15.4 - 20.1 MJ/m2/day, 6.3% photosynthetic efficiency
Wijffels (2007) - Best Case	77	280	Solar irradiation of 21.7 MJ/m2/day, 9% photosynthetic efficiency
Goldmann (1979) - Best Case	58	212	Solar irradiation of 33.5 MJ/m2/day
Actual Outdoor Pond			
Benemann (1982)	10	37	Scenedesmus, California
Garcia-Gonzales (2003)	2.36	9	Dunalliella, Spain
Huntley & Redalje (2007)	12.6	46	Haematococcus pluvialis, Hawaii
Laws (1998)	7.15	26	Phaeodactylum, Hawaii
Moheimani & Borowitzka (2006)	9.7	35	Pleurochrysis, Australia
Olaizola (2000)	11	40	Haematococcus, Hawaii
Oliguin (2003)	11	40	Spirulina, Mexico
Pushparaj (1997)	18	66	Arthrospira, Italy

Richmond & Cheng Wu (2001)	10.5	38	Nannochloropsis, Israel

Like carbohydrate, protein also have structural and metabolic functions as they take form in enzymes for growth catalysts, are embedded in the lipid membranes for structure and transport, and many other roles. Nucleic acids (RNA and DNA) provide the basis for algal division and growth. Although nucleic acids only make a small percentage of the whole biomass, they house most of the cell's phosphate and are the second most important site of nitrogen. Lipids, meanwhile, serve as both energy reserves mostly in simple fatty acid triglycerides, and as membrane components in the form on phospholipids and glycolipids. The two major elements that need to be supplied other than carbon are nitrogen and phosphorous. Other elements in lower quantity are also needed to support biomass growth, which include potassium, magnesium sulfur, iron, vitamins, and silica in the case of diatoms.

To produce liquid fuels with long hydrocarbon chain from algae, the lipid fraction within the biomass is the main of interest, while the rest is considered by-product. Species that are able to have a high percentage of lipids would therefore be favorable for biofuel production. However, we have to consider that as the lipid fraction increases, the fractions of other components go down. The shift in protein fraction is especially critical because firstly protein molecules manage the level of cell's metabolism and secondly together with nucleic acids they determine the biomass productivity (Williams, 2010). The inverse relationship between lipid content and productivity should be carefully balanced so that in the end an optimum oil yield is achieved. A cultivation procedure largely adopted to obtain high overall oil yield is by initially providing the supportive environment for high biomass productivity, and then shifting to nutrient depravation mode where there would be a decrease in the rate of growth allowing for lipid content to increase as it provides energy reserves. Just like biomass productivity, the lipid content in algae varies across species. Figure 2.1 shows the lipid content of several green algae and Cyanobacteria species (Griffiths & Harrison, 2009). The nutrient sufficient lipid content for green algae has an average of 23% dry weight, while for Cyanobacteria it is lower at 8%. When nutrient-deprived, the lipid content of green algae increases to an average of 41%, almost a two-fold increase. For Cyanobacteria, due to limited data, this trend is not clearly confirmed, but since they have low lipid content in the first place, they are not widely considered for biofuel production.

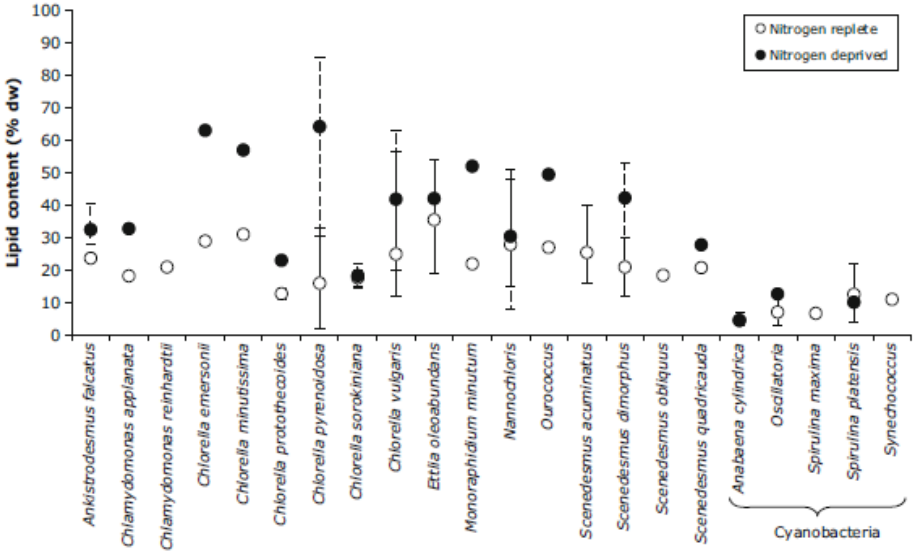

Figure 2.1: Average laboratory lipid content in green algae and Cyanobacteria. Solid lines show minimum and maximum reported values for nitrogen replete condition, dashed line shows the same for nitrogen-deprived condition (taken from Griffith & Harrison, 2009).

CO_2 is needed as a carbon source for algae growth. Carbon dioxide is present in the atmosphere at very low concentrations (0.032% by volume in dry air). Passive flux of atmospheric CO_2 through the surface of algal mass cultures is inadequate to supply the amount of carbon dioxide required to support intensive productivity (Neenan, 1986). Assuming that the transfer rate of CO_2 gas across the air/seawater interface is 1000 g/m^2/year (Regan and Gartside, 1984) the estimation of growth is as following:

$$\text{Biomass growth} = 1000\,\frac{g\ CO_2}{m^2\ year} \div 1.68\,\frac{g\ CO_2}{g\ dwb*} \times \frac{1\ year}{365\ days} = 1.63\,\frac{g}{m^2 day}$$

*dwb: dry weight biomass

From this simple calculation it is established that an additional CO_2 source would be needed to produce a growth rate needed for profitable biofuel production. Flue gas is commonly considered to provide an elevated CO_2 source. Flue gas is an emission from combustion

processes from furnace, boiler, or steam generator that is largely used in a fossil fuel power plant. It is composed mainly of N_2 from the unreacted part of air intake that is used in the combustion, CO_2, water vapor, excess O_2, and a small percentage of air pollutants like particulate matter, CO, nitrogen oxides, sulfur oxides, and mercury. Rather than directly disposing this flue gas, using it as CO_2 source in algal biofuel provides a recycling avenue which adds a functional value before it is finally emitted as a product of combustion in vehicle use. There are two ways of using this flue gas: CO_2 recovery to produce pure CO_2 via an absorption process (eg. using monoethanolamine) or direct injection of the gas. No inhibition of growth with 150 ppm NO_x and 200 ppm SO_2 has been reported by Zeiler et al. (1995), which is in compliance with 1990 US Clean Air Act (CAA) levels. The limit for concentrations to have an effect on growth rate is about 240 for NO_x and 400 ppm for SO_2 (Stepan, 2002).

2.3 **Microalgae Cultivation**

The three major cultivation methods in microalgae production are by using raceway pond, photobioreactor, or a hybrid of both. The advantages and disadvantages of these reactors are described below. However, despite differences in these configurations, the success of cultivation still depends primarily on the algae species and environmental conditions.

2.3.1 Raceway Pond

A raceway pond is essentially a closed loop channel where the algae grow suspended in water and circulated or mixed using a paddlewheel (Chisti, 2007). Figure 2.2 below shows a typical design of a raceway pond. The raceway pond is kept at a shallow depth of about 0.15 m to 0.35 m to ensure sufficient light penetration that supports photosynthesis, but at the same time does not cause photoinhibition. The paddlewheel mixing is optimally set at 20 to 30 cm/s of channel velocity to avoid biomass settling and O_2 build up that could lead to lower photosynthetic rate. At a higher mixing velocity, the energy cost would be too high and it could also reduce the life time of the liner or scour unlined ponds (Lundquist, 2010). A small section of the pond, downstream of the paddlewheel, is covered by a plastic hood under which the flue gas is

sparged. The gas is bubbled into a sump with countercurrent water flow which would increase the bubble rise time and minimized CO_2 outgassing.

Figure 2.2 : Raceway ponds (taken from http://algae.ucsd.edu/research/algae-farm.html)

It is important that the design and construction of these growth ponds be as simple as possible to keep costs low. Most raceway ponds are constructed out of concrete, but they may also be made out of compacted soil, which would greatly reduce the capital cost. Either way, lining the pond would be important to prevent leakage, reduce contamination, and prevent scouring. The liner material should be waterproof, relatively slow to degrade, flexible and strong, and has good resistance to ultraviolet light (Regan and Gartside, 1984).

While using raceway brings economic benefits due to lower construction and operational costs, there is less control possible over the cultivation environment. Temperature fluctuation, evaporative water loss, CO_2 outgassing, and contamination of other microorganisms are some of the typical problems encountered in raceway cultivation. The biomass concentration also tends to be lower in a raceway compared to a PBR due to more competition with other organisms, resulting in lower productivity. A strategy commonly adopted for sustainable production in open pond is keeping extreme culture conditions favorable only for the intended species, such as high salinity, extreme alkalinity, or giving specific nutrient types (Lee, 2001).

2.3.2 Photobioreactor

Photobioreactors (PBRs) are closed systems, in which algae can be cultivated under sterile and controlled conditions, potentially resulting in higher productivities. There are two main types of PBRs for algal biofuel production, a tubular PBR and flat-plate PBR. Both types are designed

especially for photo-autothropic growth which needs a high surface area to volume ratio (Carvalho, 2006). These PBR units are equipped with a gas exchange unit to bubble in CO_2 and pumps to circulate the culture for better gas exchange, nutrient absorption, and light exposure. This circulation has to be designed carefully to avoid high shear force that could destroy algal cells.

There are several types of tubular PBRs: a vertical tubular PBR, a horizontal tubular PBR, and a helical tubular PBR which are made out of a tube coiled in a circular framework (Carvalho, 2006). The typical design for the different types of PBR is shown in Figure 2.3 below. The body of the reactor may be made out of polyethylene or glass, which transparency allows for sufficient light penetration. How these different designs, including the flat-plate reactor fair against each other has not been thoroughly investigated. However, horizontal tubular PBRs have the highest footprint area, while the helical tubular PBR has the smallest footprint. Flat-plate PBRs may have a high light harvesting efficiency because it is easier to orient these towards the light source. However, at the same time flat-plate reactors may require more cooling, since most algal species are intolerant to high temperature. A study comparing cultivation of algae in a horizontal tubular PBR and the flat-plate PBR (Jorquera, 2009) concludes that the energy cost for mixing in a tubular PBR is too high at 2500 W/m^3 of culture and makes it energetically unfeasible. The mixing energy burden for flat-plate PBR is only quoted at 53 W/m^3 making it a clear winner. However, Jorquera states that the mixing energy value for a tubular PBR lacks published information, thus he uses data that is not validated with other sources and is highly uncertain. Typical design for the different types of PBRs are shown in Figure 2.3 below.

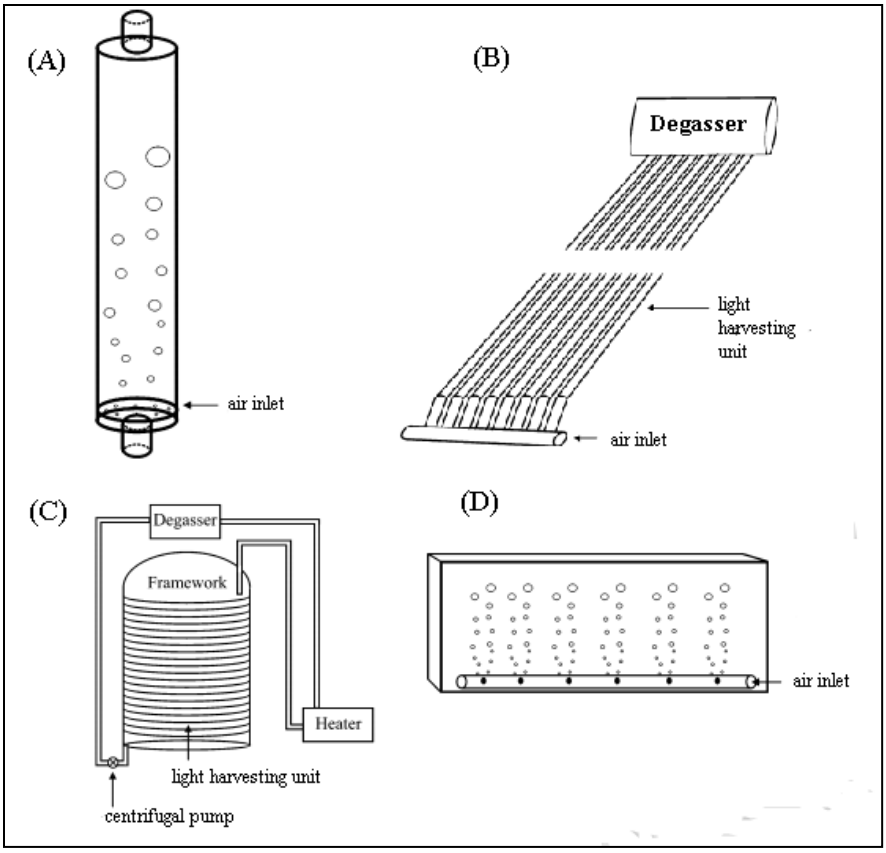

Figure 2.3: (A) Vertical tubular PBR, (B) Horizontal tubular PBR, (C) Helical tubular PBR, (D) Flat-plate PBR). Taken from Carvalho (2006)

Compared to raceway ponds, the technology for PBRs has not matured yet with continued active research. Due to the high complexity of operation, capital costs, and costly maintenance associated with PBRs, none of the current pilot plants uses PBR for the main cultivation reactor. It is very unlikely that they will be used exclusively at large-scale production operations in the near future. However, PBRs in hybrid operations to inoculate open raceway with "clean" algal feedstock may have high potential for improvement that would allow more consistent cultivation conditions, and subsequently higher quality biomass. Table 2.3 below summarizes the comparison between raceway and PBR as a cultivation reactor.

Table 2.3: Summary of comparison between open pond and PBR systems

Feature	Open Pond	PBR
Area to volume ratio	Large	Small
Algal species	Restricted mainly to local species, selected based on growth competition, monoculture is hard to achieve, susceptible to contamination	More flexible choices, selected based on shear-resistance, monoculture is possible, less contamination occurs
Productivity	Low	High
Population density	Low density, lower harvesting efficiency	High density, higher harvesting efficiency
Gas transfer	Low efficiency in CO_2 transfer to the culture, less O_2 build up	High efficiency in CO_2 gas transfer, there is a problem of O_2 build up
Temperature control	Cooling is achieved only through evaporation, poor control	Good control
Capital investment	Small	High
Operation and maintenance	Simple operation and cheaper maintenance	More complex operation, need sterilization of reactors when cleaning, more expensive maintenance
Scale-up	Easy to scale up by adding the number of ponds	Difficult to scale-up the size due to addition of compartments and support materials, temperature control, gas exchange, and possibility of algal wall growth

2.3.3 Hybrid Cultivation

Hybrid cultivation is a two-stage process using PBR for the first stage and raceway pond for the second (Huntley & Redalje, 2007). In the PBR, the cultivation is maintained at controlled conditions that maximizes continuous cell division and is protected from contamination. When the culture reaches a certain concentration, it is rapidly transferred to the raceway pond, where the cells are cultivated under a nutrient deprivation that lead to an increase in oil content. This hybrid cultivation uses the strengths of both PBR and raceway, potentially achieving less culture crashes and higher productivity at reduced capital investment.

2.4 **Harvesting and Dewatering**

Microalgae concentrations are very low while growing, typically 0.02% to 0.05% biomass dry matter in raceways and 0.1% to 0.5% dry matter in PBRs (Rodolfi, 2009). This results in about 200 m^3 to 5000 m^3 water to be recovered from the cultivation system, after being separated from the algae which has a size in the order of micrometers. Harvesting, dewatering, and further concentrating of algae are, therefore, difficult, energy intensive, and costly. In order for biofuel production from algae to be feasible, this step has to be as technically simple and economical as possible.

Harvesting and dewatering can be done in the raceway pond, or out of the pond in a separate basin. Out-of-pond dewatering adds to the construction and material cost, as well as increase of land use, but it allows time flexibility without a possibility of disrupting the growth cycle in the raceway pond. Dewatering in the pond can be done if the algae have the property of easy settling, making the time fraction of raceway pond used for dewatering low. Either way, the algae biomass has to eventually be transferred out of the raceway pond. In pilot scale ponds, this is done by sweeping manually, but as we move towards industrial scale, an automatic harvesting unit such as a travelling bridge has to be installed (Personal communication with Cellana). Several dewatering options and their details are listed in Table 2.4.

Table 2.4: Dewatering processes for microalgae

Processes	Description	Yield	Energy	Limitation
Auto-flocculation and sedimentation	Spontaneous floc formation of microalgae is commonly simulated by increase in alkalinity or excretion of macromolecules. These bigger flocs facilitate quicker sedimentation. Species with bigger cell size or higher ash content also results in more effective sedimentation. Sedimentation rates need to be at least 1 m/h.	0.5% to 3% TSS (Total Suspended Solids)	0 - 0.1 kWh/m3 (Wiley, 2011)	Relatively unreliable, slow process
Flocculation and sedimentation	Flocculation of biomass could be chemically induced, usually by using aluminum sulfate, ferric chloride, or ferric sulfate. Bigger flocs will sediment faster leaving clear water on top to be decanted.	~20% TSS	No energy input assuming mixing of flocculant is achieved when culture is transferred	Expensive flocculant, flocculant could downgrade the biomass quality
Flocculation and flotation	Dissolved air flotation involves injection of water stream pre-saturated with pressured air which generates bubble that rise through the liquid carrying the suspended solids to the surface to be skimmed off.	~1%-6% TSS	10-20 kWh/m^3 (Uduman, 2010)	Energy intensive, extra mechanical unit for skimming
Centrifugation	Centrifugal forces separate solids and liquids. The separation is based on the particle size and density difference of the medium components. Centrifugation is reliable and fast.	~ 20% TSS	1 kWh/m3, self-cleaning disc-stack 0.9 kWh/m^3 nozzle discharge 8 kWh/m^3, decanter bowl 0.3 kWh/m^3, hydrocyclone (Grima, 2003)	Expensive unit, energy intensive, potentially breakage the cells
Filtration	A separation method utilizing permeable medium through which a suspension is passed. The permeable medium retains the solids and allows the liquid to pass through.	~1%-6%, natural filtration ~5%-27% pressure filtration	0.4 kWh/m^3, vibrating screen filter 0.88 kWh/m^3, chamber filter press 2.06 kWh/m^3, tangential flow	Hard to implement on a large scale production, filter needs to be backwashed and periodically

			filtration (Uduman, 2010)	replaced on fouling
Electrocoagulation/ electroflocculation	Flotation technology that generates coagulating species for destabilizing algal suspensions in situ, through the electrochemical oxidation of consumable metal electrodes.	~3%-5% TSS	0.3-2 kWh/m^3	At early stage of research and development

2.4.1 Drying

When bulk dewatering has been achieved, depending on the concentration of algal slurry needed for the biodiesel processing, further drying might be needed. Drying to more than 90% biomass dry weight is an extremely energy intensive process as has been identified in some LCA studies. Although seen as a bottleneck, there has not been much discussion regarding finding an optimum drying process to realize the energetic feasibility of algal biofuel.

Rotary drum drying is a reliable thermal drying method that has been proven to work well for algae as it has been for other biomass drying. The energy need to operate rotary drum drying is high at 5 MJ per kg of water extracted (Verhoven, 2009). This means that we would need 20 MJ of energy to completely dry off a 20% dry weight algal paste. Assuming that the algal biomass has 40% oil content with 42.2 MJ/kg specific heating value (approximated from vegetable oil), the energy recovered in the form of oil after drying is only 16.9 MJ, lower than the energy input to obtain it. Other drying methods may be less reliable and have not been thoroughly tested on algal biomass, but they generally consume less energy and could potentially be implemented. Some of the methods to be considered are Carver-Greenfield drying used to dry wastewater sludge, fish meal drying, and dimethyl ether drying originally used for coal.

Sun drying is another viable option especially in areas with low precipitation. Most of the energy requirement is fulfilled by the solar radiation and the addition of fans for faster drying will only need minor additional energy inputs. The success of this method is very dependent on weather conditions, but on a sunny day it could very well compete with the more expensive heat sources. A flat surface with dark color should be used as a drying bed. The algae paste is spread on the drying bed at a thickness of approximately 0.5 cm. It is found that at that depth, there

would be less chance of putrefaction, and at an initial solid concentration of 6%, at a daily radiation of 480 cal/cm^2/day, drying to more than 90% dwb is achievable in a day (McGarry & Tongkasame, 1971). Additional land area required for sun drying could be large, but should not take more than 10% of the whole farm facility.

2.5 **Algal Oil Extraction**

2.5.1 Hexane Extraction

Solvent extraction, commonly with n-hexane (to be referred to as "hexane" from this point forward), is the standard method for extracting oils from biomass feedstocks. For example, hexane is very commonly used to extract soybean oil from soybeans and can also be used to extract oil from rape and canola seeds; therefore, hexane is being considered as a possible solvent for algae oil extraction. One drawback of this technique is the fact that it works better on dry biomass–90 wt% solids to be exact (Sheehan et al 1998). Halim et al (2011) conducted experiments that show hexane extraction on wet biomass (30% dwb) extracts 33% less oil than hexane extraction on 90% dwb.

The process of solvent extraction of algae oil via hexane in a counter-current extractor is modeled using data for soybean oil extraction with hexane from Sheehan *et al* (1998) and Emmenegger et al (2007) because no industry data concerning hexane extraction were available. Biomass is contacted with hexane in a counter-current extractor. Lipids from the biomass dissolve in the hexane, leaving behind carbohydrates and protein (and inorganic residues or "ash" in the case of diatoms) that is sent to an anaerobic digester or could be used as animal feed. The solids are heated to recover hexane. Residual hexane left in the solids was assumed to be 400 ppm according to analysis by Sheehan et al (1998). Hexane is recovered from the lipid fraction via multi-effect evaporation (Sheehan et al used three effects in their analysis). Figure 2.4 contains a flowchart of the hexane extraction process. It is important to note that hexane extraction of algae oil has not been proven on a large scale; this LCA assumes it would work with comparable performance to the extraction of other plant oils.

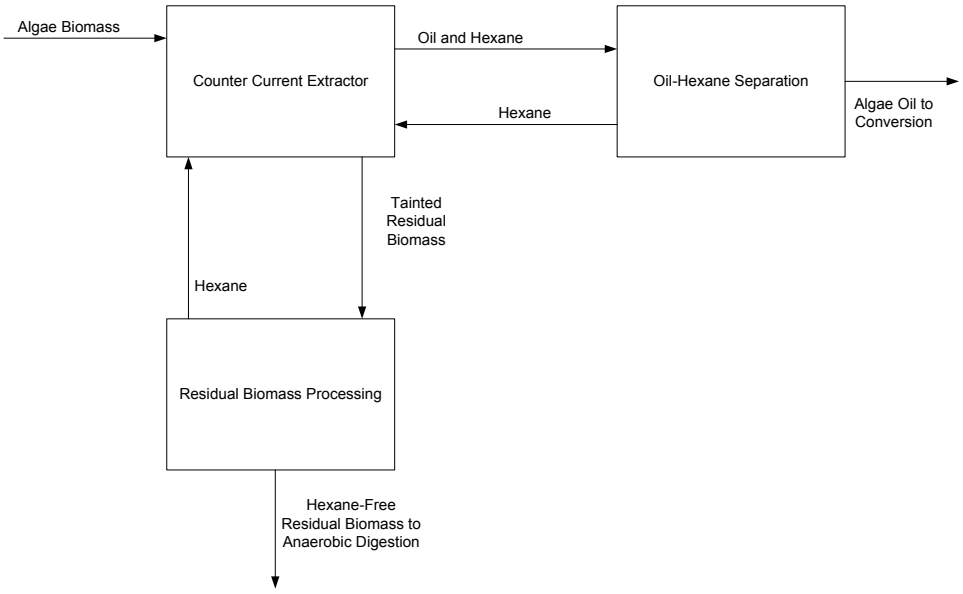

Figure 2.4: Process flow diagram for hexane extraction

One technological method of improving energetic return of algae biofuel is to develop a wet extraction technique to allow the elimination of drum drying. SRS Energy is studying a wet extraction technique for algae oil and is currently partnering with Cellana. Because of the recentness of the partnership, a full process description is not available at this moment, but several important things about the SRS process are known. One is that the process accepts algae biomass that is between 10 and 20% dwb (Czartoski, 2010). The separation process uses an organic solvent and forms three phases: an aqueous phase consisting of water, sugar monomers, and water-soluble protein; an oil phase containing the lipids, and a solid phase containing hydrophobic protein, ash, and other solids. The first generation technology can recover 80% or more of the lipids, and a goal of 90% lipid recovery has been set for the second generation of the technology (Archibald, 2011). Due to the lack of process information, it is assumed that SRS Energy's wet extraction technique has the same life cycle inventory as dry hexane extraction, making the dryness requirement the only difference between the two methods.

2.5.2 Supercritical Fluid Extraction with CO2

An alternative extraction technique explored in this study is the use of supercritical CO_2 ($SCCO_2$) to selectively extract algae lipid. $SCCO_2$ is currently used in the food processing industry for decaffeination of coffee, contaminant removal, edible oil extraction, production of hops extracts, and flavor recovery from herbs and spices (Brunner 2005). $SCCO_2$ has several desirable qualities when compared to solvent extraction; unlike hexane, CO_2 is non-toxic, non-flammable, and easily recoverable from solvated products–CO_2 readily separates from products after entering the gas phase. In an supercritical fluid extraction process, feed is contacted with a supercritical fluid which dissolves the desired product. The product and fluid are separated by either cooling or expanding (i.e. across a valve) the supercritical fluid phase until it enters the lower density gas phase where the desired species precipitated since they are no longer soluble. The biggest advantage of $SCCO_2$ is the fact that it can be used to extract oil from wet biomass (20 wt% solids) with higher efficacy than on dry biomass (Halim *et al* 2011). The one drawback in the use of $SCCO_2$ is the typically higher costs associated with it. This study will compare the energy intensity of the two processes when applied to algae oil extraction.

Another possible advantage of $SCCO_2$ is its ability to fractionate higher molecular weight polyunsaturated fatty acids (PUFAs) from TAGs. Perretti *et al* conducted a study that focused on recovery of docosahexaenoic Acid (DHA) and eicopentaenoic acid (EPA), two omega-3 fatty acids that have been associated with the prevention and treatment of arthritis, cancer, and other diseases, from algal biomass. According to the study, some algae produce more EPA than can be found in fish oil, the traditional source, and some algae also produce DHA. Perretti *et al* conclude that $SCCO_2$ can extract these two high-value PUFAs with a shorter extraction times than required for conventional solvent extraction.

In this study, we assumed that CO_2 contacts biomass at 30 MPa and 55 °C (Halim *et al* 2011 and Mendes *et al* 1995) in batches. Li *et al* (2006) conclude that compression of gaseous CO_2 to the supercritical phase and CO_2 recovery via expansion is more energy-efficient than pumping liquid CO_2 to the supercritical phase or CO_2 recovery via cooling; therefore, the process scheme in Figure 2.5 is used for this study. It is important to note that $SCCO_2$ of algae

oil has not been proven on a large scale; this study assumes it would work similar to the extraction of other plant oils.

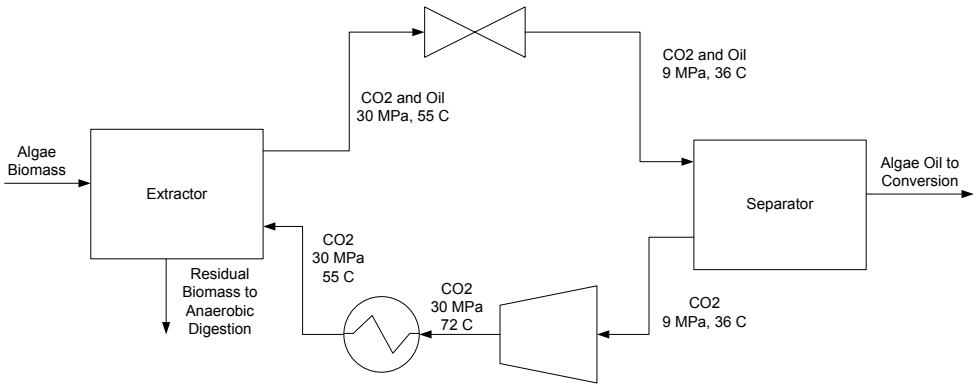

Figure 2.5: Process flow diagram for $SCCO_2$

2.5.3 Hydrothermal Liquefaction

The hydrothermal liquefaction process uses a high-pressure and high temperature condition, in a water-based medium to convert a high-lipid feedstock like algal biomass into bio-crude oils. The temperature used in this process could range from 250 to 350 °C. Water is beneficial as a reaction medium since the bio-crude oil produce will self-separate after conversion resulting in a three phase product: water phase, oil phase, and remaining solids. The aqueous medium also eliminates the need to dry the incoming feedstock completely.

In hydrothermal liquefaction, triglycerides in lipid feedstocks are continuously broken down into smaller molecules. In this fragmentation, oxygen, nitrogen, sulfur, phosphorous are removed from carbon chains, leaving mostly only hydrogen in the carbon backbone to form the bio-crude oil. Figure 2.6 shows an example of breaking down triglycerides through hydrothermal liquefaction.

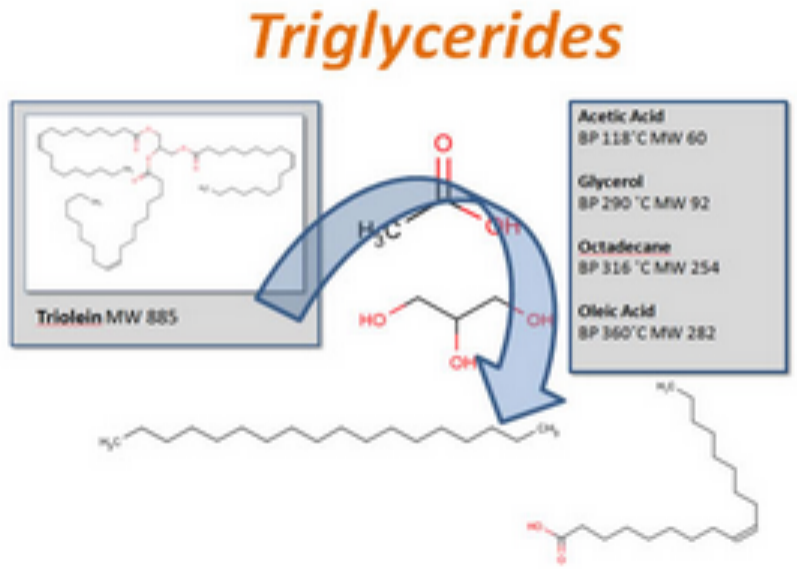

Figure 2.6: Formation of bio-crude oil from triglycerides in hydrothermal liquefaction

2.6 **Algal Biofuel Processing**

The conversion of biomass to energy encompasses a variation of technology depending on the feedstock and end use applications. This study focuses only on liquid fuel production, and limits the process option to transesterification and hydrotreating. Currently, the most preferred method of conversion is transesterification due to its success in industrial scale production of biodiesel from other types of vegetable oil. The technology for transesterification has matured and would be easier to be adapted for algal biodiesel. However, there are critical sustainability issues regarding the need for large amount of methanol and the usages for glycerol as a by-product of the process. Therefore, other alternatives have to be explored further.

2.6.1 Transesterification

The current definition of "biodiesel" in the U.S. is fatty acid methyl esters (FAME) produced from plant oils such as soybean oil, rapeseed oil, or vegetable oil. The process of

manufacturing FAME from TAGs is known as transesterification. TAGs can be transesterified with either methanol or ethanol, but industry chooses to use methanol due to its lower cost. Figure 2.7 shows the reaction between a TAG and methanol that produces FAME and glycerol. Transesterification can be undertaken using several different catalysts, most of which are homogeneous acids or bases such as sulfuric acid and potassium and sodium hydroxides. Acidic catalysts have several drawbacks. Their main disadvantage is slow reaction time, but other disadvantages include higher reaction temperature and pressure and increased reactor corrosion (Hasheminejad 2011). Therefore, typical industrial transesterification is performed with a homogeneous alkali catalyst.

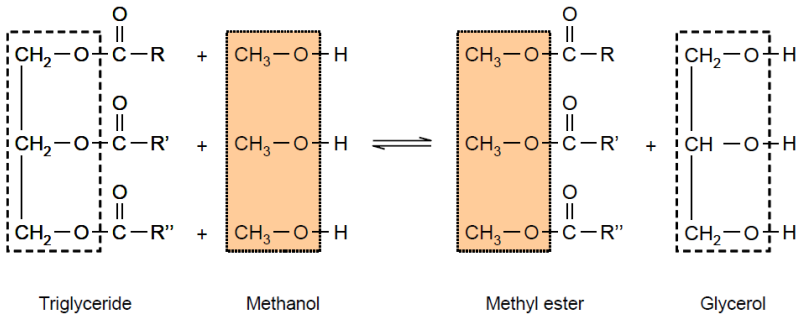

Figure 2.7: Chemistry of transesterification. From Emmenegger et al 2007

The first step in the transesterification process is pretreatment to convert PUFAs into FAME via reaction with methanol using a sulfuric acid catalyst as described by Leung *et al* (2010). In the next step, TAGs are converted to FAME via the transesterification reaction using potassium hydroxide as a catalyst. Glycerol can be separated from FAME, excess methanol, and potassium hydroxide via decanting due to its high density. Unreacted methanol is recovered via distillation. The mix of FAME and potassium hydroxide is mixed with phosphoric acid until neutral. Finally, the FAME is purified to 99.65 wt% (Pokoo-Aikins *et al* 2009) via a warm water wash that removes residual catalyst, salts, methanol, glycerol, and soaps (formed by reaction of PUFAs with potassium hydroxide). Glycerol is purified by neutralizing potassium hydroxide with phosphoric acid and further decanting to 88% purity (Leung *et al* 2010). Figure 2.8 gives a flow diagram of the transesterification process.

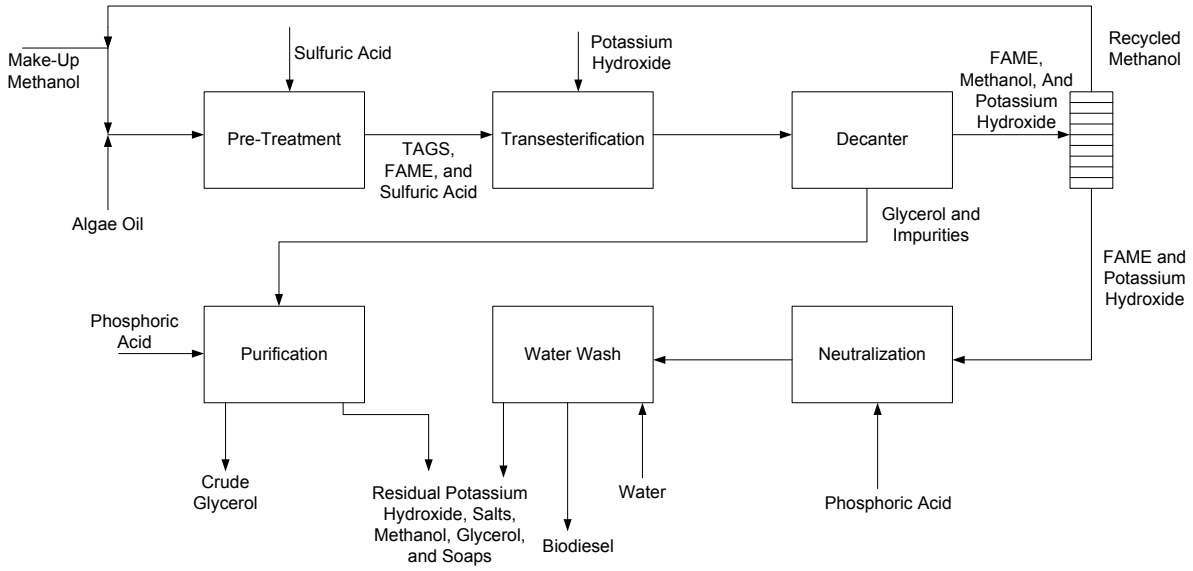

Figure 2.8: Transesterification process flow diagram.

2.6.2 Hydrotreating

An alternative method of converting algae oil to liquid fuel is hydrotreating, which is a common petroleum refinery unit operation. Traditionally, hydrotreating is used to remove nitrogen and sulfur from petroleum fractions as shown in Figure 2.9. Hydrotreating can be similarly used to deoxygenate TAGs and form straight-chain alkanes, called green diesel, that are very similar to petroleum diesel. The backbone of TAGs is converted to propane during the reaction, and some of the product diesel cracks into lighter gasoline components, providing additional by-products. Hydrotreating of TAGs can result in three different reactions all from the same catalyst, typically a mix of cobalt, molybdenum, and aluminum oxide. When lipids are contacted with hydrogen gas, their double bonds saturate, and the backbone is removed from TAGs. Then, the lipids are deoxygenated through one of several pathways. The possible reactions are hydrodeoxygenation, decarboxylation, and decarbonylation, which are shown in Figure 2.10. The occurrence of the hydrodeoxygenation reaction, which requires more hydrogen, increases with increased reactor temperature and pressure. The other two reactions are favored in milder conditions. Huber *et al* (2007) found decarboxylation and decarbonylation usually have equal occurrences, as evidenced by the equal volumes of CO and CO_2 formed by the reaction.

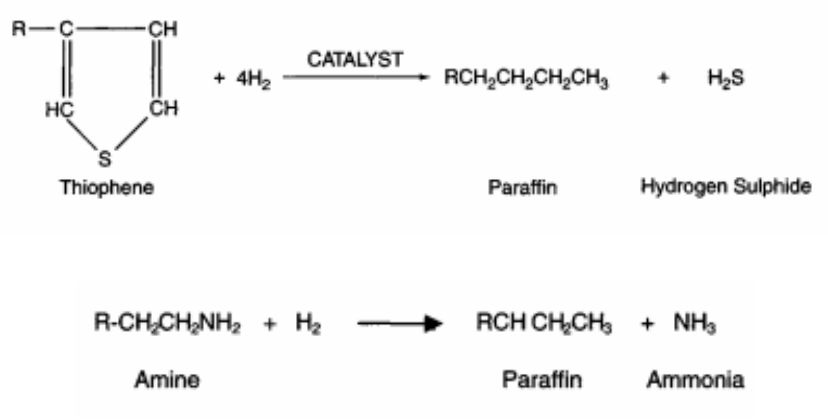

Figure 2.9: Petroleum refining desulfurization and denitrification reactions. From Parkash 2003, pp. 62-63.

$$R{-}CH_2{-}COOH \rightarrow R{-}CH_3 + CO_2$$

$$R{-}CH_2{-}COOH + H_2 \rightarrow R{-}CH_3 + CO + H_2O$$

$$R{-}CH_2{-}COOH + 3H_2 \rightarrow R{-}CH_2{-}CH_3 + 2H_2O$$

Figure 2.10: Top: decarboxylation reaction. Middle: decarbonylation reaction. Bottom: hydrodeoxygenation reaction (Huber et al, 2007)

One proposal for the hydrotreatment of bio-oil is to co-process it with heavy vacuum gasoil (VGO) in an existing hydrotreater. However, there are several issues with this. Marker *et al* (2005) point out that a stand-alone unit has the advantages of improved catalyst performance, a simpler isomerization process (Figure 2.11), and lower operating temperature and pressure and, therefore, lower hydrogen use. Therefore, a stand-alone algae oil hydrotreater is modeled in this study.

The process begins with algae oil being pumped to reaction pressure (between 36 and 50 bar) and heated to process temperature (about 325 °C). The oil reacts with hydrogen in a reactor and then is isomerized to reduce the solubility and viscosity of the oil, which improves cold temperature flow properties. The reactor products are cooled and sent to a water-oil-gas separator. Water from the reaction is sent to be purified in the refinery's sour water treatment

plant. The oil-phase is sent to a stripper where propane and gasoline are separated from the diesel product via steam injection. The gas phase is sent to a pressure swing adsorption (PSA) unit which recovers excess hydrogen to be reused in the hydrotreater. The tail gas from PSA, a mix of hydrogen, CO, and CO_2, is sent to the water-gas shift reactors in the hydrogen plant to convert CO to CO_2 and produce extra hydrogen. A process flow diagram for hydrotreating can be found in Figure 2.12.

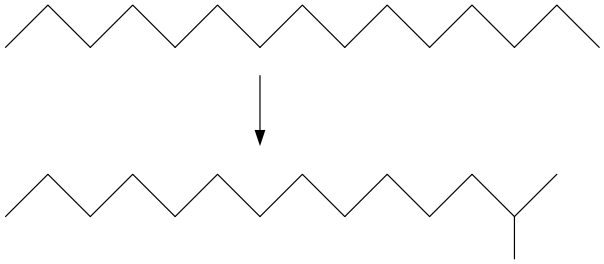

Figure 2.11: Isomerization of normal alkane to iso-alkane

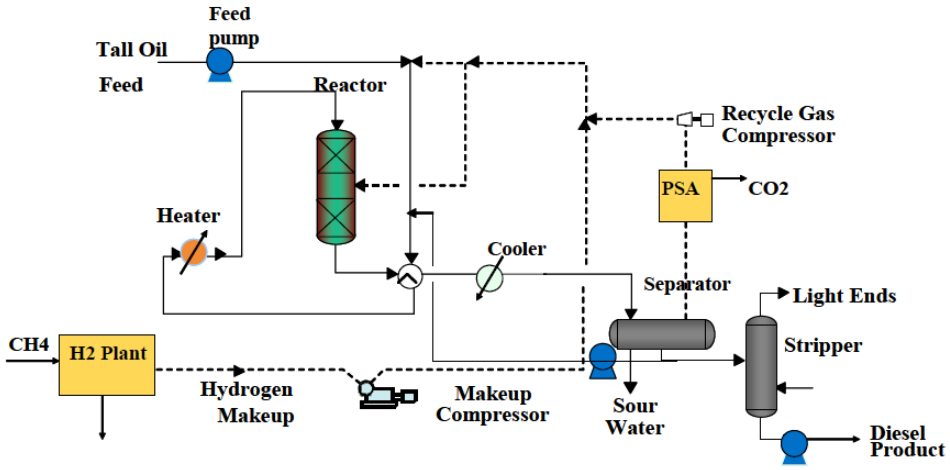

Figure 2.12: Process flow diagram for hydrotreating of algae oil (Marker et al 2005)

There are several desirable qualities of green diesel when compared to both petroleum diesel and biodiesel. Green diesel does not consist of double bonds and, therefore, has a lower autoignition temperature (as indicated by a higher cetane number) than petroleum diesel. Also,

green diesel has a lower sulfur content than petroleum diesel. Compared to biodiesel (FAME), green diesel has a higher energy density due the lack of oxygen in its molecules. The cloud point of green diesel is highly variable based on the degree of isomerization achieved. Table 2.5 shows a comparison of the properties of petroleum diesel, green diesel, and biodiesel.

Table 2.5: Comparison of diesel properties (Kalnes et al., 2009)

	Diesel (ULSD)	Biodiesel (FAME)	Green diesel
% Oxygen	0	11	0
Specific gravity	0.84	0.88	0.78
Sulfur (ppm)	<10	<1	<1
Heating value (MJ/kg)	43	38	44
Cloud point (°C)	−5	−5 to +15	−20 to +20
Cetane	40	50–65	70–90
Stability	Good	Marginal	Good

REFERENCES

Altõn, R., Cetinkaya, S., & Yucesu, H. S. (2001). The potential of using vegetable oil fuels as fuel for diesel engines. *Energy Conversion and Management, 42*, 529-538.

Archibald, I. (2011, March 8). Personal communication with Cellana.

Bai, X., Knurek, E., Workman, M., Hamilton, S., Hertz, C., Bernhardt, B., Rangelova M., Obbard, J. (2011). Algal autotrophic and heterotrophic lipid synthesis for biodiesel production. *The First International Conference on Algal Biomass, Biofuels, and Bioproducts.*

Benemann, J., Goebel, R., Weissman, J., & Augenstein, D. (1982). *Microalgae as a Source of Liquid Fuels.* Solar Energy Research Institute.

Brunner, G. (2005). Supercritical Fluids: Technology and Application to Food Processing. *Jounal of Food Engineering 67*, pg 21-33.

Carlsson, A. S., Beilen, J. B., Moller, R., & Clayton, D. (2007). *Micro- and Macro-algae: Utiliy for Industrial Applications.* University of York.

Carvalho, A. P., Meireles, L. A., & Malcata, F. X. (2006). Microalgal Reactors: A Review of Enclosed System Designs and Performances. *Biotechnol. Prog., 22*, 1490−150.

Chisti, Y. (2007). Biodiesel from Microalgae. *Biotechnology Advances, 25*, 294-306.

Czartoski, T. (14 Dec. 2010). SRS Energy Presentation to Cellana. Cellana Kona Pilot Facility, Kona.

Emmenegger, M. F., Dinkel, F., Stettler, C., Doka, G., Chudacoff, M., Dauriat, A., et al. (n.d.). *Life Cycle Inventories of Bioenergy. Rep. no. 17*.

García-González, M., Moreno, J., Canavate, J., Anguis, V., Prieto, A., Manzano, C., et al. (2003). Conditions for open-air outdoor culture of Dunaliella salina in southern Spain. *Journal of Applied Phycology, 15*, 177-184.

Goldman, J. C. (1979). Outdoor Algal Mass Cultures - Photosynthetic Yield Limitations. *Water Research, 13*, 119 -136.

Griffiths, M. J., & Harrison, S. T. (2009). Lipid productivity as a key characteristic for choosing algal species for biodiesel production. *J Appl Phycol, 21*, 493–507.

Grima, E. M., Belarbia, E., Fernandez, F. A., & A. Robles Medina, Y. C. (2003). Recovery of microalgal biomass and metabolites: process options and economics. *Biotechnology Advances, 20*, 491–515.

Halim, R., Gladman, B., Danquah, M. K., & Webly, P. A. (2011). Oil Extraction from Microalgae for Biodiesel Production. *Bioresource Technology 102* , 178-85.

Hasheminejad, M., Tabatabaei, M., Mansourpanah, Y., Far, M. K., & Javani, A. (2011). Upstream and Downstream Strategies to Economize Biodiesel Production. *Bioresource Technology 102*, 461-68.

Hu, Q., Sommerfeld, M., Jarvis, E., Ghirardi, M., Posewitz, M., Seibert, M., et al. (2008). Microalgal Triacylglycerols as Feedstocks for Biofuel Production: Perspectives and Advances. *The Plant Journal 54.4*, 621-39.

Huntley, M. E., & Redalje, D. G. (2007). CO2 Mitigation and Renewable Oil from Photosynthetic Microbes: A New Appraisal. *Mitigation and Adaptation Strategies for Global Change*, 12: 573–608.

Jorquera, O., Kiperstok, A., Sales, E. A., Embiruçu, M., & Ghirardi, M. L. (2010). Comparative energy life-cycle analyses of microalgal biomass production in open ponds and photobioreactors. *Bioresource Technology, 101*, 1406–1413.

Kadam, K. (2001). Microalgae Production from Power Plant Flue Gas: Environmental Implications on a Life Cycle Basis. *NREL Report*.

Kalnes, T. N., Koers, K. P., Marker, T., & Shonnard, D. R. (2009). A Technoeconomic and Environmental Life Cycle Comparison of Green Diesel to Biodiesel and Syndiesel. *Environmental Progress & Sustainable Energy 28.1*, 111-20.

Lee, Y.-K. (2001). Microalgal mass culture systems and methods: Their limitation and potential. *Journal of Applied Phycology, 13*, 307-315.

Leung, D. Y., Wu, X., & Leung, M. (2010). A Review on Biodiesel Production Using Catalyzed Transesterification. *Applied Energy 87*, 1083-095.

Li, Y., Griffing, E., Higgins, M., & Overcash, M. (2006). Life Cycle Assessment Of Soybean Oil Production. *Journal of Food Process Engineering 29.4* , 429-45.

Lundquist, T., Woertz, L., Quinn, N., & Benemann, J. (2010). A Realistic Technology and Engineering Assessment of Algae Biofuel Production. *Energy Biosciences Institute*, 1-178.

Marker, T., Petri, J., Kalnes, T., McCall, M., Mackowiak, D., Bob Jerosky, B. R., et al. (2005). *Opportunities for Biorenewables in Oil Refineries.*

Mendes, R. L., Coelho, J. P., Fernandes, H. L., Marrucho, I. J., Cabral, J. M., Novais, J. M., et al. (1995). Applications of Supercritical CO2 Extraction to Microalgae and Plants. *Journal of Chemical Technology AND Biotechnology 62.1* , 53-59.

Neenan, B., Feinberg, D., Hill, A., McIntosh, R., & Terry, K. (1986). *Fuels from microalgae: technology status, potentials, and research requirements.* Golden, Colorado: Solar Energy Research Institute.

Noue, J. D., & Pauw, N. D. (1988). The Potential of Microalgal Biotechnology: A Review of the Production and Uses of Microalgae. *Biotech. Adv., 6*, 725-770.

Pagliaro, M., Ciriminna, R., Kimura, H., Rossi, M., & Pina, C. D. (2007). From Glycerol to Value-Added Products. *Angewandte Chemie International Edition, 46*, 4434 – 4440.

Pokoo-Aikins, G., Nadim, A., El-Halwagi, M. M., & Mahalec, V. (2009). Design and Analysis of Biodiesel Production from Algae Grown through Carbon Sequestration. *Clean Techn Environ Policy*.

Regan, D., & Gartside, G. (1983). *Liquid fuels from micro-algae in Australia.* Melbourne: CSIRO.

Rodolfi, L., Zittelli, G. C., Bassi, N., Padovani, G., Biondi, N., Bonini, G., et al. (2009). Microalgae for Oil: Strain Selection, Induction of Lipid Synthesis and Outdoor Mass Cultivation in a Low-Cost Photobioreactor. *Biotechnology and Bioengineering, 102*, 100-112.

Schenk, P. M., Thomas-Hall, S. R., Stephens, E., Marx, U. C., Mussgnug, J. H., Posten, C., et al. (2008). Second Generation Biofuels: High-Efficiency Microalgae for Biodiesel Production. *Bioenergy Resources, 1*, 20–43.

Sheehan, J., Dunahay, T., Benemann, J., & Roessler, P. (1998). *A Look Back at the U.S. Department of Energy's Aquatic Species Program: Biodiesel from Algae.* U.S. Department of Energy's Office of Fuels Development.

Sialve, B., Bernet, N., & Bernard, O. (2009). Anaerobic digestion of microalgae as a necessary step to make microalgal biodiesel sustainable. *Biotechnology Advances, 27*, 409–416.

Spolaore, P., Joannis-Cassan, C., Duran, E., & Isambert, A. (2006). Commercial Applications of Microalgae. *Journal of Science and Bioengineering*, Vol. 101, No.2, 87-96.

Stepan, D. J., Shockey, R. E., Moe, T. A., & Dorn, R. (2001). *Carbon dioxide sequestering using microalgal system.* U.S. Department of Energy.

Tongkasame, G. M. (1971). Water reclamation and algae harvesting. *Journal (Water Pollution Control Federation), 43*, 824-835.

Uduman, N., Qi, Y., Danquah, M. K., Forde, G. M., & Hoadley, A. (2010). Dewatering of microalgal cultures: A major bottleneck to algae-based fuels. *JOURNAL OF RENEWABLE AND SUSTAINABLE ENERGY 2*.

Verhoven, J. (2009). *Life Cycle Assessment of Biodiesel and Feed Production form Microalgae: A review of the Cellana project.* Cellana Internal Report.

Weyer, K. M., Bush, D. R., Darzins, A., & Willson, B. D. (2010). Theoretical Maximum Algal Oil Production. *Bioenergy Resources, 3*, 204–213.

Wijffels, R. H. (2007). Potential of sponges and microalgae for marine biotechnology. *Trends in Biotechnology, 26*.

Wiley, P. E., Campbell, J. E., & McKuin, B. (2011). Production of Biodiesel and Biogas from Algae: A Review of Process Train Options. *Water Environment Research, 83*, 326-338.

Williams, P. J., & Laurens, L. M. (2010). Microalgae as biodiesel & biomass feedstocks: Review & analysis of the biochemistry, energetics & economics. *Energy & Environmental Science, 3*, 554–590.

Zeiler, K. G., Heacox, D. A., Toon, S. T., Kadam, K. L., & Brown, L. M. (1995). The use of microalgae for assimilation and utilization of carbon dioxide from fossil fuel-fired power plant flue gas. *Energy Conversion Management, 36*, 707-712.

3 METHODOLODY

3.1 Framework of an LCA

An LCA is a structured method to provide compilation and quantitative evaluation of the inputs, outputs and the potential environmental impacts of a product system throughout its life cycle (ISO, 2006). It is also known as a "cradle-to-grave" analysis because it takes into account the impacts from raw material acquisition, production, use, and disposal. Conceptually, it consists of set of energy and material inputs associated with emissions to the environment, as well as a loss of energy due to imperfect efficiencies. A life cycle is made of a combination of unit operations linked together, where the output of one unit process becomes an input to another unit process. From such a systematic approach, the energy and resource utilization effectiveness and environmental burden between life cycle stage or individual process can be identified and quantified. This methodology exposes areas for improvement.

For the production of algal biofuel, the raw material acquisition which is the starting unit process is crop cultivation and the last unit process is the combustion of biofuel in an engine. Figure 3.1 shows a linear process flow diagram representing a generic model for algal biofuel LCA. The detailed explanation of specific unit processes that make up each of the blocks was explained in Chapter 2.

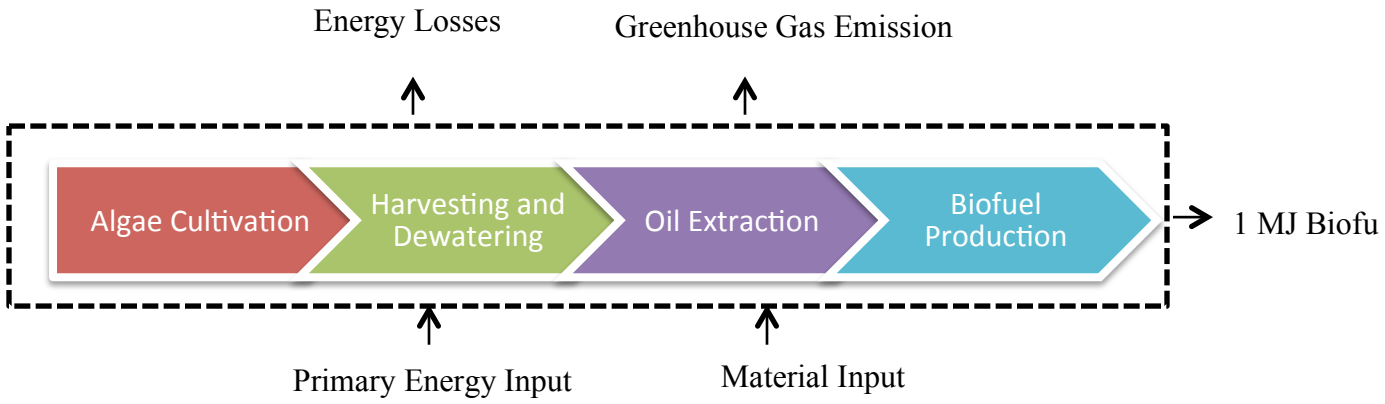

Figure 3.1: Flow diagram of microalgal biofuel LCA

The framework to conduct an LCA has been developed by the International Standard Organization (ISO) and is documented under ISO14040. LCA can be used as a method to identify points where improvement to reduce impacts could be made, to compare several similar products or processes, to assist in strategic planning and priority setting by an industry, governmental, or non-governmental organizations, and to produce eco-labeling scheme or environmental claim in product marketing. The steps in this standard are depicted in Figure 3.2 below and will be the guide for the LCA in this thesis. The backbone phases include goal and scope definition, inventory analysis, and impact assessment.

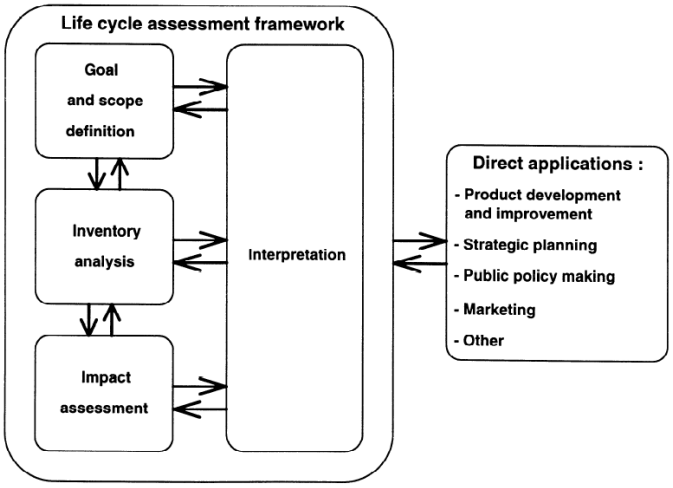

Figure 3.2: Methodological framework of an LCA: phases of an LCA (taken from ISO 14040)

The goal and scope definition phase is the first phase of an LCA, and it establishes the goal of the intended study, the functional unit, the reference flow, the product systems, and the breadth and depth of the study in relation to the goal. The functional unit is a crucial element that describes the primary functions fulfilled by a product system. It will be used as a basis for selecting one or more alternative systems that might provide these functions (Guinee & Heijungs, 2005). For example, based on the flow diagram on Figure 3.1, the functional unit to be used to compare final biofuel products is 1 MJ. Sometimes, when conducting comparison of processes in the subsection of the life cycle, we use a different functional unit. If we are only looking at comparing oil extraction processes, for example, the functional unit would be 1 kg of algal oil extracted. This way, the best process option at each subsection could be identified before conducting the whole life cycle.

The inventory analysis is the second stage where an accounting method is used to track the input and output of material and energy flows associated with each step in a process or in the production of a product. For example, in the algal cultivation step, the materials input would include fertilizer, water, carbon dioxide, raceway pond materials, etc., for which the amount of each material has to be determined.

The impact assessment is the third phase of LCA aimed at understanding and evaluating the magnitude and significance of the potential environmental impacts of the product system. At this stage, chemical outputs are assigned qualitatively to a particular impact category which is quantified in terms of a common unit. The common unit allows numerical outputs to be aggregated into a single number. For example, if the global warming potential for time horizon 100 years (GWP100) of CO_2 is 1 and the GWP100 of CH_4 is 21, the indicator result for an emission of 2 kg CO_2 and an emission of 3 kg CH_4 for climate change using the GWP100 characterization factors is:

$$(1\times 2kg\ CO_2) + (21\times 3kg\ CH_4) = 65\ kg\ CO_2\ equivalent$$

After the focus has been set in the goal and scope definition, data collection and calculations have been done in the inventory analysis, and impact assessment has been conducted, the fourth phase of interpreting the results can begin. In this phase results are summarized, analyzed and evaluated to develop conclusions and make recommendations for the target audience.

3.2 **Uncertainty in LCA**

The outcomes of an LCA are subject to uncertainty and variability within the model. Variability can be defined here as inherent variation in the real world, while uncertainty comes from inaccurate measurement, lack of data, model assumptions, etc. that are integrated in the LCA outcome (Huijbregts, 1998). The implementation of uncertainty and variability analysis in LCAs could be useful for decision makers in judging the significance of the differences in products and processes. Options for improvement can then be evaluated. While the use of such analysis is recommended in any kind of LCA work, it is particularly important for life cycle studies of biofuel systems due to its wide variation of feedstock source, conversion processes,

research results, and assumptions made in scaling experiment data up to industrial-scale operation. By implementing uncertainty analysis, we may obtain a more balanced and holistic view of the reality of processing algae to biofuels.

In general, there are two types of uncertainty: parametric and scenario uncertainty (Johnson, 2006). Parametric uncertainty deals with variation in data and process options, while scenario uncertainty deals with variation in LCA methodology such as choosing system boundary or emission accounting. The analysis in this thesis focuses largely on parametric uncertainty, while scenario uncertainty is taken into account in the end as a completion check to ensure correctness of result when a different modeling procedure is used.

3.2.1 Parametric Uncertainty

A high volume of data is usually needed in the inventory stage, which makes it time consuming and challenging to obtain necessary information. During this stage, data are collected to complete all the material and energy inputs and outputs, and emissions for each of the processes are in the life cycle. Parametric uncertainty may be caused by imprecise measurements, inconsistency of data and lack of data, or variability that is inherent to a process as a whole such as temporal, spatial, and process variability. As an example, nitrogen fertilizer is an important input to algae cultivation which exists in several forms – ammonia, urea, ammonium nitrate, etc. When it has been decided to use a particular form, there is a variation in the way that fertilizer is produced depending on the age of the facility and the technology used to manufacture. Moreover, the amount of fertilizer needed would also vary depending on the algae species, knowledge-based decision from practitioners, environmental conditions, location and time of growth, and other factors.

Process and product information is often protected by intellectual property (IP) rights which can make some data is impossible to be obtained. To overcome IP issues, generic process simulations can be used to estimate values for specific processes. Generic life cycle inventories have been publishes for many processes, especially the upstream ones for energy production or resource extraction, which greatly assists in the construction of an LCA study. For specific or new processes, more detailed models have to be developed by the investigator using the most

current data to represent material and energy balances for the system. This specific model would be more reliable than the general one, although variability for different facility, locations, and day to day operations still cannot be neglected. In a case where there is lack of knowledge of certain distribution values and correlations between parameters, expert judgment should be used to estimate values for the material and energy balances. While this solves the problem of data gap in the LCA, it does not compensate for the issue of unreliability. It should be pointed out that more studies would be needed to improve the accuracy of the data used.

3.2.2 Scenario Uncertainty

Scenario uncertainty results from the different choices available in the modeling procedure. This includes the choice of functional unit, system boundary, allocation method for by-products, and characterization factors. Characterization factors group together chemicals disposed to the environment. The amount of waste chemicals is translated into specific impacts such as acidification, global warming potential (GWP), human toxicity and eutrophication. Understanding these impacts is very useful for decision makers as having a focus on just several key impacts would simplify factors affecting the decision. However, these characterization factors use simplified environmental models with many uncertainties embedded in them. The different combinations of model uncertainties would lead to highly dispersed probability distributions of the actual impact.

The system boundary chosen can also significantly impact LCA results. The boundaries of an LCA study are subjective. The more expanded the analysis is, the more complete it will be. However, there is always a restriction of time, energy, and money such that a decision on boundary has to be made to ensure that the benefits of doing so pay for the costs. Sometimes, the processes yield beneficial co-products. In the algal biofuel production, for example, after oil extraction, we are left with a portion of the biomass that is mostly consisted of carbohydrate and protein. This co-product could be used as an animal feed. There is uncertainty on how much weight the life cycle impacts should give to co-products compared to the biofuel itself. Different allocation methods chosen would lead to considerable changes in the LCA results. These decisions on where system boundaries should be drawn, or the type of allocation method used,

are a discrete type of uncertainty, and should be analyzed differently compared to the previously mentioned levels of uncertainty.

3.3 Uncertainty Assessment Methods

Monte Carlo simulation was used in this study to manage the parametric uncertainties. Monte Carlo simulation uses an iterative problem solving method to assess uncertainty propagation (Groode, 2008). Inputs to parameters have to be in the form of a probabilistic density function (PDF), which represents the probabilistic range of values an input could have. The PDF types used here are normal, log-normal, triangular, and uniform/range distribution , shown in Table 3.1, which are chosen accordingly based on data availability.

Table 3.1: Distribution types used to describe probabilistic density function of input parameters (SimaPro Manual)

Distribution	Data needed	Graphical presentation
Range	Min and Max value	
Triangular	Min and Max value plus best guess value	
Normal distribution	Standard deviation and best guess value	
Lognormal distribution	Standard deviation and best guess value	

Parameter input values will then be sampled randomly from these distributions for multiple trials to generate a set of output results that can be presented also as a probability distribution. These uncertainties are, therefore, propagated in the life cycle model through to the last unit process and are accounted for in all stages. Each simulation is set to iterate for 1000 times. The Monte Carlo simulation tool is embedded within the SimaPro LCA software. While it may reduce the transparency of the simulation, it makes it easier for the practitioner to analyze the input distribution and constantly link it to the LCA model.

Data collection process or the inventory analysis stage is usually identified as the most difficult and time-consuming stage of an LCA. Including the characterization of uncertainty ranges for the Monte Carlo simulation would make it an even overwhelming task, especially when there are numerous parameters to be considered. To simplify data collection, a screening method to assess key parameters with the most important input uncertainties is applied. A sensitivity analysis of deterministic input values is used to rank and determine the parameters that are important for the Monte Carlo simulation.

3.4 **Data Acquisition and Software**

Various data sources are used to complete the inventory analysis within the system boundaries of this LCA, in the form of material and energy input and output, as well as to come to assumptions or best guesses for parameters with data gap. The first data source is the scientific literature which has been deeply analyzed in this study to determine uncertainty ranges and understand the different conclusions that are reached by various researchers. With the collaboration that Cornell has with Cellana Inc., a Hawaii based algal cultivation company, we are also able to obtain some data that is based on operation of a demonstration-scale plant in Kona, Hawaii.

The LCA software used, which is SimaPro 7.2, comes with several databases that provide input and output values for background processes or materials that are commonly used. The databases used in this study include Ecoinvent 2.0 and US LCI (US Lifecycle Inventory). Ecoinvent v2 LCI database (http://www.ecoinvent.org) is included with the SimaPro software and is used to fill in data that are not just specific to algal biodiesel production. Because of the depth and breadth of the data modules and the consistent inclusion of infrastructure impacts, Ecoinvent system processes were used to maintain consistency throughout the process. For these and other reasons, Ecoinvent data are commonly used in LCAs done by other researchers, improving comparability of our results to other studies. Ecoinvent data is primarily focused on European conditions but contain many worldwide modules with datasets ranging from energy, building materials, and transport to chemicals, agriculture, and waste management.

REFERENCES

Groode, T. A. (2008). *Biomass to Ethanol: Potential Production and Environmental Impacts.* Massachusetts Institute of Technology.

Guinee, J., & Heijungs, R. (2005). Life Cycle Assessment. In *Kirk-Othmer Encyclopedia of Chemical Technology.*

Huijbregts, M. A. (1998). Application of uncertainty and variability in LCA. *The International Journal of Life Cycle Assessment, III*(5), 273-280.

International Standard Organization. (2006). *Environmental Management - Life Cycle Assessment Principles and Framework.*

Johnson, J. C. (2006). *Technology Assessment of Bioethanol: A Multi-objective, Life Cycle Approach Under Uncertainty.* Massachusetts Institute of Technology.

PRe Consultant. (2008). *Introduction to LCA with SimaPro 7.*

4 ANALYSIS OF MICROALGAL BIOFUEL LCA STUDIES

A literature review is presented in this chapter of earlier studies that have reported the net energy return (NER) of biofuel production using microalgae as feedstock. In the last couple of years a significant number of life cycle studies of microalgae biofuels have been published. Unfortunately, there is no clear consensus among these studies of the advantages, challenges, or feasibility of producing algal biofuel in a sustainable large-scale process.

Comparing NER values across LCA studies that model algal biofuels production is complex. For one, published studies vary with respect to the type of biofuel produced (e.g. methane and biodiesel) as well as the functional unit on which each model is based (e.g. 1 MJ of biodiesl or 1 kg of TS algae). Additionally, the scope, boundaries, and parameter values vary across studies. Moreover, previous authors have shown that NER values associated with corn ethanol are extremely sensitive to changes in model boundaries and parameter values (Chambers et al., 1979; Farrell et al., 2006). For example Farrell et al. (2006) demonstrated that differences among choices in co-product allocation resulted in wide variations of net energy values for six cases which modeled NER for corn ethanol. There is a need to develop a set of metrics by which we can compare multiple cultivation and processing schemes associated with algal biofuels.

While it is important to model the energy and environmental impacts to predict the feasibility of producing biofuels from algae, the uncertainty of the currently available model parameters present additional challenges. Published LCA models are based on many parameter values that are taken from bench-scale experiments or untried processes. With many parameters having huge uncertainties, the results of the analysis may be misleading, making it difficult for decision makers to reach a general conclusion on how to perceive the future of algal biofuel.

The net energy metrics have been commonly used as a parameter to quantify the performance of renewable energy systems. Net energy ratio (NER) is one of the common energy metrics and is defined in this thesis as:

$$NER = \frac{Energy\ content\ of\ algal\ biofuel + Energy\ allocation\ to\ the\ by-products}{Total\ non-renewable\ energy\ input}$$

Based on this definition, an NER above one would indicate a positive energy return demonstrating the possibility of the renewability nature of the fuel. Due to the large number of studies published on this topic, we chose to look at studies that either present values of NER or studies that report sufficient data from which NER may be calculated.

Examples of LCA works that are not included in this chapter are studies by Jorquera et al. (2009) and Clarens et al. (2009); which both look at production of algal biomass, without any further processing into fuels. Although studies by Sturm et al. (2011), Campbell et al. (2010), Pfromm et al. (2010), and Sazdanoff (2006) report results on energy inputs and outputs, these values are presented in a form that makes it difficult to calculate NER as defined above. There are also LCA studies that do not emphasize energy usage such as that by Yang (2010) which looks at water use and nutrients requirements, making it hard to be compared to others.

NER values from thirteen studies that could be compared are listed in Table 4.1.

Table 4.1: List of microalgal biofuel LCA publications with liquid fuels as a final product with reported or calculated NER value

Ref #	Lead Author	Title
(1)	Alabi et al. (2009)	Microalgae technologies and processes for biofuels/bioenergy production in British Columbia: current technology, suitability, and barriers to implementation
(2)	Baliga & Powers (2010)	Sustainable algae biodiesel production in cold climates
(3)	Batan et al. (2010)	Net energy and GHG emission evaluation of biodiesel derived from microalgae
(4)	Clarens et al. (2011)	Environmental impacts of algae-derived biodiesel and bioelectricity for transportation
(5)	Dufour et al. (2011)	LCA of biodiesel production from microalgae oil: effect of algae species and cultivation system
(6)	Ehimen et al. (2010)	Energy balance of microalgal-derived biodiesel
(7)	Lardon et al. (2009)	LCA of biodiesel production from microalgae
(8)	Sander & Murthy (2010)	Life cycle analysis of algae biodiesel
(9)	Sawayama et al. (1999)	Possibility of renewable energy production and CO_2 mitigation by thermochemical liquefaction of microalgae
(10)	Shirvani et al. (2011)	Life cycle energy and greenhouse gas analysis for algae-derived biodiesel
(11)	Stephenson et al. (2010)	LCA of potential algal biodiesel production in the United Kingdom: a comparison of raceways and air-lift tubular bioreactors
(12)	Razon & Tan (2011)	Net energy analysis of the production of biodiesel and biogas from the microalgae: *Haematococcus pluvialis* and *Nannochloropsis*
(13)	Verhoven (2009)	LCA of biodiesel and feed production from microalgae

The comparison is organized based on three assumptions generally taken in the growth system: open raceway, PBRs, or a combination of the two referred to as the hybrid system. Growth system used is one of the major assumptions in conducting an LCA. Therefore, grouping

together studies according to their growth system would allow for fairer comparison and easier analysis of the differences in other more minor assumptions. Figure 4.1 below summarizes the NER results for LCA with raceway growth system.

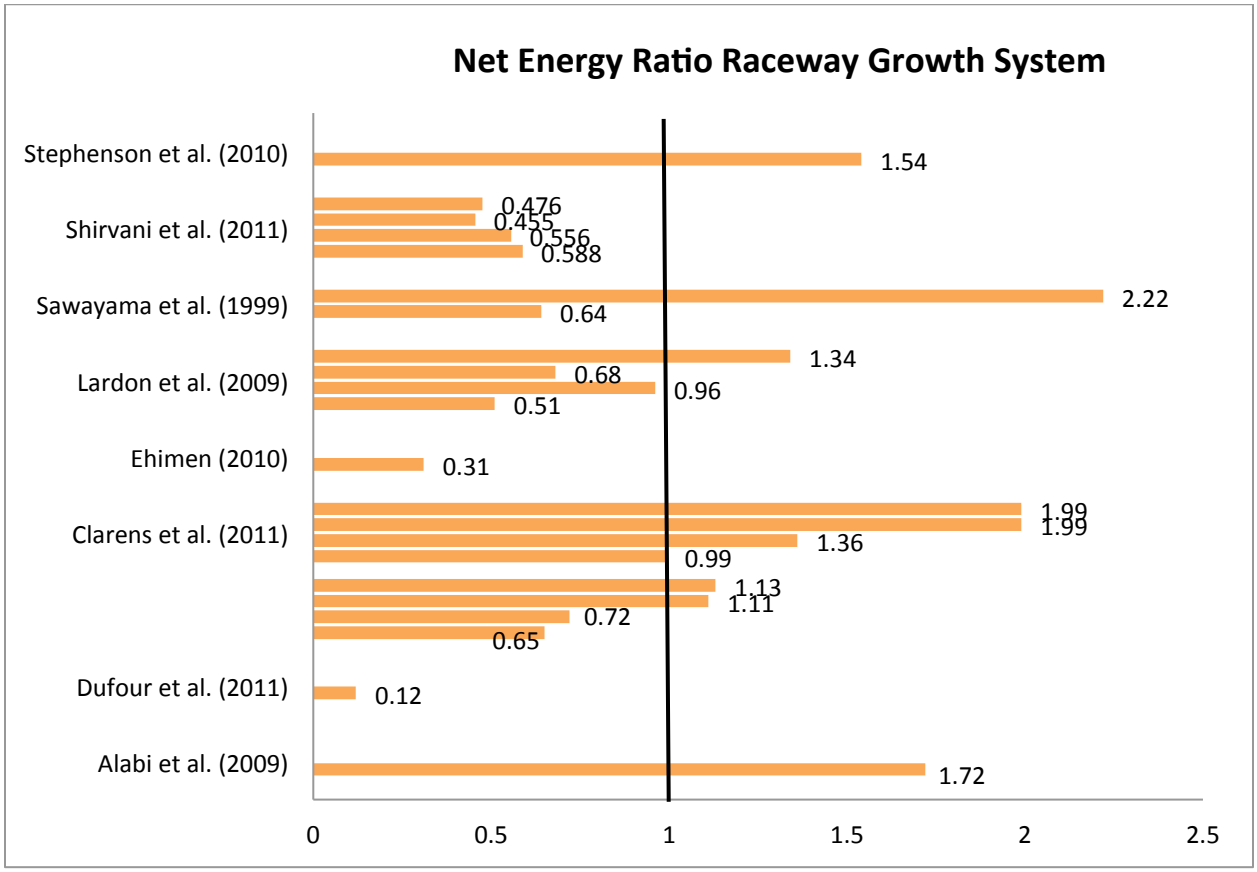

Figure 4.1: NER of microalgal biofuel with raceway pond growth system

Some of the studies have considered several cases or sensitivity analysis resulting in multiple NER results. There are a total of 22 cases included in the graph, of which 10 show an NER above 1. The highest NER is from Sawayama et al (1999) which stems from the assumption that the final biofuel is green diesel from hydrothermal liquefaction process which does not need the biomass to be dried before processing. In Sawayama study, they compare two strains of algae: *Botryococcus braunii* (NER of 2.22) and *Dunaliella tertiolecta* (NER of 0.64). The different NER calculated for the two species is due to the lower fertilizer needed in cultivating *B. braunii* and from the larger diameter of *B. braunii* resulting in lower energy use for harvesting. This

study shows that while the fuel conversion method and the need for drying affect NER result, the choice of algal strain and nutrient input are very important determinants.

The rest of the studies use transesterification from microalgal oil to biodiesel as the conversion method. The issue of high energy use for drying is confirmed in Lardon's study where four conditions are evaluated: low nitrogen culture with wet extraction (NER of 1.34), low nitrogen culture with dry extraction (NER of 0.68), normal culture with wet extraction (NER of 0.96), and normal culture with dry extraction (NER of 0.51). This result shows that while lowering nutrient input is important, only when drying need is eliminated could an NER above 1 be achieved.

Ehimen (2010) and Stephenson (2010) have very similar process pathways and system boundaries, but different assumptions on co-products. Ehimen does not consider the production of any co-product while Stephenson does, which explains the NER below 1 for Ehimen's analysis and the opposite for Stephenson. Based on these observations, a summary is made out of the main assumptions that differentiate these studies: nutrient provision, drying, fuel processing, and co-product. The table below shows the different assumptions in the studies highlighting their importance in affecting the NER results.

Table 4.2: Summary of LCA studies with raceway pond growth system and their main assumptions

Author	Nutrient	Drying from 20% to 90% dwb	Fuel Processing	Co-products	NER
Alabi et al. (2009)	Urea (109 g N/kg dwb), Diammonium phosphate (49 g P/kg dwb), free CO2 from flue gas	No	No	Ethanol from carbohydrate	1.76
Clarens et al. (2011)	Ammonium phosphate based on Redfield ratio, virgin commercial CO2	No	TE	Anaerobic digestion producing methane	0.65
	Ammonium phosphate based on Redfield ratio, carbon capture CO2 from flue gas	No	TE	Anaerobic digestion producing methane	0.72
	Ammonium phosphate based on Redfield ratio, CO2 directly from flue gas	No	TE	Anaerobic digestion producing methane	1.11
	Nutrient from wastewater, CO2 direction from flue gas.	No	TE	Anaerobic digestion producing methane	1.13
	Ammonium phosphate based on Redfield ratio, virgin commercial CO2	No	TE	Direct combustion producing electricity	0.99
	Ammonium phosphate based on Redfield ratio, carbon capture CO2 from flue gas	No	TE	Direct combustion producing electricity	1.36
	Ammonium phosphate based on Redfield ratio, CO2 directly from flue gas	No	TE	Direct combustion producing electricity	1.99
	Nutrient from wastewater, CO2 direction from flue gas.	No	TE	Direct combustion producing electricity	1.99
Dufour et al. (2011	f/2 recipe, 3.5 kg CO2/kg dwb	No	TE	No	0.12
Ehimen (2010)	Urea (80 g N/kg dwb), Triplesuperphosphate (20 g P/kg dwb), free waste CO2 from combustion.	No	TE	No	0.31
Lardon et al. (2009)	Calcium nitrate (46 g N/kg dwb), single superphosphate (9.9 g P/kg dwb), CO2 (2 kg CO2/kg dwb)	Belt dryer	TE	Algae cake	0.51
	Calcium nitrate (10.9 g N/kg dwb), single superphosphate (2.4 g P/kg dwb), CO2 (1.8 kg CO2/kg dwb)	Belt dryer	TE	Algae cake	0.68
	Calcium nitrate (46 g N/kg dwb), single superphosphate (9.9 g P/kg dw), CO2 (2 kg CO2/kg dwb)	No	TE	Algae cake	0.96
	Calcium nitrate (10.9 g N/kg dwb), single superphosphate (2.4 g P/kg dwb), CO2 (1.8 kg CO2/kg dwb)	No	TE	Algae cake	1.34
Sawayama et al. (1999)	Nitrogen and phosphorous fertilizer, total of 2.37 MJ/kg oil	No	HL	No	2.22
	Nitrogen and phosphorous fertilizer, total of 20.13 MJ/kg oil	No	HL	No	0.64

Shirvani et al. (2011)	Ammonia (80 g N/kg dwb), superphosphate (20 g P/kg dwb), CO2 from flue gas	Yes	TE	Algae cake co-fired with coal	0.59
	Ammonia (80 g N/kg dwb), superphosphate (20 g P/kg dwb), CO2 from flue gas	Yes	TE	Algae cake combusted in biomass heating system	0.56
	Ammonia (80 g N/kg dwb), superphosphate (20 g P/kg dwb), CO2 from flue gas combustion.	Yes	TE	Algae cake used in CHP	0.46
	Ammonia (80 g N/kg dwb), superphosphate (20 g P/kg dwb), CO2 from flue gas.	Yes	TE	Algae cake as livestock feed	0.48
Stephenson et al. (2010)	Ammonium Nitrate and triple superphosphate	No	TE	Anaerobic digestion producing methane	1.54

In Table 4.2, we are able to see clearer what the different assumptions do to the NER results. The cases that are highlighted in red are those with at least one of these 3 assumptions: drying need, no co-products allocation, or highly processed CO_2 (pure or from carbon capture). As a result, all of them have NER significantly lower than 1. This is with the exception of one case from Sawayama et al. (1999) which although has it no co-product allocation, has an NER of 2.22 due to using hydrothermal liquefaction and having low fertilizer input. All of the other cases that are not highlighted, on the other hand, do not need drying and include co-products. They have an NER above one, or really close to 1 (above 0.95). These variations can be due to slight differences in amounts of fertilizer input and different co-products as listed in the table.

The results of LCA studies using PBRs and hybrid (PBRs and raceway pond) growth systems are also compared. The comparison is less clear because there are several PBR types as explained in Chapter 2. These different types lead to different methods of mixing, aeration, cooling, and light provision, which results in large variation of energy use (Jorquera., 2009). The PBR system is far less developed than raceway pond, therefore, even within the same type of PBR, variation in many parameters like size and mixing speed is significant. In addition to that, we still have differing assumptions in other parts of the cycle just like that in the raceway pond case. Figure 4.2 below shows the NER results from studies with PBRs (shown in blue) and hybrid growth systems (shown in green).

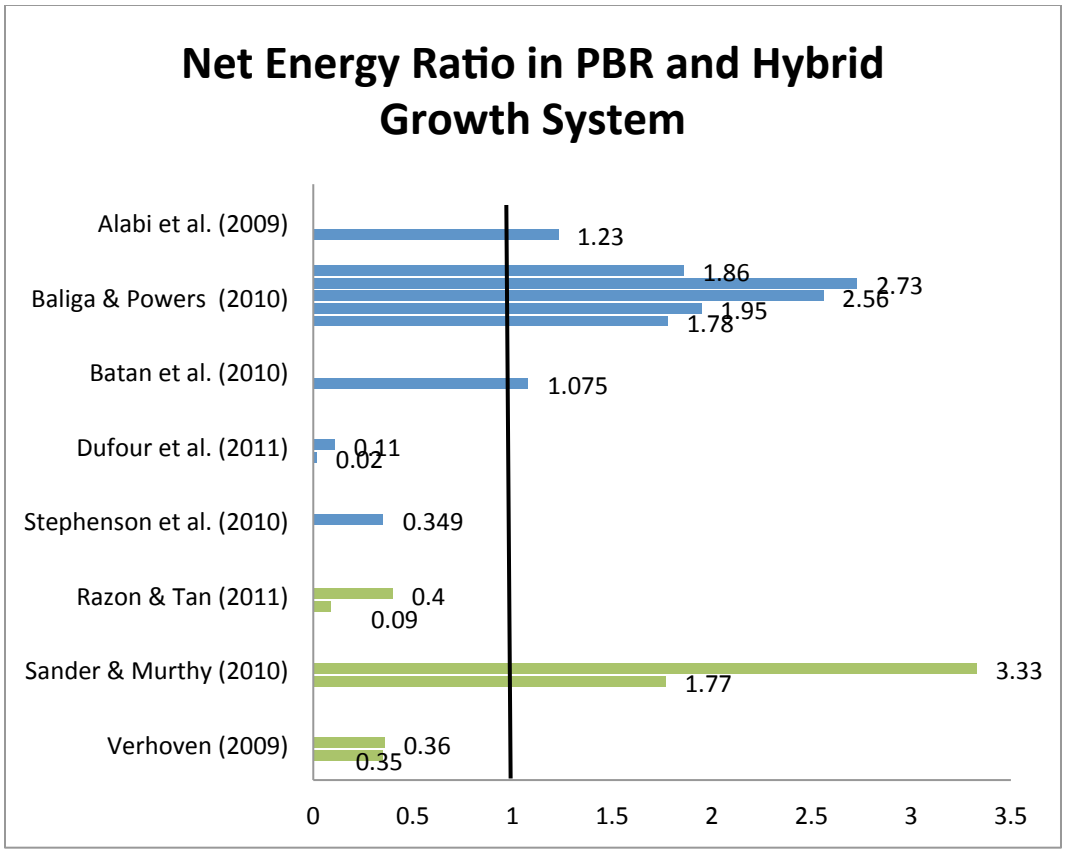

Figure 4.2: NER of microalgal biofuel with PBR (blue bars) and hybrid (green bars) growth systems

Amongst the five studies compared for NER in PBR growth system, Stephenson (2010) and Dufour (2010) reaches a conclusion of NER below 1. The highest energy burden in Stephenson's study lies on the electrical power needed in mixing, which amounts to about 9 times that of a raceway pond, and 5 times more than the value used in Alabi & Tampier's study. Stephenson uses an air-lift PBR which is analyzed in the study by Jorquera (2009) as much more energy consuming than a flat-panel PBR. However, Dufour (2011) has two cases comparing the use air-lift and flat-panel PBR, both also based on the data taken from Jorquera (2009), and in both cases, the NER values are below 1. These two studies conclude that using PBRs would not be energetically viable. Alabi (2009) and Batan (2010), unfortunately, do not specify the PBR type used and there is not much detail regarding the operation. Therefore, it is hard to find the parameter within the PBR design and operation that would lead to the lower energy input.

Baliga (2010), meanwhile, focuses the study on algal biodiesel production in cold climates which houses the PBR inside a greenhouse. Two locations are considered: Syracuse and Albany, and three heat sources are analyzed: natural gas heat, waste heat, and insulated design. With no natural lighting and full dependence on artificial light, and insulated design, the NER is promising at 1.86. When greenhouse heating is needed, using waste heat instead of natural gas would result in higher NER (2.73 for Albany and 2.56 for Syracuse using waste heat; 1.95 for Albany and 1.78 for Syracuse using natural gas), as predicted. Cultivation located in Albany has a higher NER than that in Syracuse due to higher temperature and solar irradiation that reduces the need for heating and artificial lighting. The highest energy burden in this study is in providing the heating and lighting, as well as dewatering.

Three studies are compared for the cultivation system using hybrid method. The studies from Verhoven (2009) and Razon (2011) conclude an NER that is below one while Sander & Murthy (2010) calculate an NER above one. The difference in NER result from Sander & Murthy might stem from the system boundary used in the assessment. For example, although CO_2 provision from flue gas is mentioned, the energy need for delivering CO_2 and sparging it to the culture is not included. Sander and Murthy also make an assumption that all the nutrients could be provided from wastewater, therefore eliminating the high embedded energy associated with providing fertilizers. Other than that, just as in the PBR case, it is hard to find parameters in the growth system that causes these differences in the results.

From the NER, Sander and Murthy conclude that dewatering process using a filter press would be more energetically viable than using a centrifuge (NER of 3.33 vs. 1.77). In Verhoven's study, it is found that there is very little difference between fuel production via direct transesterification and hydrotreatment. In Luiz's study, two species are compared, namely *Haematococcus pluvialis* (NER of 0.4) and *Nannochloropsis* (NER of 0.09), showing the importance of choosing the species that is not only producing a high yield of oil, but also easily harvested and processed.

Appendix A shows the details of the assumptions made in the LCA studies included in the graphs.

REFERENCES

Alabi, A. O., Tampier, M., & Bibeau, E. (2009). *Microalgae Technoligies and Processes for Biofuels/Bioenergy Production in British Columbia: Current Technology, Suitability, and Barriers to Implementation.* British Columbia.

Baliga, R., & Powers, S. E. (2010). Sustainable Algae Biodiesel Production in Cold Climates. *International Journal of Chemical Engineering*.

Batan, L., Quinn, J., Willson, B., & Bradley, T. (2010). Net Energy and Greenhouse Gas Emission Evaluation of Biodiesel Derived from Microalgae. *Environ. Sci. Technol., 44*, 7975–7980.

Campbell, P. K., Beer, T., & Batten, D. (2010). Life cycle assessment of biodiesel production from microalgae in ponds. *Bioresource Technology, 102*(1), 50-56.

Chambers, R. S., Herendeen, R. A., Joyce, J. J., & Penner, P. S. (1979). Gasohol: Does It or Doesn't It Produce Positive Net Energy? *Science, 206*(4420), 789-795.

Clarens, A. F., Nassau, H., Resurreccion, E. P., White, M. A., & Colosi, L. M. (2011). Environmental Impacts of Algae-Derived Biodiesel and Bioelectricity for Transportation. *Environ. Sci. Technol.*

Clarens, A. F., Resurreccion, E., White, M. A., & Colosi, L. M. (2010). Environmental Life Cycle Comparison of Algae to Other Bioenergy Feedstocks. *Environ. Sci. Technol., 44*, 1813 - 1819.

Dufour, J., Moreno, J., & Rodríguez, R. (2011). Life Cycle Assessment of Biodiesel Production from Microalgae Oil: Effect of Algae Species and Cultivation System. In M. Finkbeiner, *Towards Life Cycle Sustainability Management.*

Ehimen, E. A. (2010). Energy Balance of Microalgal-derived Biodiesel. *Energy Sources*.

Farrell, A. E., Plevin, R. J., Turner, B. T., Jones, A. D., O'Hare, M., & Kammen, D. M. (2006). Ethanol Can Contribute to Energy and Environmental Goals. *Science, 311*(5760), 506-508.

Jorquera, O., Kiperstok, A., Sales, E. A., Embiruçu, M., & Ghirardi, M. L. (2010). Comparative energy life-cycle analyses of microalgal biomass production in open ponds and photobioreactors. *Bioresource Technology, 101*, 1406–1413.

Lardon, L., Hlias, A., Sialve, B., Steyer, J.-P., & Bernard, O. (2009). Life-Cycle Assessment of Biodiesel Production from Microalgae. *Environmental Science and Technology*, 6475–6481.

Pfromm, P. H., Amanor-Boadu, V., & Nelson, R. (2011). Sustainability of algae derived biodiesel: A mass balance approach. *Bioresource Technology, 102*(2), 1185-1193.

Razon, L. F., & Tan, R. R. (2011). Net energy analysis of the production of biodiesel and biogas from the microalgae: Haematococcus pluvialis and Nannochloropsis. *Applied Energy*.

Sander, K., & Murthy, G. S. (2009). Life cycle analysis of algae biodiesel. *LCA FOR ENERGY SYSTEMS*.

Sawayama, S., Minowa, T., & Yokoyama, S.-Y. (1999). Possibility of renewable energy production and CO2 mitigation by thermochemical liquefaction of microalgae. *Biomass and Bioenergy, 17*, 33-39.

Sazdanoff, N. (2006). *Modeling and Simulation of the Algae to Biofuel Cycle.* Department of Mechanical Engineering, Ohio State University .

Shirvani, T., Yan, X., Inderwildi, O. R., Edwards, P. P., & King, D. A. (2011). Life cycle energy and greenhouse gas analysis for algae-derived biodiesel. *Energy & Environmental Science*.

Stephenson, A. L., Kazamia, E., Dennis, J. S., & Howe, C. J. (2010). Life-Cycle Assessment of Potential Algal Biodiesel Production in the United Kingdom:. *Energy Fuels*.

Sturm, B. S., & Lamer, S. L. (2011). An energy evaluation of coupling nutrient removal from wastewater with algal biomass production. *Applied Energy*.

Verhoven, J. (2009). *Life Cycle Assessment of Biodiesel and Feed Production form Microalgae: A review of the Cellana project.* Cellana Internal Report.

Yang, J., Xu, M., Zhang, X., Hu, Q., Sommerfeld, M., & Chen, Y. (2010). Life-cycle analysis on biodiesel production from microalgae: Water footprint and nutrients balance. *Bioresource Technology*.

5 LCA OF MICROALGAE: SCOPE DEFINITION & INVENTORY

5.1 Goals and Scope Definition

The main objectives of the work of this LCA study are to provide insights into the currently proposed production system of algal biofuel as a base case which is through dry hexane extraction and transesterification and compare it to other processes such as supercritical CO_2 extraction, hydrothermal liquefaction, and hydrotreating. A second goal is to analyze the uncertainties inherent in the parameters used in the calculation using Monte Carlo simulation.

The results to be compared include the net energy return of the processes and the environmental impacts of greenhouse gas emission. With these comparisons, we hope to provide an objective analysis for policy makers and stakeholders in the government, industry, and academia of the current state of algal biofuels and what it takes for this technology to reach sustainability.

5.1.1 Life Cycle Boundary & Stages

The life cycle boundary was drawn from the cultivation of algal biomass to combustion of the fuel. There were 5 main stages before combustion: cultivation, harvesting and dewatering to 20% dwb, oil extraction, biofuel production, and co-product allocation. In each of the stages, there were different process options to consider. Before the whole life cycle was assembled, each of the stage was analyzed independently of other stages to determine which process options would be the most energetically viable and environmentally friendly. Figure 5.1 shows the life cycle stages and the process options for each of them.

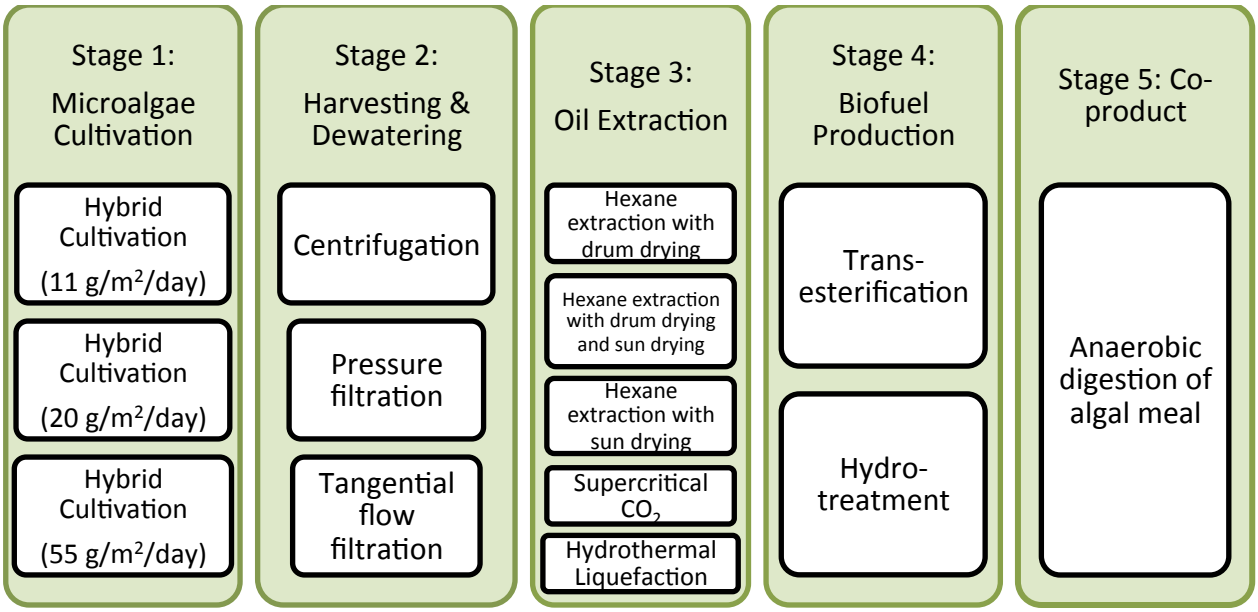

Figure 5.1: Stages in the life cycle and assumptions/process options considered in each stage

5.1.2 Functional Unit

The comparison of different industrial systems could only be achieved if they performed the same function. When a function had been defined, a unit of measure was chosen to compare the systems on the same quantitative basis. Before the full cycle was analyzed, each of the cycle stage was analyzed independently to compared processes or assumptions. Therefore, for each of the stage and also for the whole cycle, we would have different functional units. The functional units were:

Stage 1 (cultivation) : 1 kg of algal biomass

Stage 2 (dewatering to 20% dwb) : 1 kg of algal biomass

Stage 3 (oil extraction) : 1 kg of algal oil

Stage 4 (fuel conversion) : 1 MJ of fuel

Stage 5 (co-product allocation) : 1 kg of algal meal

Life cycle : 1 MJ of fuel

5.1.3 Plant Design & Operation

The design of an industrial-scale algal biofuel plant was based off a facility with an area of approximately 1210 ha. The facility would have 748 ponds and 3740 PBRs. The breakdown of area allocation is as follows:

Total plant area: 1210 ha
Raceway ponds: 860 ha
PBRs: 131 ha
Processing/access: 219 ha

The hybrid process based on Cellana's projected design was used as a basis of calculation. The algae were first cultivated in a horizontal tubular PBR which would serve as an inoculum for the cultivation in the raceway. This way a monoculture grew in the PBR without significant competition with other organism, and when transferred to an open pond, culture crashes could be minimized because the chosen species was already growing at a higher density than others. The reactor design specifications are listed in the Table 5.1 below.

Table 5.1: Design on PBR and raceway pond

	PBR	Raceway Pond
Unit Configuration	Length: 500 m Diameter: 0.4 m Total reactor volume: 63 m^3 Culture volume: 50 m^3	Pond length: 366 m Pond width: 32 m Pond depth: 0.15 m Culture volume: 1500 m^3
Main construction materials	Clear polyethylene bags for reactor body	Concrete blocks or bricks for walls and baffle, lined with reinforced polypropylene, cover for CO_2 sump
Supporting units	End assembly for nutrients, CO_2, mixing air, and water input	Paddlewheel, CO_2 sump of 1 m deep, water and nutrient inlet
Mixing	Air-lift mixing	Paddlewheel mixing
Footprint	350 m^2	11,500 m^2

The PBRs were designed as “U” shaped tubular plastic reactors with airlift-driven systems. The PBR was operated in a semi-batch mode where half of the PBR content was transferred to the pond in a gravity-driven flow. Water was added to refill the PBR and at the end of the next day the biomass would reach the same concentration and ready to be harvested again. During the cultivation time, the culture was constantly circulated and mixed using an air blower that provided a motive force of 20 scfm. Air was vented through a check valve to ensure only enough backpressure that would keep the PBR inflated. Seawater served as a nutrient medium and was run through a 5-micron filtration to remove sands, and an industrial UV sterilization to minimize any contamination. Concentrated nutrients and CO_2 were added to the seawater flow to allow for optimum growth condition. The end assembly was located at one end of the PBR and had a height of 1 m situated in a trench which houses the material refill and harvest headers. It was essentially an extension of the PBR loop tubing, consisting of a vertical U-shaped PVC tube of 1 m height where the compressed air entered in for air-lift mixing. All the PBRs were set side-by-side so that their end assembly could share a common trench.

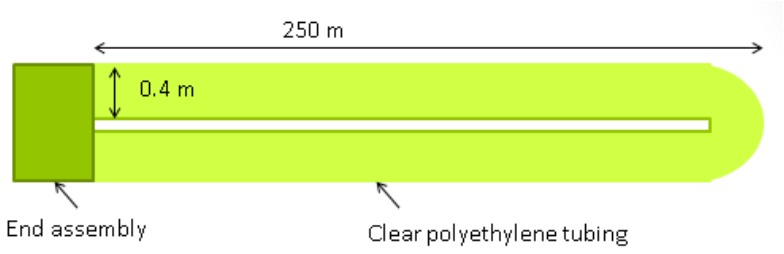

Figure 5.2: Schematic of PBR design

The raceway pond was operated in a batch mode with 4 days residence time. Through many trial runs done in Cellana’s pilot plant, it was concluded that when the residence time is higher than 4 days, a culture crash was likely to occur. On the morning of day 1, the pond was inoculated with the culture from PBR. Twenty PBRs were needed to supply the culture which amounted to a total of 500 m^3 in volume. Additional 1000 m^3 of seawater was supplied to fill up the pond, and the PBRs were also refilled. The nutrients were supplied on day 1 based on the need to grow at an optimum rate. Day 3 and day 4 cultivations were considered as nutrient deficient state, where the supply of nutrients except for CO_2 was stopped to allow the biomass to accumulate lipid. Figure 5.3 shows the design of the open pond in side view and top view.

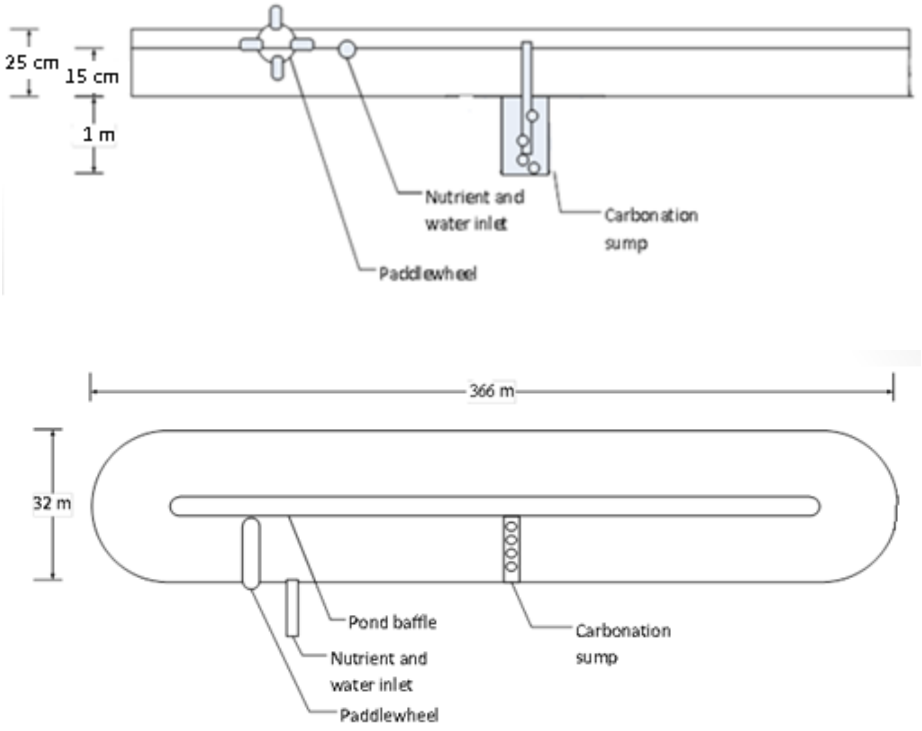

Figure 5.3: Schematic of open raceway pond design

Since the PBRs were operated in a semi-batch mode and half of the volume was harvested every day, they were able to inoculate three other ponds on the cultivation day 2, 3, and 4 of the first pond. This meant that the 20 PBRs were dedicated to supply a biomass culture for 4 ponds, making a total PBR to pond ratio of 5. The number of operation days is 360 days/year, making 90 harvests for every pond annually and 67,320 harvests for the whole facility.

5.2 Life Cycle Inventories

The SimaPro software allowed the modeling of complex life cycles and the running of detailed sensitivity or uncertainty analysis to determine the important parameter variability. Whenever possible, custom SimaPro process modules were developed to specify conditions needed for algal biodiesel production. Modules within the SimaPro model are designed to define material, energy, and environmental inputs and outputs that were required for a particular process within

the lifecycle. For example, a module may define the electricity, steam, and water need for algal oil extraction, required fertilizer for algae cultivation, or impacts of constructing the algae ponds.

The sections below describe the data inventories and assumptions used to define the case scenarios. The detailed data and calculation for this chapter can be referred to in Appendices.

5.2.1 Microalgae Cultivation

The module for microalgae cultivation was based on 1 growth cycle which includes 1 day cultivation in 20 PBRs and 4 days cultivation in the raceway pond. This calculation to grow the biomass from 1 growth cycle was then normalized to material and energy input and output to produce 1 kg of algal biomass. The picture below shows the input and output to the module.

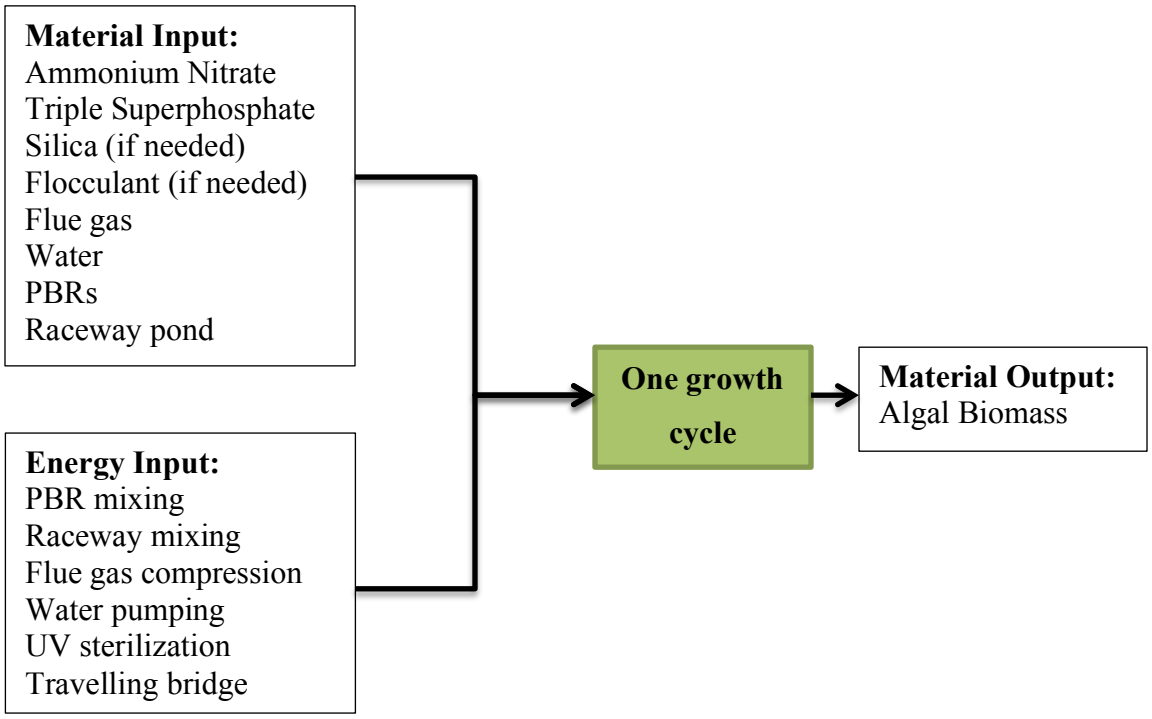

Figure 5.4: Input and output module for microalgae cultivation stage

5.2.1.1 Productivity and Composition

Productivity and composition of algae determines the amount biomass and oil that we obtain in the cultivation stage. Productivity of microalgae biomass was measured in g/m^2/day of ash free dry weight. The range for productivity was very large and uncertain. It was dependent on the species used, environmental conditions, solar insolation, provision of nutrient, presence of other organisms, and many other factors. The relationship of these factors to productivity was hard to analyze, therefore, the productivity value used in this study was not quantitatively correlated to any factor. The productivity is divided as:

Productivity 1: reported values of real outdoor ponds experiments

Productivity 2: predicted achievable values in the literature

Productivity 3: theoretical calculation of best case scenarios

By breaking down the productivity data into these three types, we would be able to assess the state of current production system, the results of mid-term (10 to 15 years) advancement, and the optimized production system. The 1 m^2 area basis in the productivity unit referred to the area of raceway pond only. Although in reality the PBR was also used for growth, it was treated as a supporting system that ensures sustained growth throughout the year with minimum contamination and not included in this area unit. This was done to be consistent the data sources which mostly refers solely to open pond and not a hybrid system.

A common problem with outdoor cultivation was the presence of contaminants that would result in culture crashes. The use of PBR which supplied a high concentration of microalgae and the use of UV sterilization for sea water before it was transferred to the PBRs helped minimize culture crashes (Huntley & Redalje, 2006). Culture crashes was assumed to happen 3% of the time, in which none of the biomass grown could be harvested.

The composition of algal cells was assumed to be of lipids, carbohydrate, and protein, with insignificant amount of nucleic acid. Lipid data from marine algae was collected and from experiments with nutrient replete condition during the end of growth period, the range of lipid content is determined. The remaining of the biomass is assumed to be protein and carbohydrate

with a mass ratio of 3 to 2 (Williams & Laurens, 2010). Table 5.2 summarizes the data inventory used for productivity and lipid content.

Table 5.2: Inventory for productivities and lipid content of microalgae

Parameter	Unit	Mode	Distribution	Min	Max
Productivity 1	$g/m^2/day$	11	Triangular	2.4	18
Productivity 2	$g/m^2/day$	20	Triangular	10	33
Productivity 3	$g/m^2/day$	55	Triangular	33	77
Culture crash	%	3	Triangular	0	6
Lipid content	%	34	Triangular	8.9	66

5.2.1.2 Nutrients

The productivity value would affect the amount of fertilizers and CO_2 needed for cultivation. The higher the productivity value, the more nitrogen, phosphorus, and CO_2 had to be supplied to support biomass growth.

The major nutrients needed for algae growth are nitrogen and phosphorus. In this analysis ammonium nitrate would be used as nitrogen source due to its wide availability and application, and the triple super phosphate was used as phosphorus source due to its large market share and relatively lower environmental impact. Both were the fertilizers used in KPF operation which have been proven to support algal growth very well. Silica may also be needed when diatoms were grown, which would be supplied in the form of sodium silicate (Royal Haskoning, 2009). These three nutrients were provided when the biomass was growing in PBRs and the first 2 days of raceway pond cultivation. In the last two days, they were nutrient deprived to stimulate accumulation of lipids. Therefore, we could assume that 100% of the nutrients provided would be assimilated into the biomass.

The supply of CO_2 comes from the flue gas of coal-fired power plant that was located adjacent to the facility. The amount of CO_2 in the flue gas was taken to be 15%wt. Because it was a material that would otherwise be emitted to the air, it was treated as a "free" input, which means that there were no financial and no energetic costs associated in producing it. A CO_2 supply sump was present directly downstream of the paddle wheel over the full width of one raceway (16 m). Water loaded with algal biomass flows downwards, was saturated with CO_2 in a counter

flow direction, passed underneath a vertical plate in the sump and flowed upwards again. By matching closely the downflow velocity with the average bubble rise velocity, long contact times were achieved, resulting in high CO_2 absorption efficiencies (Jackson & Lee, 2009). Table 5.3 below summarizes the inventories for nutrients and CO_2 needs.

Table 5.3: Inventories for nutrient and CO_2 inputs to the growth system

Parameter	Code	Units	Mode	Distribution	Min	Max
Nitrogen	N	g N/kg dwb	70	Triangular	26	90
Phosphorous	P	g P/kg dwb	6	Triangular	4.2	10
Silica	Si	g Si/ kg dwb	77.7	Triangular	74.35	81
Nutrient Absorption Efficiency		%	100	NA		
CO_2	CO2	kg/kg dwb	1.23	Triangular	1.75	1.88
CO_2 Absorption Efficiency	CO2_Eff	%	85	Uniform	70	95

The energy cost for CO_2 injection to the pond only included compression of flue gas. The assumption that the algae ponds were located next to the power plant eliminated energy consumption in gas transportation and since the distribution to individual ponds was predicted to be negligible, it was not included in the calculation also. The compression of gas from 1 to 2 bar absolute at the entrance of the facility was needed to have sufficient pressure for distribution to all the PBRs and ponds in the 1210 ha facility. The energy required for the adiabatic compression is calculated below, assuming ideal gas behaviour which is reasonable at these pressures.

$$W_c = \frac{C_p T_i}{\eta}\left[\left(\frac{P_o}{P_i}\right)^{\left(\frac{\gamma-1}{\gamma}\right)} - 1\right] = 77.3\ kJ/kg$$

Where W_c = compression energy (kJ/kg flue gas)

C_p = specific heat capacity of flue gas, 1 kJ/kg K

T_i = inlet temperature, 300 K

η = adiabatic compression efficiency, 85%

P_o = outlet pressure, 2 atm

P_i = inlet pressure, 1 atm

γ = constant, 1.4

Assuming CO_2 takes 15% of the flue gas by mass, the compression energy became 0.515 MJ/kg CO_2. The inventory for the air compressor and lubricant need was based off an air compression system listed in Eco-invent. For every 1 kg of CO_2 supplied, the input parameters listed in the Table 5.4 below were needed.

Table 5.4: Inventories for CO2 compression

Parameter	Unit	Amount	Distribution	GSD^2
Air compressor	piece	6.615×10^{-8}	Lognormal	3.06
Lubricating oil	kg	2.184×10^{-6}	Lognormal	1.24
Electricity	MJ	0.515	Lognormal	1.13

5.2.1.3 Mixing

The PBRs used airlift mixing to circulate the culture through the loop and at the same time stripping the oxygen from the broth to ensure optimum growth rate. The volumetric air needed for this circulation is 20 ft^3/min. For a day of PBR operation, 28,800 ft^3 of air would be supplied. The calculation for mixing energy need in the PBR was based on the following formula (Weissman & Goebel, 1987):

$$P_{mix,PBR} = \frac{0.039 V^{2.75} A\, t}{\eta d^{0.25}}$$

Where $P_{mix,PBR}$= Power need for mixing in PBR (W/m^2)

V = flow velocity, 30 cm/s

A = PBR footprint area, 350 m^2

t = operation hours per day, 20 hours

d = diameter, 40 cm

η = airlift pump efficiency, 60%

The PBRs were mixed 20 hours a day since it needed 2 hours to be filled up and 2 hours for half of their content to be transferred to the ponds. Based on this calculation, the mixing energy needed for 1 PBR is 1.97 kWh/day. In Cellana's internal report, this mixing energy was calculated to be 3.6 kWh/day. Since there were not many sources regarding this energy need, the value was set to range uniformly from 1.97 to 3.6 kWh/day.

In the pond, one paddlewheel per pond was used to keep the water moving at a velocity (V) of 25 cm/s (Q of 0.6 m^3/s) for 12 hours/day which covered the daylight period when photosynthesis happened and several hours before daybreak to ensure that biomass was well suspended when it received light in the morning.

Based on Green, Lundquist, and Oswald (1995), the mixing power needs are calculated as below:

$$P_{mix,raceway} = 9.8 \cdot Q \cdot \rho_{water} \cdot \Delta_{head} \cdot \eta$$

$$\Delta_{head} = \Delta_{head,frictional} + \Delta_{head,kinetic}$$

$$\Delta_{head,frictional} = \frac{V^2 . N^2 . L}{R^{4/3}}$$

$$\Delta_{head,kinetic} = \frac{K . V^2}{2g}$$

$$R = W_{channel} + 2D_{pond}$$

Table 5.5: Parameters for raceway mixing energy calculation

Parameter	Value	Unit	Explanation
$\mathbf{W_{channel}}$	16	m	Channel width/Half of pond width
$\mathbf{D_{pond}}$	0.15	m	Pond depth
$\mathbf{A_{channel}}$	2.4	m^2	Cross sectional area of channel

$P_{channel}$	32.3	m	Wetted perimeter of channel
R	0.0743	m	Hydraulic radius of pond channel
g	9.81	m/s^2	Gravitation
K	2		Kinetic loss for 180˚ bend
N	0.01		Manning's friction factor for plastic
L	366	m	Channel length
ρ_{water}	1030	kg/m^3	Density of water
η	0.4		Efficiency of paddlewheel

This calculation resulted in an energy input of 31.82 kWh/pond/day. Assumptions regarding energy need for paddlewheel operation seen in other studies varied in the power per paddlewheel, number of paddlewheels per hectare of pond, mixing speed, and the number of hours of operation per day. Based on the set of data taken from other studies as well as the above calculation, the value used in this analysis had a triangular distribution with a minimum of 6.23 kWh/pond/day and a maximum of 51.8 kWh/pond/day. The mixing energy requirement is tabulated below.

Table 5.6: Summary of energy need for PBR and raceway pond mixing

Parameter	Code	Unit	Amount	Distribution	Min	Max
PBR Mixing	PBR_Mix	kWh/day	2.79	Uniform	1.97	3.60
Raceway Mixing	R_Mix	kWh/day	31.82	Triangular	6.23	51.8

5.2.1.4 Water Supply and Transport

Daily water supply was needed to refill all 3740 PBRs, inoculate 187 open ponds, replace water loss through evaporation, and clean the 187 ponds after harvesting. The evaporation loss was set at 10% of pond volume or 150 m^3/pond/day and the water needed in clean up procedure was estimated to be 20% of pond volume which is 300 m^3/pond. The breakdown of daily water need for the whole facility is shown below.

Table 5.7: Daily water need for the whole facility

Usage	Amount	
3740 PBR refill	93,500	m^3
187 Pond fill	187,000	m^3
Replacing evaporation loss	112,200	m^3
187 Pond clean up	56,100	m^3
Total daily need	448,800	m^3

The calculation for water pumping (head of the pump and the total head loss) was based on Cellana's internal report explaining their vision for an industrial-scale production. The water supply was taken from seawater using a pipeline from offshore. Based on the daily need, 448,800 m^3 of water was transported from the sea to the intake canal in 20 hours. The required design capacity of the intake pumping station and transport pipes was therefore 22,400 m^3/h. Three pumps would be used to transport the seawater, each one delivering water was a rate of 7500 m^3/h or 2.083 m^3/s. The static head requirement of the pump was the maximum level difference between the intake reservoir canal and mean seal level (+0 m MSL) which was set at 5.2 m. The dynamic losses in the pipes with length of 5 m, and internal diameter of 1600 mm and losses in the pumping station and header was assumed to be 2 m. The friction loss over the pipe was calculated as follows, where λ is friction factor based on White-Colebrook with k of 3 mm.

$$H_{pipe} = \frac{\lambda L v^2}{D\ 2g} = 14.8 \text{ m}$$

With a total head loss of 22 m, density of seawater of 1030 kg/m3, and pump efficiency of 0.8, the power required by the three pumps could be calculated as follows.

$$P = \frac{3\rho g Q H}{1000\eta} = 1736.4 \text{ kW}$$

The daily energy need for water transport from the sea to storage canal was therefore 34,728 kWh/day, which translated to 0.07738 kWh/m^3.

From this storage canals, the seawater was distributed to the PBRs and ponds. The storage canal and the PBRs were designed to be located at a higher ground than the ponds. Therefore, the filling of the ponds as well as the water transport from the pond back to the sea was always by gravitation. Before the seawater fills up the PBRs, they passed through 5 micron UV sterilization unit and sand filter to ensure the water was clean and contamination was minimized. The sterilization unit and filter required energy of 0.04 kWh/m^3 seawater passed. The loss of energy head in the distribution system between the canal and PBRs had been calculated to be 10.5 m, which already included 0.5 m over the check valve, 5 m over the sand filters, and 1 m over the control valve. With a total head of 10.5 m, filling the PBRs with 93,400 m3 over a period of 4 hours required a total pump power of:

$$P = \frac{\rho g Q H}{1000\eta} = 983.1 \text{ kW}$$

This resulted in an energy requirement of 0.0421 kWh/m^3.

On the fourth day of the growth period in the open pond, the biomass was ready for harvesting. The paddlewheel was switched off to let the biomass settle on the bottom for several hours to a concentration of about 2.5%wt and the supernatant was transported back to the sea by gravity. The algal slurry that was left behind is piped to a centrifuge which concentrated it further to 20%wt. The volumetric rate of algal slurry to be transported per day depended on the productivity that was achieved in the growth period and would be calculated as a function of that. The head requirement of the pump was calculated to be 90 m with the assumption that the viscosity of the algal slurry would be 10 times that of water. This assumption was not well tested and should be investigated further in the future to obtain a more accurate calculation of pumping energy need. Taking a productivity of 25 g/m2/day (Q of 7293 m^3 algal slurry/day) for a calculation example, the pumping power needed was:

$$P = \frac{\rho g Q H}{1000\eta} = 1315.9 \text{ kW}$$

The energy needed to pump the slurry for 2 hours per day was 0.361 kWh/m^3. The summary for energetic costs related to transfer of water and slurry is summarized in Table 5.8.

Table 5.8: Summary of energy need for water transport and treatment

Parameters	Code	Unit	Amount
Pumping , sea to canal	Sea_Canal	kWh/m^3	0.0774
Pumping, canal to PBRs	Canal_PBR	kWh/m^3	0.0421
Pumping, canal to ponds	Canal_Pond		(By gravitation)
UV sterilization	UV	kWh/m^3	0.04
Supernatant from pond back to sea	Pond_Sea		(By gravitation)
Pumping, pond to dewatering*	Pond_DW	kWh/m^3	0.361

**Pumping energy will vary depending on the biomass productivity which will affect the amount of slurry to be pumped over 2 hours from the pond to the centrifuge. Productivity of 25 g/m2/day is used for the value listed in the table.*

5.2.1.5 Construction

There were two main components of the PBR. The first was the low-density polyethylene (LDPE) sleeve bag and the second was the polyvinyl chloride (PVC) fitting at the end of the bag. The PVC fitting was where the end assembly was constructed to provide air circulation input, water, nutrients, and CO_2 input, and to harvest the culture. The lifespan of LDPE was set at 2 years due to effect of UV radiation, temperature, thermal cycling, and daily contact with rigid surfaces, biomass culture, and chemicals. The PVC fitting lifespan was set at 10 years. In order to produce 1 PBR, 1,040 kg of LDPE and 14.07 kg of PVC was needed.

The open pond wall and mid divider are constructed from bricks with total length of 1,098 m per pond. With a width of 0.1 m and a height of 0.25 m, the volume of bricks needed would be 12.5 m^3. The pond had to be lined to reduce seeping of water and contamination. The liner material chosen was reinforced polypropylene (RPP) which was tough, flexible, and has good resistance to fatigue. Each pond would need 1.25 ha of RPP with a thickness of 1 mm which resulted to a mass of 11,825 kg. Cover over the CO_2 sump was also needed to increase CO_2 gas dissolution into the culture and ensure lower rate of degassing from the pond. Since the CO_2 sump spanned across half of the pond width, the cover of a same width was needed. The life time of the liner, cover, and bricks were 20 years.

5.2.1.6 *Harvesting*

In-pond sedimentation was used as the first step in harvesting. When a diatom was used, it was able to sink at a fast rate of about 0.5 to 1 hour. Other species types might not be able to sink in as well and flocculant had to be added. In this study, the flocculant added was in the form of aluminum sulfate (alum). The ideal case would be when a non-diatom species was able to auto-flocculate, eliminating the need of adding silica and flocculant. In-pond sedimentation would reduce the space and capital cost needed to have a separate basin.

When the biomass had settled, the water above it was drawn out of the pond and transported back to the sea. The remaining algal slurry would have a concentration of 1% to 2.5% and would be taken out for further dewatering. While manual shoveling worked well to ensure that all of the slurry could be taken out, in a large industrial setting this process should be automated. A travelling bridge would be used to sweep through the bottom of the pond to obtain the biomass. The sedimentation process would have an efficiency ranging in a triangular distribution of 90% to 100%. Table 5.9 shows the parameter values pertinent to in pond sedimentation.

Table 5.9: Inventory for harvesting via in-pond sedimentation

Parameter	Code	Units	Mode	Distribution	Min	Max
Sedimentation Efficiency	Sed_eff	%	95	Triangular	90	100
Sedimentation Concentration	Sed_conc	%	1.5	Triangular	1	2.5
Alum	Alum	g/m^3	145	Triangular	80	250

5.2.1.7 *Life Cycle Inventory for 1 time Harvest*

To obtain a single harvest worth of biomass, 1 day of 20 PBR units operation and 4 days of a raceway pond operation were needed. Table 5.10 below summarizes the input and output material as well as energy to obtain algal biomass from 1 growth cycle. The values that are given in terms of formulas indicate the use of some parameters in the form of a distribution.

Table 5.10: Inventories for producing 1 time harvest worth of biomass

Output (Abbr.)	Unit	Value	Note
Algal Biomass (AB)	g	Productivity * 4 days * 10,000 m^2 * (1-Culture Crash)	Amount of algal biomass from 1 growth cycle
Harvested Biomass (HB)	g	AB * Sed_eff	Amount of biomass harvested
Algal Lipid (AL)	g	Lipid Content * HB	Amount of lipid in algal biomass from 1 growth cycle
Material Input		**Value**	**Note**
Seawater	m^3	2310	Amount of water to fill half of 20 PBRs, open pond, replace 4 days of evaporated water, and pond clean up.
PBR Construction			
PVC Pipe	kg	0.005617	End assembly of PBR, for 5 PBRs (20 PBRs used to fill 4 raceway ponds), 2 years life time.
Low-density polypropylene	kg	14.25	Plastic tube of PBR, for 5 PBRs (20 PBRs used to fill 4 raceway ponds), 10 years life time.
Raceway Construction			
PVC film	kg	6.4	Liner and sump cover of 1 pond, with 20 years life time.
Brick	kg	57.55	Pond walls and mid divider, with 20 years life time
Ammonium Nitrate	g N	(AB/1000) * N	Amount of nitrogen fertilizer
Triple Superphosphate	g P_2O_5	(AB/1000) * P* 141.9/31	Amount of phosphorus fertilizer. (141.9/31) is conversion from P to P_2O_5
Sodium Silicate	g Si	(AB/1000) * Si* 122/28	Amount of silica fertilizer. (122/28) is conversion from Si to sodium silicate
CO_2	g CO_2	AB * CO_2 / CO_2_Eff	Amount of CO_2
Alum	g Alum	Alum*1500	Amount of alum in 1500 m3 pond
Travelling Bridge	kWh	1.25	Energy needed to operated travelling bridge
Energy Input		**Value**	**Note**
PBR Mixing	kWh	PBR_Mix* 20	1 day mixing energy for 20 PBR
Raceway Mixing	kWh	R_Mix * 4	4 day mixing energy for 1 raceway pond
Flue gas Compression	kWh	CO_2 /1000 * Compression	Compression material and energy input as listed in table 5.4
Water Transport, Sea to Canal Storage	kWh	Sea_Canal * 2310	Pumping energy to transport water from sea to canal storage
Water Transport, Canal to PBR	kWh	Canal_PBR * 500	Pumping energy to transport water from canal to 20 PBRs storage
Sterilization and Filtration	kWh	UV * 500	Energy needed to clean seawater before it enters PBRs.

The sources of inventory data included in the algal cultivation stage is presented in Appendix B.

5.2.2 Dewatering and Drying

After in-pond sedimentation, the algal slurry was transported from the pond to the dewatering station that would concentrate it further to 20 %wt of dry weight biomass (dwb). There were three dewatering options that we considered: decanter centrifuge, pressure filtration, and tangential flow filtration.

After the dewatering to 20% dwb, it was ready for further processing if SC-CO_2 oil extraction or hydrothermal liquefaction processes are used. If the hexane extraction was used, the biomass had to be further dried to a concentration of 90%wt. Drying up to that level using thermal drying alone took a lot of energy which would not be economically nor energetically feasible for a sustainable industrial process. Therefore, as much as possible, it should be done by sun drying, in which the algal paste was spread on a drying bed for 1 day at a thickness of 1 cm. We assumed three kinds of drying: thermal drying by drum dryer, sun drying, or a combination of the two (50% of the time by drum drying, 50% remaining by sun drying). Tables 5.11 and 5.12 below list parameters used in calculation and the input/output inventories for harvesting, dewatering, and drying process for the amount of biomass in 1 harvest.

Table 5.11: Parameters for harvesting, dewatering, and drying processes

Parameter	Code	Unit	Amount	Distribution	Min	Max	SDev
Dewatering Energy	DW_E						
Centrifugation	Cent	kWh/m^3	8	Triangular	2.5	9.88	
Filter Press	Fpress	kWh/m^3	0.88				
Tangential Flow Filtration	Tflow	kWh/m^3	2.06				
Drying Energy	Dry_E						
100% Drum Dryer	DD	MJ/kg H_2O	5	Normal			0.36
100% Sun Drying	SD	MJ/kg H_2O	0				
Combination	DD_SD	MJ/kg H_2O	0.5*Dry_DD				

Table 5.12: Inventories for harvesting, dewatering, and drying processes

Output	Unit	Amount	Note
Water Transport, Pond to Dewatering Unit	kWh	HB * (100-Sed_conc)/Sed_conc / 10^6 * Pond_DW	Pumping energy to transport algae sludge from pond to dewatering.
Dewatering	kWh	HB * (100-Sed_conc)/Sed_conc / 10^6 * DW_E	Dewatering energy to concentrate to 20% dwb
Drying	MJ	Dry_E * (4-0.11) * HB/1000	Drying energy from 20% to 90% dwb

5.2.3 Algal Oil Extraction

The modeling of extraction processes were done by two other students in our group: Michael J. Franke and Michael Johnson.

5.2.3.1 Hexane Extraction

Hexane would not dissolve all lipids in the algae biomass. It was uncertain how efficient the process would be, so the extraction efficiency was modeled as variable with a triangular distribution. The minimum value for efficiency is 80%, the lowest efficiency achieved with the SRS Energy process (Archibald, 2011). The maximum value was 96%, the efficiency at which hexane extracts oil from soybeans (Sheehan *et al,* 1998). The mode was 90%, the efficiency SRS Energy expected to obtain with its second generation technology (Archibald, 2011).

Inputs for the process included construction materials, tap water, make-up hexane, electricity from fuel oil, heat from fuel oil, and phosphoric acid used to "degum" the oil, making it fit for transport and storage (Eshratabadi et al., 2008). Input values for construction materials (bundled together under the title of "Oil Mill" in ecoinvent), tap water, make-up hexane, and phosphoric acid were taken from Emmenegger et al (2007) and multiplied by a factor of 1/0.195, the reciprocal of the mass fraction of lipids in soybeans, to convert the basis from 1 kg oil to 1 kg biomass and by another factor of 1/0.345, the reciprocal of Emmenegger et al's economic allocation factor to oil, to undo ecoinvent's 34.5%/65.5% split between allocation of inputs to oil and residual biomass, thus putting all allocation on the algae oil. The mass balance on hexane was closed by defining a hexane emission to the atmosphere equal to the hexane input.

Table 5.13 and Table 5.14 summarize electricity and heat use, respectively, per kg oil in biomass. The data in the tables were based on a study by Sheehan et al (1998). Their numbers were multiplied by a factor of 1/0.195, the reciprocal of the mass fraction of lipids in soybeans, to convert the basis from kg biomass to kg oil in biomass.

Table 5.13: Summary of electricity use (Sheehan et al, 1998)

Process Unit	Electricity Use (Wh/kg oil)
Counter-Current Extractor	18.46
Hexane Recovery from Oil	1.95
Residual Biomass Processing	102.4
Total	**122.8**

Table 5.14: Summary of heat use (Sheehan et al, 1998)

Process Unit	Heat Use (MJ/kg oil)
Hexane Recovery from Oil	0.4469
Residual Biomass Processing	2.8572
Total	**3.3041**

For stochastic studies, all inputs were assumed to have the same distribution shape (i.e. lognormal) and geometric standard deviation found in Emmenegger *et al* (2007). Table 5.15 gives the complete inventory for hexane extraction.

Table 5.15: Inventories for hexane extraction (Emmenegger et al, 2007). Basis is 1 kg of oil in algae biomass.

Input/Output	Amount	Unit	Distribution	GSD^2
From Technosphere				
Oil Mill	4.6592E-09	p	Lognormal	3.284
Tap Water	2.33831	kg	Lognormal	1.1668
Hexane	0.05833	kg	Lognormal	1.1668
Phosphoric Acid	0.0045959	kg	Lognormal	1.0752
Electricity	0.12281	kWh	Lognormal	1.1668
Heat	3.3041	MJ	Lognormal	1.1668
To Atmosphere				
Hexane	0.05833	kg	Lognormal	1.5046

5.2.3.2 *Supercritical Fluid Extraction with CO_2 ($SCCO_2$)*

As in hexane extraction, $SCCO_2$ does not extract all lipids. However, laboratory experiments expect that the extraction efficiency should be higher than that of hexane extraction (Halim *et al*., 2011 and Mendes *et al.,* 1995). Halim *et al* (2011) report the lowest extraction efficiency, 81%, so that is defined as the minimum value. Sahena *et al* (2009) report a range of values from 83% to 100%, and Demirbas and Demirbas (2011) report that $SCCO_2$ can extract nearly 100% of the lipids, so 100% is defined as the maximum value. Given Halim *et al* (2011) and Mendes *et al's* (1995) expectations that $SCCO_2$ should be more efficient than hexane extraction, it is assumed that the best value for the mode is 90%, equivalent to the mode of the distribution of hexane extraction efficiency.

The basis for the $SCCO_2$ inventory was 1 kg of oil in the algae biomass. No public data existed for industrial-scale algae oil $SCCO_2$, so soybean oil $SCCO_2$ was used as a model. Li *et al* (2006) reported a solvent-to-solute weight ratio of 29.2:1, and McHugh and Krukonis (1986) reported a value of 99:1. Therefore, a uniform distribution using these two ratio values was used.

Inputs to the $SCCO_2$ process included electricity from fuel oil, pure CO_2, and tap water. CO_2 released to the atmosphere are the only non-product output. CO_2 losses, and hence CO_2 make-up, were assumed to be 1 wt% of CO_2 used in a batch. Compression energy was 0.01163 kWh/kg CO_2 when assuming a compressor efficiency of 70% (McHugh and Krukonis 1986). Electricity and tap water make-up were also required for post-compression cooling. The heat duty of the cooler was equal to the enthalpy rise across the compressor (i.e. compressor electricity input). Assuming cooling water temperature rised 10 °C, there were 158.4 kJ of cooling duty in a gallon of cooling water. Therefore, 0.2637 gal of cooling water was needed per kg of CO_2. Tap water make-up to the cooling water system was assumed to be 1% of cooling water use. Also, it was assumed 1.5 Wh was used per gallon of cooling water circulated (Towler and Sinnott, 2008). The resulting inventory is shown in Table 5.16.

Table 5.16: Inventories for SCCO2. Basis is 1 kg of oil in algae biomass.

Input	Amount	Unit	Distribution	Min	Max
From Technosphere					

CO_2	0.641	kg	Uniform	0.292	0.99
Electricity, Compression	0.746	kWh	Uniform	0.340	1.151
Electricity, Cooling Water	0.025	kWh	Uniform	0.0116	0.0392
Tap Water	0.0640	kg	Uniform	0.029	0.099
To Atmosphere					
CO2	0.641	kg	Uniform	0.292	0.99

5.2.3.3 Hydrothermal Liquefaction

Michael Johnson used his experimental results to model hydrothermal liquefaction reaction for microalgae. In the end of liquefaction process, the products phase separated into three parts: oil, water, and solids. 90% of the lipid content would end up in the oil phase, together with small portions of liquefied proteins and carbohydrate.

The inputs to the process were electricity to run pumps, cooling of the process, and light heating oil to heat the streams. The Aspen flowsheet was synthesized to minimize input energy. The biomass mixture entered the process and was pressurized in two stages to 200 bar. The pressurized mixture was preheated in a heat exchanger with the reaction effluent. The remaining heat was supplied by a boiler to reach the reaction temperature. After cooling, the effluent was depressurized to 20 bar and flashed to separate the oil from water in a separation drum. The heat exchanger used an assumed 300 W/m^2 K transfer coefficient and achieved a temperature approach of 15°C. The cooling needs for the effluent were ignored, as the heat exchanger cooled to a suitable temperature.

Table 5.17: Inventory to produce 1 kg of oil phase from hydrothermal liquefaction

Input	Amount	Unit	Distribution	Min	Max
From Technosphere					
Electricity	0.743	MJ	Lognormal	0.340	1.151
Heat	0.248	MJ	Lognormal	0.0116	0.0392
Methanol Plant	3.72×10^{-11}	piece			

5.2.4 Biofuel Processing

5.2.4.1 Transesterification

The basis for the transesterification LCI was 1 kg of biodiesel output. Each kg of biodiesel had a HHV of 38 MJ (Kalnes *et al.,* 2009). The transesterification process used for oil extracted from hexane and $SCCO_2$ extraction would be different from that of hydrothermal liquefaction. This was because the oil compositions obtained from the processes are significantly different.

In the transesterification process following hexane or $SCCO_2$ extraction, 0.109 kg of glycerol was produced per kg of biodiesel produced (Emmenegger *et al.,* 2007). Inputs included algae oil, methanol, electricity from fuel oil, heat from fuel oil, construction materials, tap water, phosphoric acid, potassium hydroxide, and sulfuric acid. Input values for construction materials (bundled together under the title of "Veggie Oil Esterification Plant" in Ecoinvent), algae oil, methanol, electricity, heat, tap water, and phosphoric acid are taken from the "Veggie Oil Methyl Ester at Esterification Plant/FR" inventory from Ecoinvent (Emmenegger et al, 2007) and multiplied by a factor of 1/0.871, the reciprocal of Emmenegger's economic allocation factor to biodiesel, to undo Ecoinvent's 87.1%/12.9% split between allocation of inputs to biodiesel and glycerol, thus putting all allocation on biodiesel. It is important to note that the vegetable oil input in the Ecoinvent inventory is replaced with an algae oil input of the same mass. It was also assumed that the pretreatment process did not alter the ratio of construction materials, algae oil, methanol, electricity, heat, tap water, and phosphoric acid input to biodiesel output. Potassium hydroxide and sulfuric acid requirements were calculated in Appendix C. The inventory for transesterification is shown in Table 5.18.

Table 5.18: Inventory for transesterification following hexane or SCCO2 extraction to produce 1 kg of biodiesel

Input	Amount	Unit	Distribution	GSD^2
From Technosphere				
Algae oil	1.0276	kg	Lognormal	1.209
Methanol	0.11355	kg	Lognormal	1.0722
Electricity	0.042280	kWh	Lognormal	1.0722
Heat	0.92344	MJ	Lognormal	1.0722
Veggie Oil Esterification Plant	9.34E-10	p	Lognormal	3.046
Tap Water	0.027313	kg	Lognormal	1.5642
Phosphoric Acid	0.0046008	kg	Lognormal	1.0722
Potassium Hydroxide	0.012821	kg	Lognormal	1.0722
Sulfuric Acid	0.001285	kg	Lognormal	1.0722

Unlike the oil from hexane or $SCCO_2$ extraction, the hydrothermally reacted oil phase was mostly free fatty acids, so the alkaline approach was not possible. If alkaline approach was used the free fatty acids would saponify to soaps with the alkaline and then remade to free fatty acids when FAME was neutralized after transesterification. Therefore, after hydrothermal liquefaction, an acid catalyzed transesterification must be used.

Transesterification was performed with 10 %wt sulfuric acid to fatty acids and 10 times the stoichiometric ratio of methanol. The reaction was modeled after the pretreatment approach of Canakci and Van Gerpen (2003), for one hour at 60°C. The conversion for this reaction was modeled with a mode of 0.8 and a range of 0.7 to 0.95. A settling tank allowed the water resulting from the esterification to separate out from the oil phase. The separation was modeled by 95% of the water, methanol, and sulfuric acid in the water phase, with 0.5% of the FAME and 1% of the free fatty acids.

Table 5.19: Inventory for transesterification following hydrothermal liquefaction to produce 1 kg of biodiesel

Input	Unit	Amount	Distribution	SD	GSD^2
From Technosphere					
Algae oil	kg	1.01			
Methanol	kg	0.149	Normal	0.0055	
Sulfuric Acid	kg	0.0556	Normal	0.0038	
Lime	kg	0.0318	Normal	0.0022	
Heat	MJ	3.68	Lognormal		1.081
Cooling energy	MJ	3.305	Lognormal		1.081
Veggie Oil Esterification Plant	p	9.34E-10	Lognormal		3.046

5.2.4.2 Hydrotreating

The first task in determining material inputs and outputs from the hydrotreating process was to simulate the hydrotreating reaction itself. The first step was to determine what percentage of the lipids will be deoxygenated through hydrodeoxygenation. Given the uncertainty in this parameter, it was simulated as a stochastic variable within a triangular distribution. Marker *et al* (2005) suggested that the expected reaction conditions inside a stand-alone unit would cause a 25/75 split between the hydrodeoxygenation path and deoxygenation; therefore, 25% hydrodeoxygenation was considered the mode of the distribution. Marker *et al* stated that hydrodeoxygenation was less favorable than the other two reaction paths; therefore the goal was to eliminate its occurrence completely. Because of this, a minimum value of the distribution was as 0% hydrodeoxygenation. Huber *et al* (2007) found that a 50/50 split between hydrodeoxygenation and the other two pathways occured at 450 °C. Given a stand-alone reactor temperature of 325 °C (Marker *et al.,* 2005), the reaction could be safely assumed to be less than 50% hydrodeoxygenation. Therefore, 50% hydrodeoxygenation was defined as the maximum of the distribution.

The next step was to calculate the hydrogen needed to saturate double bonds, break TAG backbones, and deoxygenate the lipids. These calculations were performed in Excel and in a Monte Carlo simulation via MATLAB detailed in Appendix D. Details for heat and electricity inputs can be found in Appendix E.

The calculated material and energy balances for the basis of 1 kg of algae oil processed are given in the LCI in Table 5.20. Also included are construction materials used per kg of algae oil processed (Hsu, 2011) as bundled together under "Refinery/RER/I with US electricity U" in SimaPro.

Table 5.20: LCI for hydrotreating following hexane and SCCO2 extractions. Basis is 1 kg of algae oil processed.
1: GSD^2 is the square of the geometric standard deviation.
2: Formula given in Appendix D.
3: Formula given in Appendix E.

Input	Unit	Amount	Distribution	Min	Max
From Technosphere					
Refinery/RER/I with US electricity U	p	4.7864E-11	Lognormal	GSD^2 = 3.046[1]	
Hydrogen, Naptha Reforming, Reactor Consumption	kg	0.018	Triangular	0.013	0.024
Hydrogen, Naptha Reforming, CO Conversion	kg	-0.0046	Triangular	-0.0030	-0.0063
Electricity, Make-Up H2 Compressor	kWh	B[3]	Formula		
Electricity, Recycle H2 Compressor	kWh	C[3]	Formula		
Electricity, Tail Gas Compressor	kWh	D[3]	Formula		
Electricity, Tail Gas Compressor Cooling Water	kWh	E[3]	Formula		
Electricity, PSA Inlet Cooling Water	kWh	F[3]	Formula		
Electricity, Sour Water Treatment	kWh	G[3]	Formula		
Electricity, Algae Oil Pump	kWh	H[3]	Formula		
Heat, Hydrotreater	MJ	I[3]	Formula		
Heat, Sour Water Stripper	MJ	0.023	Triangular	0.013	0.034
Heat, Side Stripper	MJ	J[3]	Formula		
Heat, Reformer Steam	MJ	0.0934	Triangular	0.0613	0.1264
Heat, Make-Up H2	MJ	K[3]	Formula		
Heat, Recycle H2	MJ	L[3]	Formula		
To Atmosphere					
CO2, from decarboxylation	kg	0.122	Triangular	0.080	0.165
CO2, from conversion of CO	kg	0.122	Triangular	0.080	0.165
Output					
Propane	kg	0.0544	Triangular	0.0534	0.0554
Gasoline	kg	0.0250	Triangular	0	0.07
Diesel	kg	A[2]	Formula		

Hydrotreatment of oil phase from the hydrothermal liquefaction iss similar to the one described above for oil from hexane and $SCCO_2$ extraction. The main difference is that since the oil phase from hydrothermal liquefaction contained more sulfur, nitrogen, and oxygen, more hydrogen was needed to remove these impurities. Below is the summary of inventory for hydrotreating process that follows hydrothermal liquefaction for 1 kg of algal oil that enters the process.

Table 5.21: Inventory for hydrotreating following hydrothermal liquefaction to process 1 kg of algal oil

Input	Unit	Amount	Distribution	Min	Max	SD	GSD^2
From Technosphere							
Algae oil	kg	1					
Electricity	MJ	3.158	Lognormal				1.6
Heat (sour stripper and reformer)	MJ	0.00156	Triangular	0.00131	0.00178		
Heat (hydrotreater)		-0.7765	Normal			0.06	
Hydrogen	kg	0.03065	Lognormal				1.26
Refinery	piece	4.786×10^{-11}	Lognormal				3.046
Output							
Propane	kg	0.0044	Lognormal				1.076
Gasoline	kg	0.0252	Lognormal				1.784
Diesel	kg	0.645	Lognormal				1.106
Methane	kg	0.00964	Lognormal				2.97

In comparing greenhouse gas emissions, due to its large oxygen content, FAME has a lower energy content than green diesel and therefore, more carbon emissions will be resulted from the combustion of 1 MJ FAME than 1 MJ green diesel. This difference was taken into account by calculating the CO_2 that would be release in combustion It is calculated in Appendix G that combusting 1 MJ of FAME released 0.073 kg CO_2, whereas 1 MJ of the product mix (propane, gasoline, and diesel) released 0.070 kg CO_2.

5.2.5 Co-product Allocation

The main co-product in producing algal biofuel is the residual biomass that was left after oil had been extracted. We assumed that the remaining biomass contained protein and carbohydrate in a 3 to 2 ratio. Therefore, in a 100 g of algae, assuming 34% of oil content (mode of the oil content distribution), 39.6 g is protein, and 26.4 g is carbohydrate. The products of the digestion were methane and carbon dioxide. Not all of the biomass would be gasified; therefore, in the end of anaerobic digestion there would be remaining biomass contents either in solid or liquid phase which could be recycled as fertilizer.

Using a mass balance and the molecular compositions for all components, the moles of each element could be determined. Based on Michael Johnson's experiments with model algae feedstock, the elemental composition of protein and carbohydrate after oil extraction is as shown in Table 5.22.

Table 5.22: Elemental composition of protein and carbohydrate left after oil extraction

	Protein (wt%)	Carbohydrate (wt%)	Amount from 64 g algal meal (mol)
C	0.5342	0.4494	2.75
H	0.0688	0.0617	4.32
O	0.2127	0.4889	1.33
N	0.1667		0.47

The mols of each element (based on 64 g residual algal meal) became the coefficients for Symons and Buswell's (1933) method of stoichiometry for the relative amounts of each compound shown below.

$$C_aH_bO_cN_d + \left(\frac{4a-b-2c-3d}{4}\right)H_2O$$
$$\rightarrow \quad \left(\frac{4a-b-2c-3d}{8}\right)CH_4 + \left(\frac{4a-b-2c+3d}{8}\right)CO_2 \quad + d\,NH_3 \qquad (Equation\ 2)$$

Based on this theoretical calculation the carbon split 49% ± 0.26% to carbon dioxide and the remainder became methane. As ammonia was the only nitrogen-containing product, protein

nitrogen converted to ammonia. Recovery of the gases was performed by bubbling through a slightly compressed water column. Carbon dioxide and ammonia would absorb into the water and could be recycled to the culture. Methane was almost completely insoluble, and a 97% pure gas stream could be recovered following the assumptions for Collet et al. (2011).

Theoretical maximum yields were found using a formula by Angelidaki and Sanders (2004). The proximate components each had a yield associated with it. Protein had a methane yield of 0.851 m^3/kg and carbohydrates had a methane yield of 0.415 m^3/kg. Based on this, the theoretical maximum biogas to be obtained would be 0.677 m^3/kg algal meal. Based on experiment results reported in the studies below, an inventory for real yield from algal meal was constructed. A triangular distribution with a mode of 0.3 m3 CH/kg algal meal and a minimum and maximum of 0.25 and 0.35 m3/kg algal meal were used. With a density of 0.668 kg/m3 at STP conditions, the mode of this yield would be 0.2004 kg CH_4/kg algal meal.

Table 5.23: Experimental methane yield from anaerobic digestion

Source	Yield (m^3 CH_4/kg algal meal)	Conditions
Golueke et al. (1957)	0.25	Temperature of 35 C, 11 days retention time
	0.32	Temperature of 50 C, 11 days retention time
Eisenberg et al. (1979)	0.33	Loading rate of 0.67 kg VS/L day, 30 days retention time
Rigoni-Stern et al. (1990)	0.35	
Samson and LeDuy (1986)	0.35	
Benemann et al. (2010)	0.3	Assuming 70% dissimilation, 30 days retention time
Collet (2010)	0.292	46 days retention time

CH_4 produced would be used to offset consumption of natural gas. CO_2 produced did not offset the supply of CO_2 to the pond because we considered CO_2 as a free material and regardless of the source, compression of CO_2 would still have to done. Comparing this experimental yield to the theoretical maximum, the decomposition percentage of the algal meal is 44.34%. This meant that there was 55.66% of the algal meal that remained as solids. Based on the assumption used by Collet (2010), the inorganics mineralized from organic compounds during anaerobic

digestion, which transformed nitrogen and phosphorus from proteins to ammonium and phosphates. This yield of mineralization was assumed to be 90%.

Together with the ammonia that was formed during the digestion, the nitrogen and phosphorus from the mineralization were fed back to the pond to offset fertilizer inputs (N replaced ammonium nitrate, P replaced triple superphosphate). Based on equation 2, the mole ratio of NH_3 to CH_4 was 0.361, from which the amount of NH_3 could be calculated. Table 5.24 summarizes the products of anaerobic digestion per 1 kg of algal meal (AM).

Table 5.24: Products from anaerobic digestion of 1 kg algal meal (AM)

Products	Unit	Value	Distribution	Min	Max
CH_4	m^3/kg AM	0.3	Triangular	0.25	0.35
CO_2	kg/kg AM	0.1925	Triangular	0.1604	0.225
NH_3	kg N /kg AM	0.06077	Triangular	0.0506	0.0709
N recycle	kg N/kg AM	(1-CH_4/0.667)*90%*0.1	Explanation: equation links amount of recycle N from remaining solid to amount of biomass decomposition, 90% mineralization, 0.1 kg N in 1 kg AM		
P recycle	kg P/kg AM	0.221* 4.58 * N recycle	Explanation: 0.221 is mass ratio of P to N (based on 0.1:1 mole ratio P:N). 4.58 is conversion P to P_2O_5 (unit of triple superphosphate)		

The basin where anaerobic digestion is conducted has to be heated to have acceptable reaction rates. Based on the assumption made in Lundquist (2010) report, waste heat from an on-site generator could be used, thus eliminating any additional heat input. The basin had to be stirred and based on the assumption by Collet, the energy input was 0.288 kWh/m3 CH_4 produced.

When transesterification was used as the fuel processing method, glycerine is obtained as a by-product. This glycerine production obtained environmental impacts credit as it assumed to replace the production of glycerine in soybean transesterification. Production of 1 kg of glycerine would therefore offset 9.87 MJ and 0.645 kg CO_2-eq of impacts.

REFERENCES

Archibald, I. (2011, March 8). Personal communication with Cellana.

Canakci, M., & Gerpen, J. V. (2003). Comparison of Engine Performance and Emissions for Petroleum Diesel Fuel, Yellow Grease Biodiesel, and Soybean Oil Biodiesel. *American Society of Agricultural and Biological Engineers, 46*(4), 937-944.

Collet, P., Hélias, A., Lardon, L., Ras, M., Goy, R.-A., & Steyer, J.-P. (2011). Life-cycle assessment of microalgae culture coupled to biogas production. *Bioresource Technology, 102*, 207-214.

Demirbas, A., & Demirbas, M. F. (2011). Importance of Algae Oil as a Source of Biodiesel. *Energy Conversion and Management 52* , 163-70.

Emmenegger, M. F., Dinkel, F., Stettler, C., Doka, G., Chudacoff, M., Dauriat, A., et al. (n.d.). *Life Cycle Inventories of Bioenergy. Rep. no. 17*.

Eshratabadi, P., Sarrahzadeh, M. H., Fatemi, H., Ghavami, M., & Gholipour-Zanjani, N. (2008). Enhanced Degumming of Soyabean Oil and Its Influences on Degummed Oil and Lecithin. *Iranian Journal of Chemical Engineering 5.1*, 65-73.

Green, F., Lundquist, T., & Oswald, W. (1995). Energetics of Advanced Integrated Wastewater Pond Systems. *Water Science Technology, 31*(12), 9-20.

Halim, R., Gladman, B., Danquah, M. K., & Webly, P. A. (2011). Oil Extraction from Microalgae for Biodiesel Production. *Bioresource Technology 102* , 178-85.

Huntley, M. E., & Redalje, D. (2006). CO2 mitigation and renewable oil from photosynthetic microbes: a new appraisal. *Mitigation and Adaptation Strategies for Global Change, 12*, 573–608.

Jackson, S., & Lee, H. T. (2009). *Cellana FCP CO2 Transport Key Investigation Phase: CO2 Supply & Transport from Pearl, Qatar.*

Kalnes, T. N., Koers, K. P., Marker, T., & Shonnard, D. R. (2009). A Technoeconomic and Environmental Life Cycle Comparison of Green Diesel to Biodiesel and Syndiesel. *Environmental Progress & Sustainable Energy 28.1*, 111-20.

Li, Y., Griffing, E., Higgins, M., & Overcash, M. (2006). Life Cycle Assessment Of Soybean Oil Production. *Journal of Food Process Engineering 29.4* , 429-45.

Lundquist, T., Woertz, L., Quinn, N., & Benemann, J. (2010). A Realistic Technology and Engineering Assessment of Algae Biofuel Production. *Energy Biosciences Institute*, 1-178.

Marker, T., Petri, J., Kalnes, T., McCall, M., Mackowiak, D., Bob Jerosky, B. R., et al. (2005). *Opportunities for Biorenewables in Oil Refineries.*

McHugh, M. A., & Krukonis, V. J. (1986). *Supercritical Fluid Extraction: Principles and Practice.* Boston: Butterworths.

Mendes, R. L., Coelho, J. P., Fernandes, H. L., Marrucho, I. J., Cabral, J. M., Novais, J. M., et al. (1995). Applications of Supercritical CO2 Extraction to Microalgae and Plants. *Journal of Chemical Technology AND Biotechnology 62.1* , 53-59.

Royal Haskoning. (2009). *Cellana FCP Upstream BOD Premise Document.*

Sahena, F., Zaidul, I., Jinap, S., Karim, A., Abbas, K., Norulaini, N., et al. (2009). Application of Supercritical CO2 in Lipid Extraction – A Review. *Journal of Food Engineering 95.2*, 240-253.

Sheehan, J. V. (1998). *Life Cycle Inventory of Biodiesel and Petroleum Diesel for Use in an Urban Bus.* NREL/SR-580-24089.

Towler, G., & Sinnott, R. (2008). *Chemical Engineering Design: Principles, Practice and Economics of Plant and Process Design.* Amsterdam: Elsevier/Butterworth-Heinemann.

Weissman, J., & Goebel, R. (1987). *Design and Analysis of Microalgal Open Pond Systems for the Purpose of Producing Fuels.* Golden, Colorado: Solar Energy Research Institute.

Williams, P. J., & Laurens, L. M. (2010). Microalgae as biodiesel & biomass feedstocks: Review & analysis of the biochemistry, energetics & economics. *Energy & Environmental Science, 3*, 554–590.

6 RESULTS & INTERPRETATION

The results would be organized based on the life cycle stages to compare processes or assumptions specific to the stage itself. In the stages, only non-renewable energy input is compared. The results of greenhouse gas (GHG) emission generally follows the trend of non-renewable energy input, which shows that most of the GHG impacts are due to the use on non-renewable energy. Therefore, the GHG impacts for each stage are not shown in the stages results. The whole life cycle results are also presented in the end after we have chosen the processes and assumptions to be combined. Both non-renewable energy input and GHG impacts are reported for the life cycle results.

6.1 Algae Cultivation

The functional unit in this stage was 1 kg of algal biomass. In this stage, we were basing the analysis on the hybrid system used in Cellana's pilot plant and would not compare it to raceway pond or PBR systems. Using this fixed growth system, we were able to look at assumptions within it that would be important.

The choice of algal species may play a significant role in the life cycle results. Cellana explored the possibility of using both diatom and green algae. Diatom's grown in Cellana's plant had ash content ranging from 40-50%, thus requiring silica input for optimum growth. Due to their cell weight, diatoms would settle quickly in the sedimentation stage and did not need the addition of flocculant. Green algae, meanwhile, did not need the addition of silica but needed alum as flocculant to induce the cells to agglomerate and settle. The ideal case would be one where a non-diatom species was used that was able to auto-flocculate without addition of alum. Figure 6.1 shows the results comparison between these cases, calculated using productivity of 20 $g/m^2/day$.

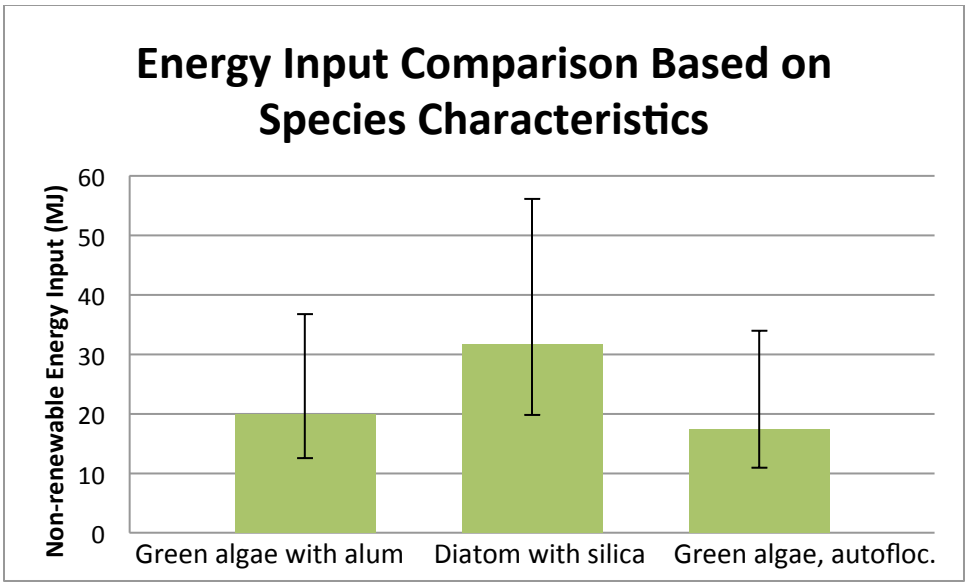

Figure 6.1: Comparison non-renewable energy input in using green algae and diatom

Figure 6.1 shows that both in terms of non-renewable energy input and greenhouse gas emission using green algae would be more beneficial than using diatom. The cost of silica and the difficulty to recycle and reuse it had driven Cellana to move away from using diatom. This result showing a higher environmental burden from adding silica added another reason why diatom might not be a good species choice. Adding flocculant increased the energy burden by 11% (from 18 MJ to 20 MJ). Just like silica, if not recovered, having flocculant on the biomass would probably affect the downstream processing. Their effects on downstream processing or the flocculant recovery methods had not been well researched. Therefore, for the rest of the analysis, we assumed that adding flocculant was not necessary and the algae cells were able to auto-flocculate and sink within two hours.

Figure 6.2 shows the energy breakdown of algae cultivation stage. The highest energy sink was in providing nitrogen nutrients followed by water transport (from sea to canal storage and from canal storage to PBRs). Therefore, recycling of nutrient or extracting nutrients from waste products should be done as much as possible to reduce this energy sink. In addition, this showed the importance of locating the cultivation site near water sources.

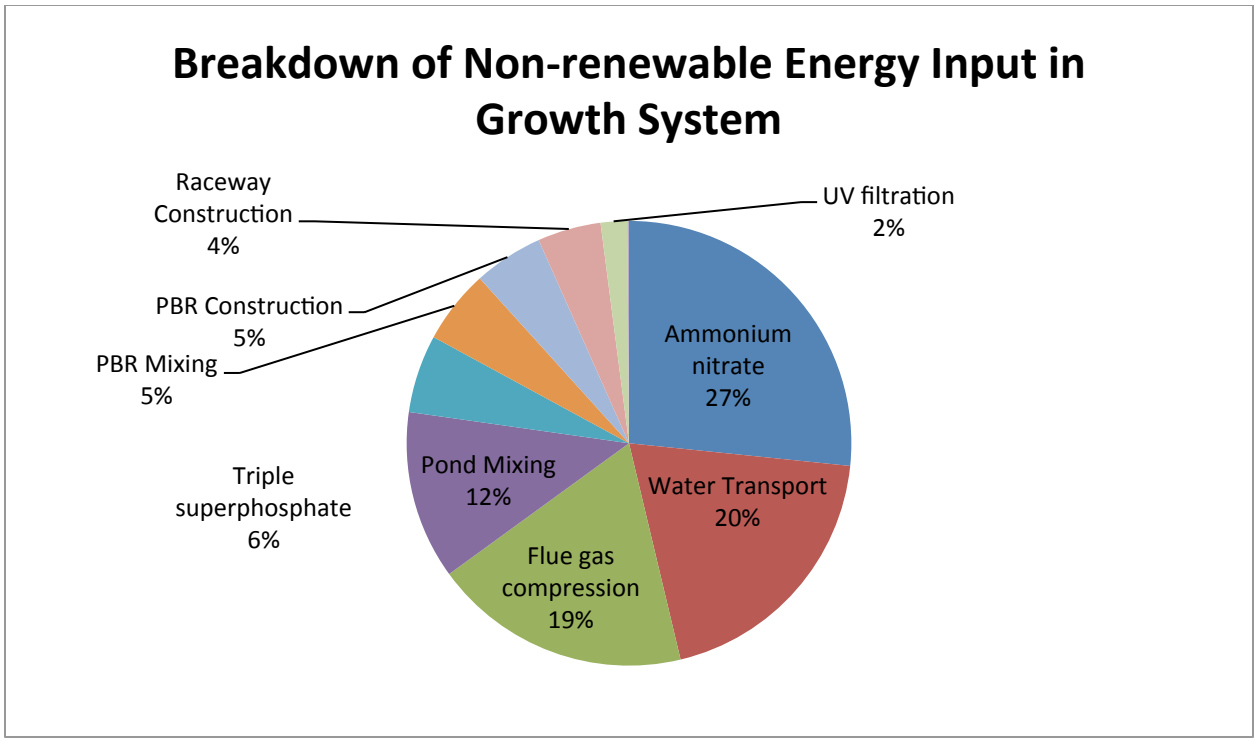

Figure 6.2: Breakdown of energy input in algal cultivation stage

To understand the importance the parameters within growth system, a sensitivity analysis was conducted. The input value of each of the parameter was altered by +/- 25% and plotted against the resulting total non-renewable energy input required to produce 1 kg of algal biomass. Figure 6.3 shows the results of this sensitivity analysis. This analysis was done using deterministic values and with productivity value fixed at 20 g/m^2/day.

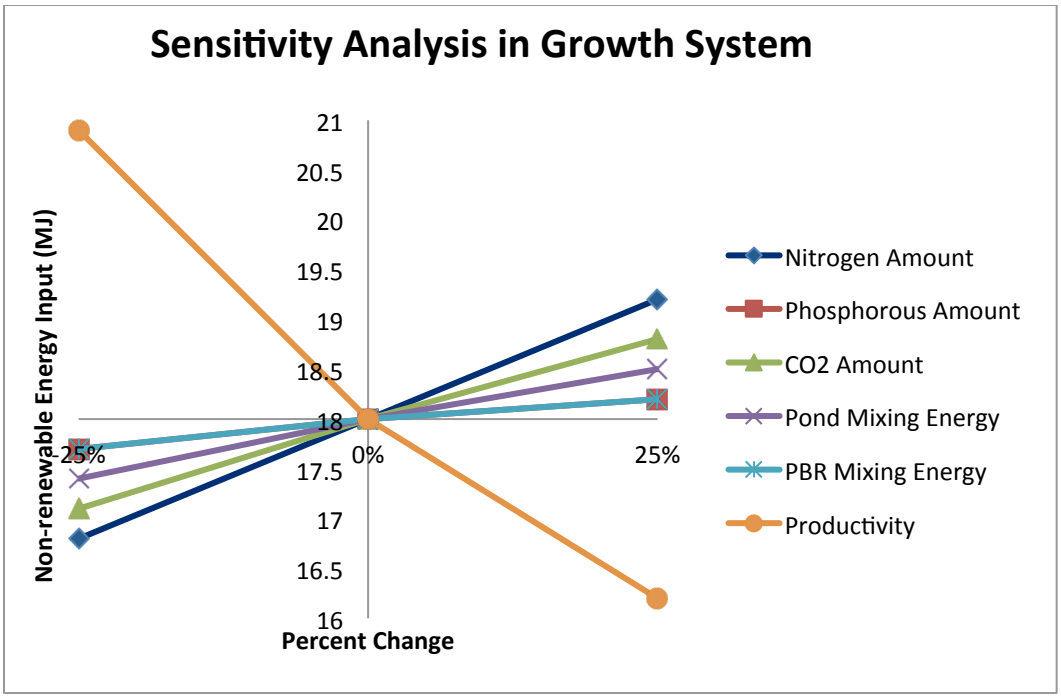

Figure 6.3: Sensitivity analysis in the hybrid growth system

The sensitivity analysis showed that productivity value was the most sensitive parameter, followed by nitrogen amount and CO_2 amount (not the CO_2 itself but the compression energy needed to supply it). Having a high productivity, provided that the lipid content could be maintained, would be crucial in ensuring the feasibility of algal biofuel. Three ranges of productivity were analyzed based on what was currently achievable (productivity 1), near future projection (productivity 2), and optimized productivity (productivity 3). This comparison is shown in Figure 6.4.

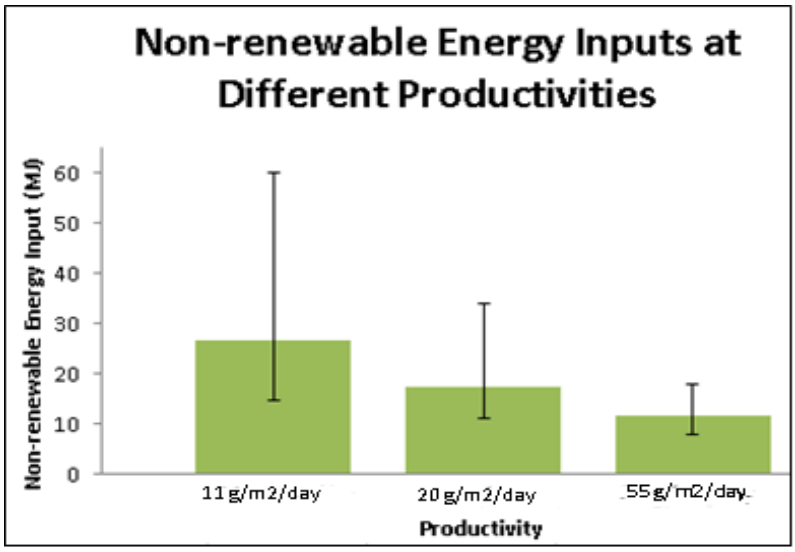

Figure 6.4: Comparison of non-renewable energy inputs at different productivities to produce 1 kg of algal biomass

6.2 Dewatering

Dewatering reduces the water from harvested biomass to obtain a paste-like consistency of 20% dwb. Three dewatering methods were considered: decanter centrifuge, filter press, and tangential filtration. Very few data existed to build the inventory of these dewatering methods. We only included uncertainties for energy input into decanter centrifuge and used deterministic values for filter press and tangential flow filtration. In Figure 6.5 where comparison of energy inputs for the three of them is shown, filter press gives the best result. This may be because it uses mechanical forces in compressing the chambers where the algal paste is contained compared to operating large electric motors like used in centrifuges. Tangential flow filtration gives about twice the energy input for filter press, but it may have the advantage of having a continuous process rather than batch and it may use less labor. Filter press needs a worker to manually clean the chambers when the pressing is done. With these factors considered, it is not clear which of the two processes would be more applicable for dewatering algae, but either one provides a good alternative to using centrifuges with high energetic costs.

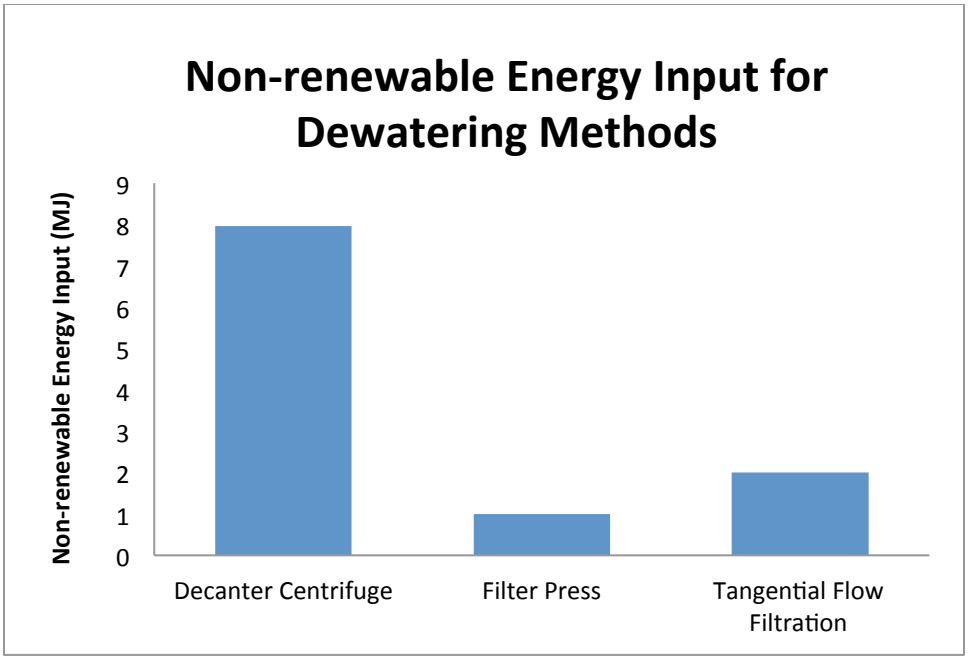

Figure 6.5: Non-renewable energy input of decanter centrifuge, filter press, and tangential flow filtration to produce 1 kg of algal biomass

6.3 Algal Oil Extraction

Five cases of algal oil extraction were considered: hydrothermal liquefaction, SCCO2 extraction, and hexane extraction with 3 methods of drying. In the case of hexane extraction, the algal paste out of the dewatering stage had to be dried from 20% to 90%. The three ways of drying were: sun drying with the assumption of negligible energy input, drum drying, and a combination of the two (half sun drying and half drum drying). Figure 6.6 shows the comparison between the 5 cases.

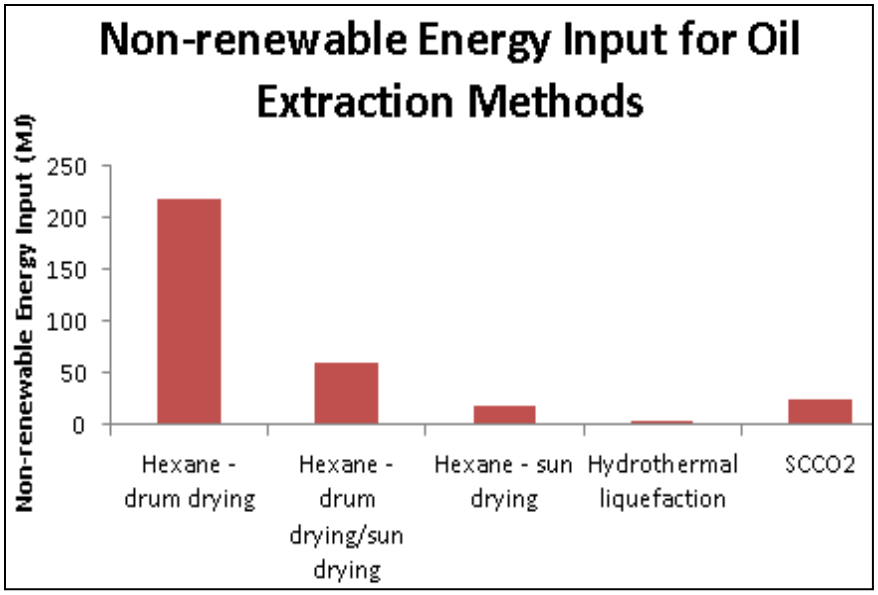

Figure 6.6: Non-renewable energy input for different oil extraction methods to produce 1 kg of algal oil

When thermal drying is used, even at 50% of the time, the energy input increases significantly. The drying energy input alone is 12 times that of the hexane extraction process. Therefore, if any type of solvent extraction is to be used, drying has to be done by sun drying with minimal energy requirement, or the process has to be able to take in wet algal biomass as input. Hydrothermal liquefaction gives the lowest energy requirement at 2.9 MJ/kg oil. $SCCO_2$ process yields a higher energy input that hexane extraction with sun drying due to the energy needed to compress the CO_2. However, CO_2 is seen as a "cleaner" solvent than hexane because it is not a processed chemical and it has lower environmental impacts. With $SCCO_2$ extraction there is also a possibility of extracting the high molecular weight carbon chains such as docosahexanoic acid (DHA) which could be a high value by-product sold as a pharmaceutical product.

6.4 Biofuel Processing

In this stage, two fuel conversion processes were considered: transesterification and hydrotreatment. The modeling done for these processes was different for oil that had been extracted using hexane and $SCCO_2$ compared to that extracted by hydrothermal liquefaction. Figure 6.7 shows the non-renewable energy input for the biofuel processing stage. The functional unit used was 1 MJ of produced fuel. For transesterification this fuel would be methyl ester (biodiesel), and in the hydrotreatment, the fuel would be a combination of diesel, propane, gasoline, and methane.

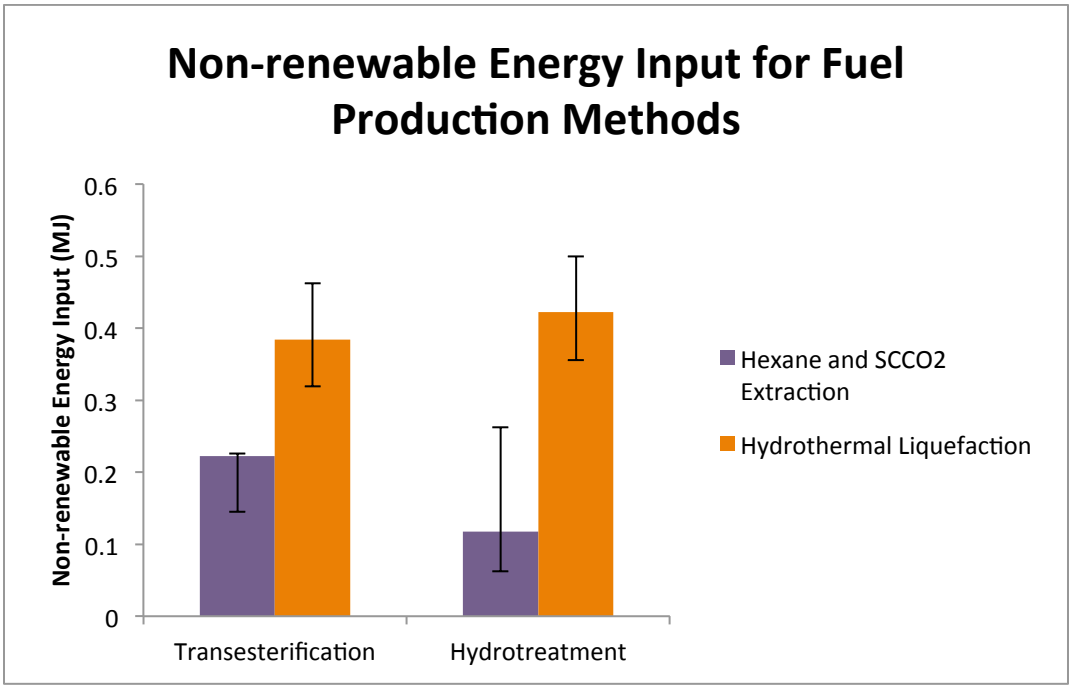

Figure 6.7: Non-renewable energy input comparison for fuel processing to produce 1 MJ of fuel

The energy input used in processes following hydrothermal liquefaction is consistently higher than that following hexane or $SCCO_2$ extraction. In the hydrotreatment, it is about 4 times higher and in transesterification, about 1.5 times higher. The transesterification process for the solvent extraction is base catalyzed while for the hydrothermal liquefaction, it would be acid catalyzed. The two processes differ in the type and amount of catalyst, and the amount of

methanol used is also higher in the acid catalyzed reaction, which explains the higher energy input for acid catalyzed transesterification.

The hydrotreatment for oil from hydrothermal liquefaction needs higher amount of hydrogen as compared to the solvent extraction methods to complete the reaction for the nitrogen and sulfur existing in the oil phase. This may increase the energy input for hydrotreating, but not as much as what we obtain in the results. Hydrotreatment is generally seen as a slightly better option than transesterification since it does not need much chemical inputs, but this is not the result we obtain for processing the oil phase from hydrothermal liquefaction. In this case, transesterification and hydrotreating consume almost the same energy, with transesterification consuming 0.038 MJ less.

6.5 Complete Life Cycle Analysis

A complete life cycle analysis combined the results from algal cultivation, dewatering, oil extraction, fuel conversion and added the credits from by-products into account. Three cases of complete life cycle were analyzed as shown in Table 6.1. These cases are:

- Best case which combines assumptions and processes that give the lowest non-renewable energy input
- Base case which combines the most common assumptions and processes used in published algal biofuel LCAs
- Worst case which combines assumptions and processes that give the highest non-renewable energy input

Table 6.1: Three cases considered in the full life cycle analysis

Case Scenarios	Producti-vity	Dewatering	Drying	Oil Extraction	Fuel Production	By-products
Best Case	55 $g/m^2/day$	Pressure filtration	None	Hydrothermal liquefaction	Transesterification	Anaerobic digestion of algal meal + glycerine
Base Case	20 $g/m^2/day$	Decanter centrifuge	Drum drying/ Sun drying	Hexane extraction	Transesterification	Anaerobic digestion of algal meal + glycerine

Worst Case	11 g/m^2/day	Decanter centrifuge	Drum drying	Hexane extraction	Transesterification	Anaerobic digestion of algal meal + glycerine

By showcasing the results from these three cases in this manner, we captured the range of results completely with respect to process and assumption choices. The results from each of these cases would also have a distribution, showing the range caused by uncertainties within the parameters used in the modeling.

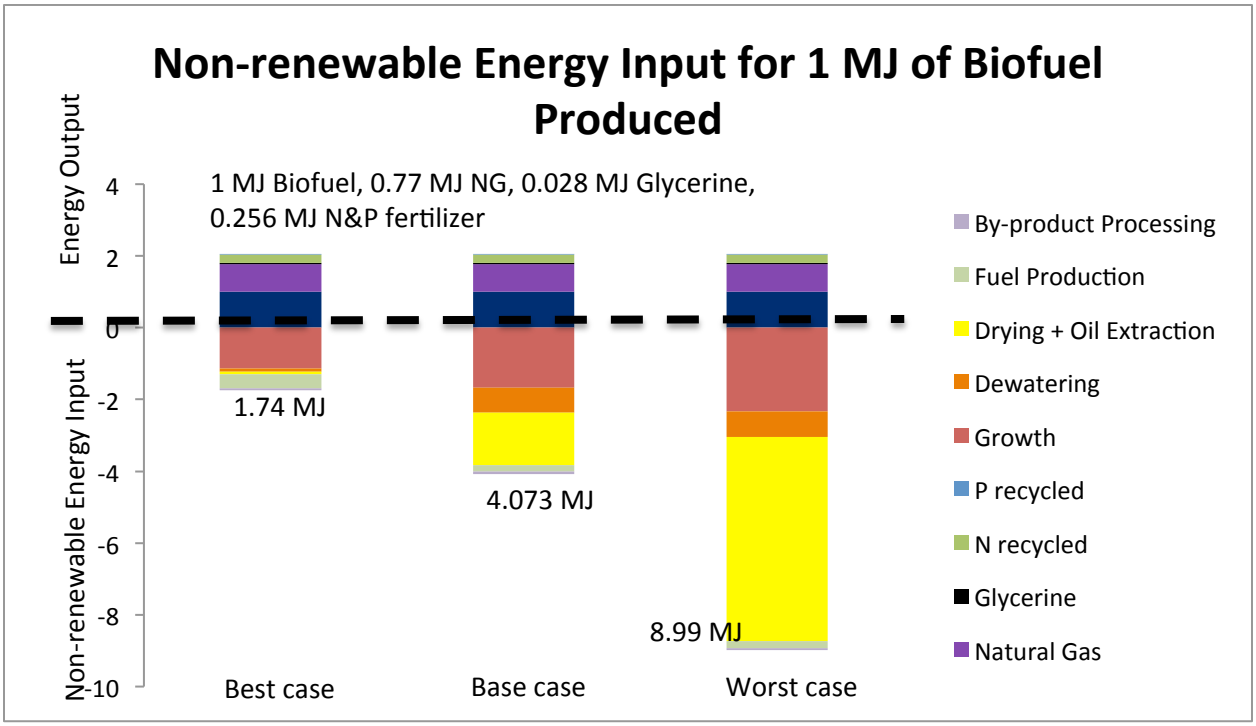

Figure 6.8: Energy input and output for full life cycle for three representative cases

Figure 6.8 summarizes the deterministic results for the three cases. For all three cases the products obtained are the same. The functional unit is 1 MJ of biofuel. The by-products include: natural gas, glycerine, and fertilizer (both nitrogen and phosphorous), each giving an energy credit of 0.77, 0.028, and 0.256, respectively.

From this result, we see that drying consumes a lot of energy, approximately a third in the base case and two-thirds in the worst case. For algal biofuel to be feasible, providing energy input for drying would not be the route to take. Sun drying, which consumes very minimal energy, is not

really reliable because it is highly dependent on the weather. It may also cause putrefaction of the biomass or decrease in the lipid composition. An extraction method that does not need to process dry algae would have a significant advantage in terms of the energy input and should be pursued in future research.

When drying is not needed, algal cultivation becomes the highest energy burden as seen in the best case scenario. Therefore, having a high productivity and keeping any parasitic energy input minimum would also be an important factor in ensuring feasibility of algal biofuel. Dewatering and fuel processing do not have significant contribution in the energy input.

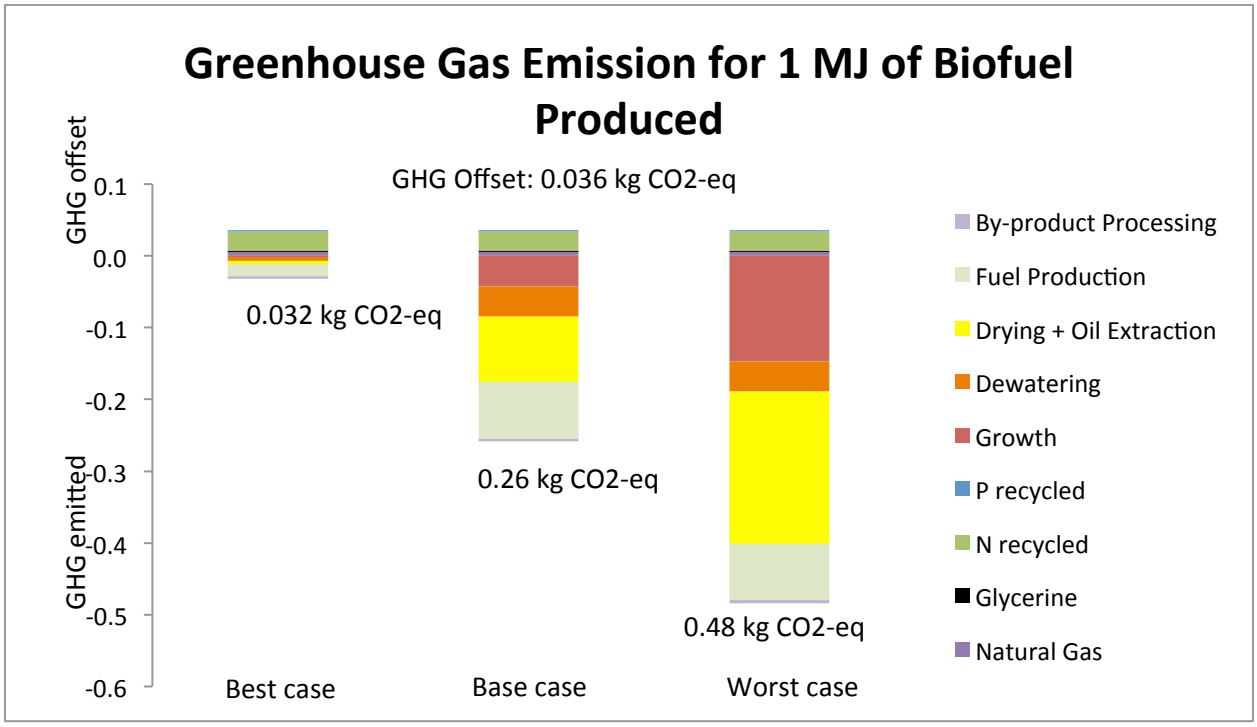

Figure 6.9: Greenhouse gas offset and emission for full life cycle for three representative cases

The net greenhouse gas emissions for the best, base, and worst case are -0.04, 0.224, and 0.444 kg CO2-eq respectively. The best case can be considered a carbon neutral process. The trend for greenhouse gas emission in this model follows the trend for the amount of non-renewable energy input because we do not consider emissions that are directly related to the processes. For example, we do not consider greenhouse gas emission due to land use change, or any decomposition of biomass.

Monte Carlo simulations are conducted for the three cases. This gives us the distribution for each of the results shown above. Figures 6.10 to 6.15 show the shape of the distribution and the distribution parameters.

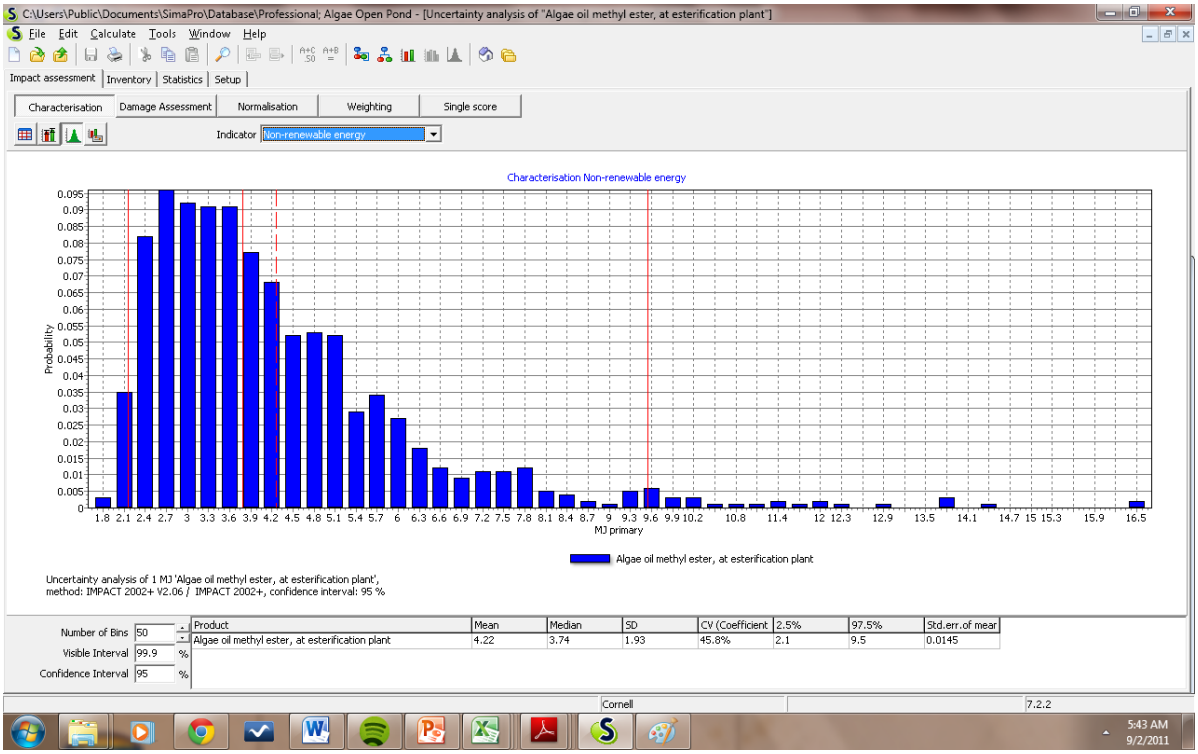

Figure 6.10: Non-renewable energy input for the base case to produce 1 MJ fuel

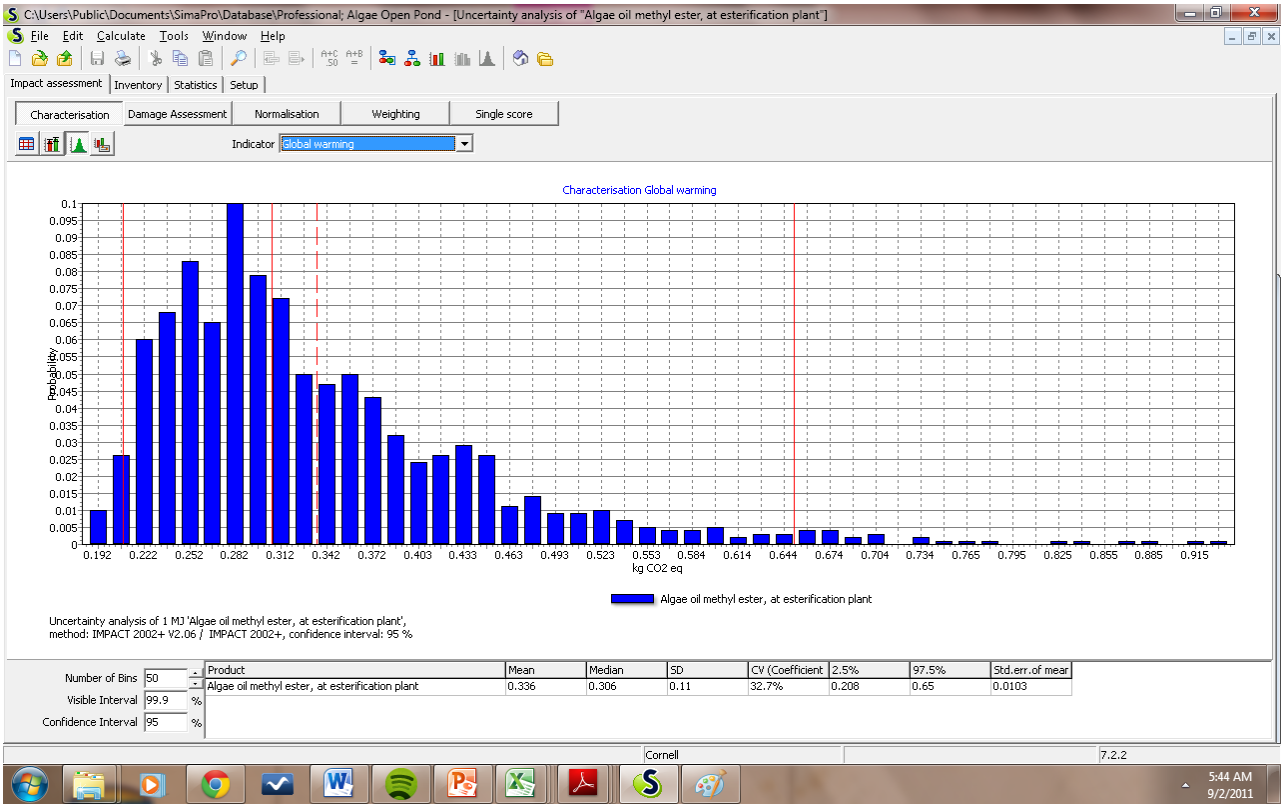

Figure 6.11: Greenhouse gas emission for the base case to produce 1 MJ fuel

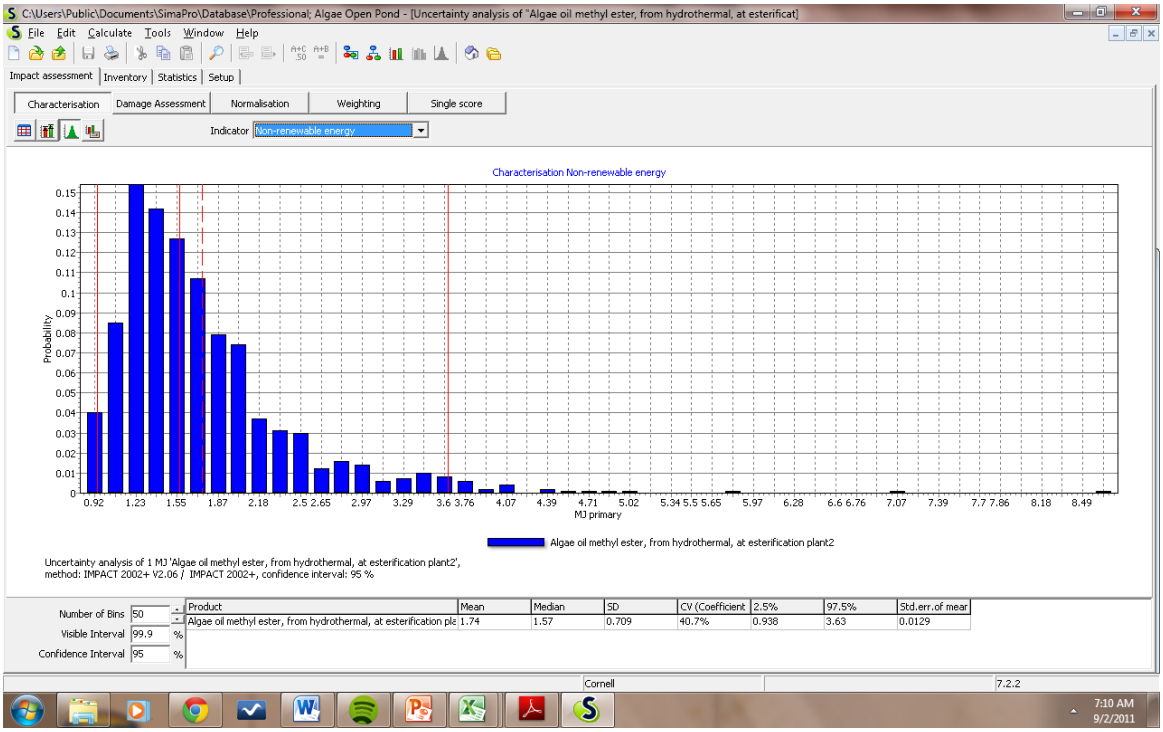

Figure 6.12: Non-renewable energy input for the best case to produce 1 MJ fuel

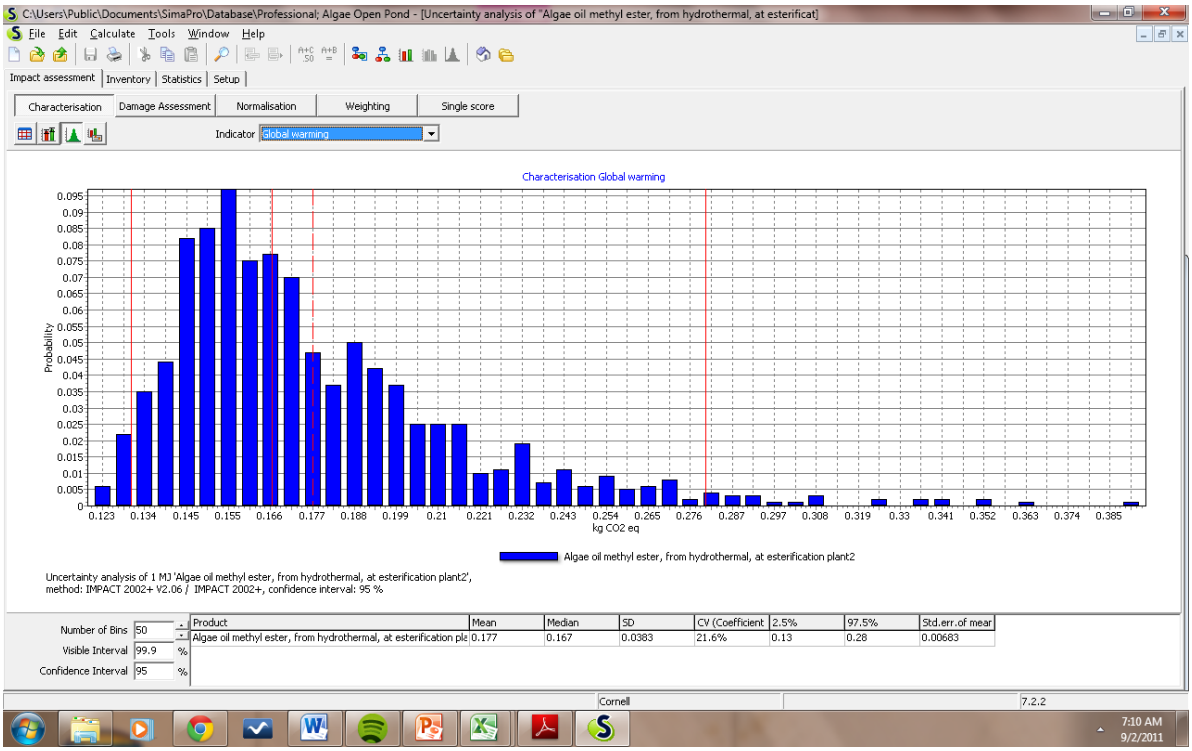

Figure 6.13: Greenhouse gas emission for the best case to produce 1 MJ fuel

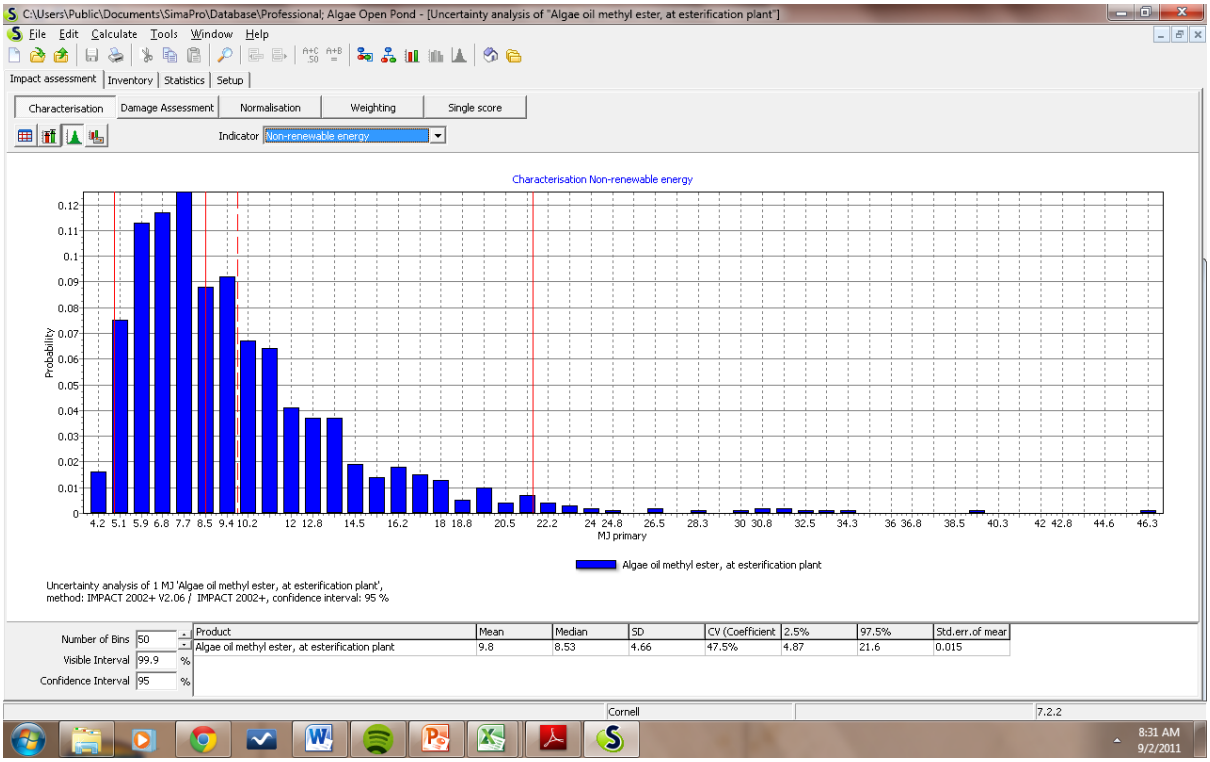

Figure 6.14: Non-renewable energy input for the worst case to produce 1 MJ fuel

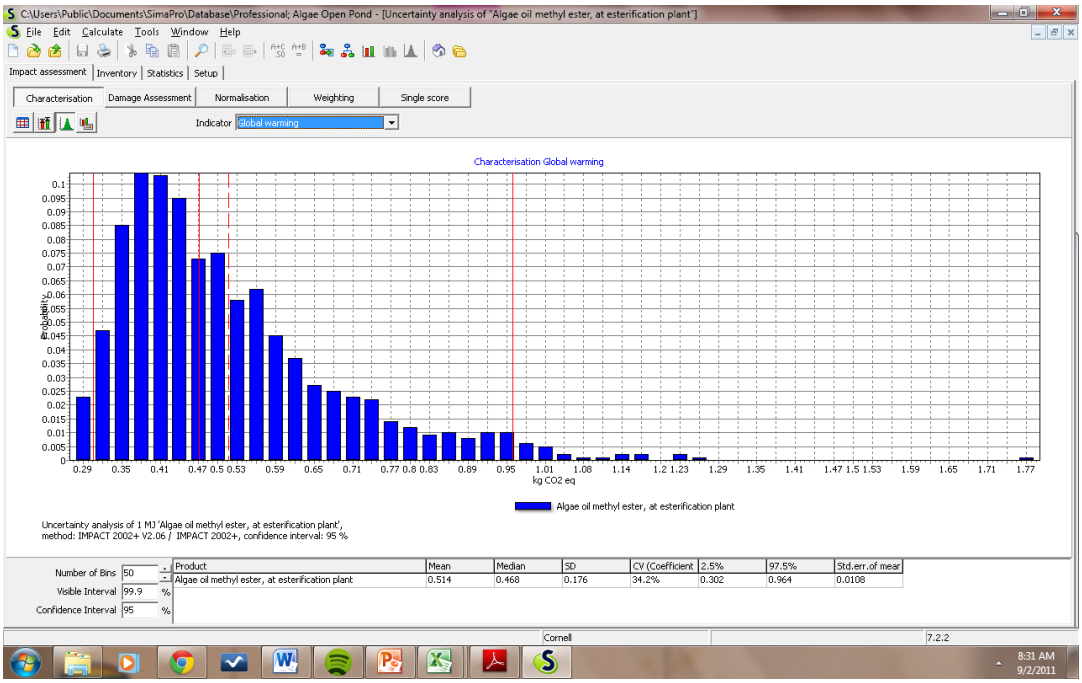

Figure 6.15: Greenhouse gas emission for the worst case to produce 1 MJ fuel

The table below gives a summary of the non-renewable energy input and the greenhouse gas emission for the three cases to produce 1 MJ of biofuel.

Table 6.2: Summary of LCA results

Cases	Non-renewable energy input (MJ)	95% Confidence Interval	GHG Emission (kg CO_2-eq)	95% Confidence Interval
Best Case	1.74	0.938-3.63	0.177	0.13-0.28
Base Case	4.22	2.1-9.6	0.336	0.208-0.650
Worst Case	9.8	4.87-21.6	0.514	0.302-0.964

From this result, NER and its range for each of the case could be calculated. The graph below summarizes the NER calculation.

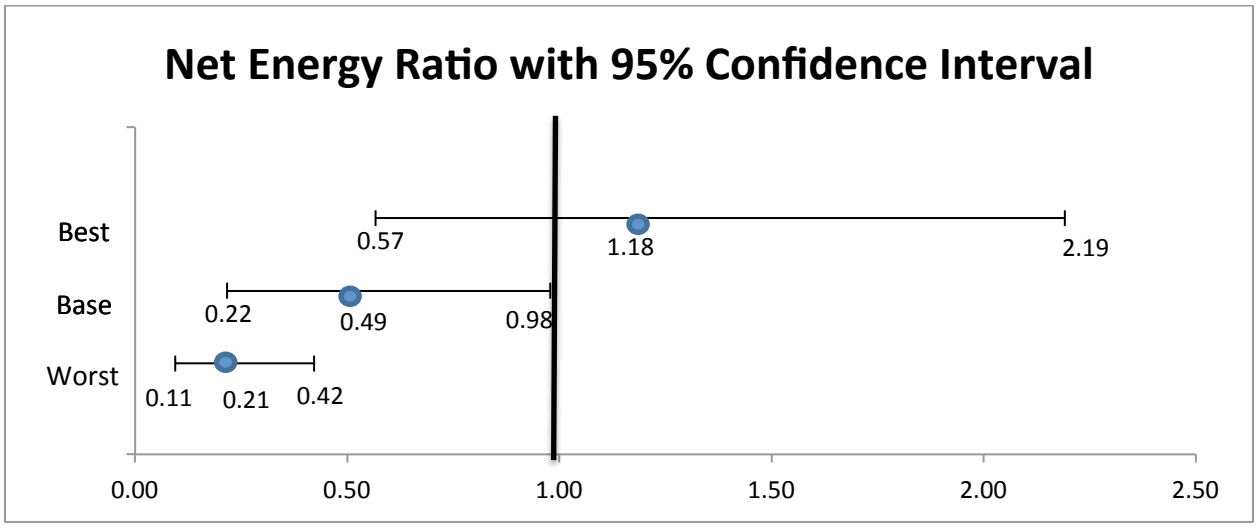

Figure 6.16: NER results for the three representative cases

Figure 6.16 shows that even with the most optimistic assumptions for base case, which is assumed as the most common processes and parameters to be used, the NER does not reach over one. For the best case scenario, the mean NER is slightly above 1, with a potential to be below one, but at the same time could be promising if the high end could be achievable sustainably in the future.

7 CONCLUSIONS

Life cycle analysis was used to assess the feasibility of producing biofuels from microalgae in terms of its energetic values and greenhouse gas emission. Due to the many process options and process combinations to build the whole life cycle, three cases were chosen as a representation of the worst case, base case, and best case scenarios. Together with using the inherent parametric uncertainties that were built in the life cycle inventory, Monte Carlo simulations were conducted to obtain results that showed 95% confidence interval, showing the final uncertainty range of the life cycle.

Based on the NER results, in the worst case and base case scenarios, an NER above 1 is not achievable. The best case scenario shows a range indicating a possibility of reaching an NER up to 2.19, which would be promising if achievable in a sustainable way. Looking at the breakdown of energy burden from each stage, downstream processes that need drying from 20% to 90% would result in very high energy input. Even when 50% of drying is done by sun drying, the energy burden from drying still occupies the highest percentage.

When drying is not needed, algal cultivation has the highest energy input. Therefore, choosing the right species that are robust, needs minimum nutrient, able to be harvested easily, and at the same time has high overall lipid productivity remains to be an important research area. Recycling nutrients by using anaerobic digestion or using waste water as nutrient source are also important since nutrient input results in a high energetic cost. Bulk dewatering that takes the harvested algae to produce a 20% dwb paste would not be a bottleneck if industrial processes such as tangential flow filtration or filter press could be used effectively. While it shows great potential in terms of the energy input, efficient technical operation has to be in place to ensure low maintenance and problems such as clogging do not occur often.

The extraction process itself has a relatively low energy input which is not significant in the whole life cycle. However, as mentioned before, only extraction processes that take in wet biomass would make the whole process feasible. The fuel conversion stage is an area where much research has been done for converting raw oil to usable fuels, based on oil from other feedstocks. In terms of the modeling, the assumptions used are robust, in the sense that they

have been proven at an industrial scale. Therefore, reducing the energy input in this stage by further process improvement would be difficult. But the question remains if the same process and its efficiencies apply closely when algal raw oil is used, or if there is other properties in algal oil that might make these processes unfeasible.

In conclusion, uncertainty analysis in the LCA shows a wide range of NER results. By analyzing each stage independently and having three cases that represent the low, middle, and high end of the process combinations, this range could be captured and assessed further. There is a possibility to have a feasible process chain at a commercial scale that gives NER above 1, but virtually all the processes have to be tested further in a large-scale production facility to really know if they could work for algal feedstock.

8 Appendices

8.1 Appendix A: Summary of LCA Studies

The file below shows the assumption used in each of the paper included in Chapter 4.

8.2 Appendix B: Distribution Data for Parameters in Microalgae Cultivation

Table A.1: Data to build inventory for lipid content in algae (lipid content N deficient is used)

Marine Algae		Lipid content N sufficient	Lipid content N deficient	Sources
Biddulphia aurita	Bacillariophyceae	18	15	Shifrin & Chisolm (1981)
Chaetoceros gracilis	Bacillariophyceae	15	28	Benemann (1986)
Chlorella sp.	Chlorophyceae	10.9	8.9	Tornabene & Benemann (1985)
Chlorella minutissima	Chlorophyceae	31	57	Illman et al (2000)
Cyclotella cryptica	Bacillariophyceae	23	37	Shifrin & Chisolm (1981)
Nitzschia sp.;	Bacillariophyceae	21	37	Smith et al (1997)
Nitzschia dissipata	Bacillariophyceae	26	66	Tadros (1985)
Phaeodactylum tricornutum	Bacillariophyceae	20	23	Thomas (1983)
Skeletonema costatum	Bacillariophyceae	23.5	25	Shifrin & Chisolm (1981)
Thalassiosira pseudonana	Bacillariophyceae	24	26	Shifrin & Chisolm (1981)
Thalassiosira weissflogii	Bacillariophyceae	22	24	Shifrin & Chisolm (1981)
Dunaliella salina	Chlorophyceae	22	9	Ben-Amotz et al (1985)
Dunaliellia tertiolecta	Chlorophyceae	24	18	Shifrin & Chisolm (1981)
Nannochloropsis (Monollantus) salina	Eustigmatophyceae	44	57	Shifrin & Chisolm (1981)
Nannochloropsis salina	Eustigmatophyceae	29	60	Tornabene (1984)
Nannochloropsis sp.	Eustigmatophyceae	19.7	16.9	Tornabene & Benemann (1985)

Nannochloropsis sp.	Eustigmatophyceae	20.8	35.5	Ben-Amotz et al (1985)
Nannochloropsis sp.	Eustigmatophyceae	32.2	60	Rodolfi (2008)
Nannochloropsis sp	Eustigmatophyceae	28	53	Benemann & Oswald (1996)
Tetraselmis ap	Prasinophyceae	18	15	Laws & Berning (1991)
Hymenomonmas carterae	Prymnesiophyceae (Haptophyceae)	20	14	Shifrin & Chisolm (1981)
Isochrysis	Prymnesiophyceae (Haptophyceae)	11.2	26	BenAmotz (1984)
Monallantus salina	Xanthophyceae	44	57	Shifrin & Chisolm (1981)
Navicula sp	Bacillariophyceae	32	58	Benemann & Oswald (1996)
Amphora sp	Bacillariophyceae	4.1	14	Benemann (1986)
Ankistrodesmus	Chlorophyceae	24	40	BenAmotz (1984)
Boekilovia sp		28	36	Benemann (1986)
Cyclotella sp	Bacillariophyceae	13	42	Tadros (1985)
Monoraphidium sp	Chlorophyceae	21	25	Benemann (1986)
Bracteacoccus minor	Chlorophyceae	25	33	Pohl et al (1971)

Table A.2: Data used to build the distribution for paddlewheel mixing

References	Energy (kWh/ha/day)	Notes
This Study	31.82	Speed of 25 cm/s for 12 hours
Clarens (2009)	8.88	Operated at 10 RPM.
Sazdannoff (2006)	12.3	Average operating hours/day is used. Paddlewheel power is referred to Benemann (1996).
Collet (2010)	50	Speed of 25 cm/s.
Verhoeven (2009)	6.23	Paddle wheel of 0.4 kW.
Weissman (1989)	50.88	Operated at 6.1 RPM in an unlined pond.
Putt (2007)	7.2	Speed of 15 cm/s.
Benemann (1987)	8.16	Power of 0.34 kW
Cellana, Design Report	38.4	Power 3.2 kW/pond, 12 hours a day
Cellana, Mark Huntley	51.8	Power 3.7 kW/pond 14 hours a day

Table A.3: Data used to build distribution for nutrient input

Reference	C:N:P ratio in %dwb	Nitrogen (g N/kg dwb)	Phosphorus (g P2O5/kg dwb)	CO_2 (kg/kg dwb)	Note
Grobbelaar (2004)	$CH_{1.83}O_{0.48}N_{0.11}P_{0.01}$	65.90	30.40	1.88	Molecular representation of high lipid algae
Redfield (1958)	$C_{106}H_{181}O_{45}N_{15}P$	86.99	29.41		
Chisti (2007)	33.6 : 9 : 1.8	90.00	41.23	1.23	
Lardon (2009) - Normal N	48 : 4.6 : 0.99	46.00	22.67	1.76	K: 8.2 and Mg: 2
Hillebrand and Sommer (1999)	46.1 : 7.7 : 1	77.00	22.90	1.69	Assuming P to be 1%
Woertz (2009)	50.0 : 8 : 1	80.00	22.90	1.83	Assuming P to be 1%
Verhoven (2008)		26.00	25.00	1.92	
Huntley – Cellana internal report (2007)		67.90	19.24	1.65	Marine diatom in KPF
Average		**67.47**	**27.79**	**1.71**	

Table A.4: Data used to build the distribution for alum

Reference	Type	Dose	Unit
Uduman (2010)	Inorganic Alum	80-250	g/m3
McGarry (1970)	Alum	75-100	g/m3
Sukenik (1988)	Alum	225 ± 21	g/m3

Table A.5: Data used to build the distribution for silica

Reference		Dose
Verhoven (2009)	81	g Si/kg dwb
Cellana Internal Report	74.35	g Si/kg dwb

8.3 Appendix C: Calculation of Sulfuric Acid and Potassium Hydroxide Use in Transesterification

The EcoInvent transesterification LCI assumes there is no pretreatment step. Therefore, the sulfuric acid input is determined by assuming the mole-to-mole ratio between TAGs and potassium hydroxide is equal to that between PUFAs and sulfuric acid. A typical TAG content of algae oil as produced by Cellana is 92.8 wt% (Cellana 2010). The remaining weight is considered to be EPA (Hu *et al* 2008). The molar ratio of EPA to TAGs is calculated below:

$$\frac{7.2\text{ g EPA}}{92.8\text{ g TAG}} \left| \frac{262.9\text{ g TAG}}{1\text{ mol TAG}} \right| \frac{1\text{ mol EPA}}{315.1\text{ g EPA}} = 0.06473\text{ mol EPA/mol TAG}$$

The mass of potassium hydroxide needed to catalyze the transesterification of TAGs is 0.011352 kg (Emmenegger *et al* 2007). The mass of sulfuric acid needed to catalyze the pretreatment process is calculated below:

$$\frac{0.011352\text{ kg KOH}}{} \left| \frac{1\text{ kg-mol KOH}}{56.1056\text{ kg KOH}} \right| \frac{0.06473\text{ kg-mol } H_2SO_4}{1\text{ kg-mol KOH}} \left| \frac{98.086\text{ kg } H_2SO_4}{1\text{ kg-mol } H_2SO_4} \right.$$

$= 0.001285\text{ kg } H_2SO_4$

Additional potassium hydroxide will need to be input to neutralize the sulfuric acid from the pretreatment step. The mass of potassium hydroxide needed for the neutralization reaction is calculated below:

$$\frac{0.001285\text{ kg H2SO4}}{} \left| \frac{1\text{ kg-mol } H_2SO_4}{98.0786\text{ kg } H_2SO_4} \right| \frac{2\text{ kg-mol KOH}}{1\text{ kg-mol } H_2SO_4} \left| \frac{56.1056\text{ kg KOH}}{1\text{ kg-mol KOH}} \right. = 1.470\text{x}10^{-3}\text{ kg KOH}$$

The sum of the masses of potassium hydroxide needed for catalysis and neutralization is 0.012821 kg, the value found in the LCI.

8.4 **Appendix D: Hydrotreating Reactor Simulation**

Three algal lipid contents are analyzed in the table below. The first column gives the fatty acids that are found in the algae oil. The next two give the number of carbon atoms (n) and the number of double bonds (d) in the fatty acid. The next column gives the molecular weight (MW) of that fatty acid in a TAG (i.e. multiply MW by three to get the molecular weight of a TAG) as found using the formula below the table. The next column gives the mass of hydrogen needed to saturate (i.e. break double bonds and break TAG backbone) a kg of TAG consisting of only that fatty acid using the formula below the table. The final three columns give typical algae oil contents by mass (Cellana 2010).

Fatty Acid	n	d	MW	kg sat H2/kg TAG	Algae 1	Algae 2	Algae 3
C14:0	14	0	241.0	0.0042	19.7	14.3	14.5
C16:0	16	0	269.1	0.0037	29.9	36.2	22
C16:1	16	1	267.1	0.0113	41.2	31.9	42.8
C18:0	18	0	297.2	0.0034	2	2.4	3.7
C18:1	18	1	295.1	0.0102	0	6.9	4.6
C18:2	18	2	293.1	0.0172	0	1.5	2.5
C20:5	20	5	315.1	0.0352	7.2	6.8	9.9

$$MW = \underbrace{32}_{2\ O\ atoms} + \underbrace{(n+1)*12.01}_{n+1\ C\ atoms} + \underbrace{[5/3+2*(n-1)+1-2*d]*1.008}_{5/3+2*(n-1)+1-2*d\ H\ atoms}$$

$$\text{kg sat H2/kg AO} = \frac{1\ \text{kg-mol TAG}}{\text{MW kg TAG}} \left| \frac{d+0.5\ \text{kg-mol H2}}{1\ \text{kg-mol TAG}} \right| \frac{2.016\ \text{kg H2}}{1\ \text{kg-mol H2}}$$

The mass of hydrogen needed to saturate and average molecular weight was calculated for each of the three algae oils. These two parameters were simulated as stochastic variables with a triangular distribution. The smallest values were used as the minimums, the largest as the maximums, and the intermediates as the modes. The table below summarizes the distributions of these two parameters. The scripts for the two simulations can be found in Appendix E.

Parameter	Minimum	Mode	Maximum
Saturation H_2	0.0090	0.0092	0.0108
Molecular Weight	265	270	275

The results of the Monte Carlo simulation are given in the table below.

Parameter	Minimum	Mode	Maximum
Hydrogen Consumption (kg/kg TAG)	0.013	0.018	0.024
Carbon Dioxide Produced (kg/kg TAG)	0.080	0.122	0.165
Water Produced (kg/kg TAG)	0.033	0.058	0.085
Propane Produced (kg/kg TAG)	0.0534	0.0544	0.0554

Given equimolar amounts of carbon dioxide and carbon monoxide are produced and all carbon monoxide is converted to carbon dioxide in the WGS reactors, another CO_2 output with equivalent mass is added to the outputs in the LCI. The amount of gasoline formed via cracking is uncertain. Marker *et al* (2005) predict that gasoline output will be 2.4% or 2.5% of the input oil mass. Huber *et al* (2007) predict this value to be between 0% and 2.5%, and Kalnes *et al*

(2009) predict this number to be anywhere between 0% and 7%. Therefore, the mass of gasoline produced is considered to be triangularly distributed with a minimum of 0 kg, a mode of 0.025 kg, and a maximum of 0.07 kg. Because one mole of hydrogen is formed per mole of CO reacted in the WGS reactors, there is a hydrogen credit equal to the mass of CO produced multiplied by the ratio of the molecular weight of hydrogen to that of CO and by 83%, the percent of hydrogen produced in a refinery's hydrogen plant that is recovered (Parkash 2003, pp. 173-175). The green diesel output is computed by closing the mass balance around the reactor in equation A below:

(A) $X_D = X_{H2} + X_{TAG} - X_{C3} - X_W - X_G - X_{CO2} - \gamma X_{CO2}$

γ is the ratio of the molecular weight of CO to that of CO_2. Each X is a mass ratio of a chemical species to input algae oil (therefore making X_{TAG} 1). The table below gives a translation of the subscripts of X.

Subscript	Meaning
D	Diesel produced.
H_2	Hydrogen consumed in reactor.
TAG	Algae oil processed.
C3	Propane produced.
W	Water produced.
G	Gasoline produced.
CO_2	Carbon dioxide produced in reactor.

8.5 Appendix E: Hydrotreating Heat and Electricity Calculations

8.5.1 Electricity Calculations

Electricity is used for compression, cooling water, and sour water treatment. 70% efficiency is assumed for all compression calculations.
Make-up hydrogen compression to the reactor is calculated in Aspen (see Appendix F for Aspen simulation details). It is assumed hydrogen from the refinery hydrogen plant is available at 20 bar (Parkash 2003, **pp.173-175**). The reaction can take place between 36 bar and 50 bar (Marker *et al* 2005) so a range of compression energies are calculated in equation B:

(B) Electricity use = $\beta_1(0.332 + 0.213d_1)$kWh/(kg make-up hydrogen)

d_1 is a uniformly-distributed stochastic variable with a minimum of 0 and maximum of 1 that represents the uncertainty in reactor pressure (i.e. a value of 0 corresponds to a pressure of 36

bar and a value of 1 corresponds to a pressure of 50 bar). β_1 is the mass ratio of hydrogen consumption in reactor to algae oil processed.
The electricity for the compression of hydrogen recycled from the PSA unit is calculated via Aspen simulation (see Appendix F). The input for the LCI is equation C:

(C) Electricity use = $\frac{\beta_1}{0.018\ \text{kg}}(0.0343 + 0.220d_1)$kWh/(kg algae oil processed)

The electricity for the compression of PSA tail-gas is calculated via Aspen simulation (see Appendix F). The input for the LCI is equation D:

(D) Electricity use = $0.0672\beta_2$ kWh/(kg make-up hydrogen)
β_2 is the ratio of tail-gas mass flow to simulated tail-gas mass flow (see Appendix F).

$$\beta_2 = \frac{[(1+\gamma)(\text{CO}_2\text{ produced in reactor, kg}) + 1.176(\text{hydrogen consumption in reactor, kg})]}{0.221\ \text{kg}}$$

γ is the ratio of the molecular weight of CO to that of CO_2.

The electricity use for the cooling water for the PSA tail gas compressor is calculated via Aspen simulation (see Appendix F). The same assumptions for cooling water that are used for SFE are employed in this analysis, except for the electricity use per gallon of cooling water, which is allowed to vary between 1 and 2 Wh/gallon. The input for the LCI is equation E:

(E) Electricity use = $4.61 \cdot 10^{-4}(1 + d_2)\beta_2$kWh/(kg algae oil processed)

d_2 is a uniformly-distributed stochastic variable with a minimum of 0 and maximum of 1 that represents the uncertainty in cooling water electricity use (i.e. a value of 0 corresponds to 1 Wh/gallon and a value of 1 corresponds to 2 Wh/gallon).
The electricity use for the cooler upstream of the PSA unit is calculated via Aspen simulation (see Appendix F). The input for the LCI is equation F:

(F) Electricity use = $3.60 \cdot 10^{-3}(1 + d_2)\beta_3$kWh/(kg algae oil processed)

β_3 is the ratio of PSA inlet mass flow to simulated PSA inlet mass flow (see Appendix F).

$$\beta_3 = \frac{[(1+\gamma)(\text{CO}_2\text{ produced in reactor, kg}) + 6.916(\text{hydrogen consumption in reactor, kg})]}{0.324\ \text{kg}}$$

Electricity and cooling water use for the sour water stripper is given by Parkash (2003, p. 266). The input for the LCI is given by equation G:

(G) Electricity use = $[1.485 \cdot 10^{-4}(1 + d_2) + 3.003 \cdot 10^{-3}]X_W$ kWh/(kg algae oil processed)

X_W is the mass of water produced in the reactor, a stochastic variable calculated in Appendix C.

Electricity for the algae oil pump upstream of the hydrotreater is calculated using the formula below (75% efficiency assumed; subscripts h and denote hydraulic and electric energy):

1 kg oil	1 m^3	ΔP, bar	10^5 Pa	2.778×10^{-7} kWh_h	1 kWh_e
	920 kg oil		1 bar	1 J_h	0.75 kW_h

= 1.51×10^{-3} kWh for 36 bar reactor pressure and 2.12×10^{-3} kWh for 50 bar reactor pressure.
The LCI input is given in equation H:

(H) Electricity use = $1.51 \cdot 10^{-3}(1 + 6.1 \cdot 10^{-4} d_1)$kWh/(kg algae oil processed)

8.5.2 Heat Calculations

Heat is generated from the hydrotreating reaction, used to make steam for stripping, WGS, and stream heating applications. Heat production from the hydrotreater is determined from data given in Marker *et al* (2005), the input for the LCI is given by equation I (note: the equation is written so that the result is negative and represents a heat credit).

(I) Heat use, MJ = $X_D[0.9 - 61.5(\text{hydrogen consumption in reactor, kg})]$

X_D is the mass ratio of diesel output to algae oil processed, as calculated by equation A in Appendix D.

Data from Parkash (2003, p. 266) is used to determine 0.401 MJ of heat is used per kg of water produced in the reactor (calculated in Appendix C). This results in a triangularly-distributed LCI input with a minimum of 0.013 MJ, mode of 0.023 MJ, and a maximum or 0.034 MJ per kg of algae oil processed. 599 g of steam per liter of diesel produced are used to strip light components from the outgoing diesel stream (Parkash 2003, p. 23). The steam sent to the diesel stripper is saturated steam at 300 °F ("Steam Strippers") , supplying a duty of 38.143 MJ/kg-mol (Perry 2008, p. 2-413). The heat use is calculated below and input to the LCI as equation J.

5.99x10^-3 kg steam	1 L diesel	1 kg-mol steam	38.143 MJ	=	0.01626 MJ/kg diesel
1 L diesel	0.78 kg diesel	18.02 kg steam	1 kg-mol steam		

(J) Heat Use, MJ = $0.01626X_D$

Steam sent to the reformer WGS reactors is saturated at 2.17 MPa, supplying a duty of 33.705 MJ/kg-mol (Perry 2008, p. 2-413). One mole of steam is consumed per mole of CO converted to CO_2 (see Appendix C for CO and CO_2 production via the hydrotreating reaction), giving a triangularly-distributed steam use with a minimum of 0.0613 , a mode of 0.0934, and a maximum of 0.1264 MJ/kg algae oil processed.
Heat duty for the reactor make-up hydrogen is calculated via Aspen simulation (see Appendix F). The input for the LCI is equation K:

(K) Heat Use, MJ = (2.95-0.76d_1) β_1

Heat duty for the recycle hydrogen is calculated via Aspen simulation (see Appendix F). The input for the LCI is equation L:

(L) Heat Use, MJ = (0.302-0.078d_1) $\frac{\beta_1}{0.018\ \text{kg}}$

It is assumed in these calculations that the heat used to warm the algae oil to reactor conditions is recovered via thermal integration of the post-reactor cooling process with other streams in the refinery. Also, no heat will be needed for downstream processing of the gasoline components stripped from the diesel. This is because these components will most likely be straight-chain heavy naphtha processes in the platformer. The reaction they will undergo is thermally neutral (Parkash 2003, p. 110).

8.6 **Appendix E: MATLAB Script**

8.6.1 Main Script

```
%  SET MATLAB TO RUN ONE MILLION SIMULATIONS
level=6;
n=10^level;

% CALCULATE MASS FLOWS
% NOTE: TRIRND IS A USER-DEFINED FUNCTION THAT CREATES A
TRIANGULAR DISTRIBUTION
figure(1)
sat=trirnd(0.009,0.0092,0.0108,n);   %   DEFINE   SATURATION   H2
PARAMETER
title('sat h2')

figure(2)
mw=trirnd(265,270,275,n); % DEFINE MOLECULAR WEIGHT PARAMETER
title('mw')

figure(3) % DEFINE PERCENT HYDRODEOXYGENATION PARAMETER
hdo=trirnd(0,0.25,0.5,n);
title('hdo')

% DEFINE 5 ARRAYS EACH WITH ONE MILLION DATA POINTS INITIALLY
SET TO ZERO
h=zeros(1,n); %HYDROGEN CONSUMED BY DEOXYGENATION
h2o=h; % WATER PRODUCED IN REACTOR
co=h; %CARBON MONOXIDE PRODUCED IN REACTOR
co2=h; %CARBON DIOXIDE PRODUCED IN REACTOR
c3=h; %PROPANE PRODUCED IN REACTOR
```

```
%FOR EACH TRIAL IN SIMULATION, CALCULATE THE FIVE VALUES DEFINED
ABOVE
for i=1:n
    h(i)=sat(i)+hdo(i)*3*2.016/mw(i)+(1-hdo(i))*.5*2.016/mw(i);
    h2o(i)=hdo(i)*2*18.02/mw(i)+(1-hdo(i))*.5*18.02/mw(i);
    co(i)=(1-hdo(i))*.5*28.01/mw(i);
    co2(i)=(1-hdo(i))*.5*44.01/mw(i)+co(i)*44.01/28.01;
    c3(i)=44.09/3/mw(i);
end

%DISPLAY VALUES OF INTEREST
figure(4)
hist(h,50)
title('h')

figure(5)
hist(h2o,50)
title('h2o')

figure(6)
hist(co2,50)
title('co2')

figure(7)
hist(c3,50)
title('c3')
```

8.6.2 TRIRND Script

The following script is available on MATLAB's website (Piantanakulchai 2007).

```
%Script by Dr.Mongkut Piantanakulchai
%To simulate the triangular distribution
%Return a vector of random variable
%The range of the value is between (a,b)
%The mode is c (most probable value)
%n is to tatal number of values generated
%Example of using
%X = trirnd(1,5,10,100000);
% this will generate 100000 random numbers between 1 and 10
(where most probable
% value is 5)
% To visualize the result use the command
% hist(X,50);

function X=trirnd(a,c,b,n)
X=zeros(n,1);
for i=1:n
%Assume a<X<c
```

```
z=rand;
if sqrt(z*(b-a)*(c-a))+a<c
    X(i)=sqrt(z*(b-a)*(c-a))+a;
else
    X(i)=b-sqrt((1-z)*(b-a)*(b-c));
end
end %for
hist(X,50); %Remove this comment % to look at histogram of X
end %function
```

8.7 Appendix F

Data from Parkash (2003, pp. 173-175) is used to construct an Aspen simulation of the water-oil-gas separator, separation via PSA, and recompression. The components of the gas input into the simulation are hydrogen, carbon monoxide, and carbon dioxide. The deterministic hydrogen and carbon oxide values are used in this simulation, and Huber *et al* (2007) run their hydrotreating reactions with excess hydrogen equal to 6.916 times the stoichiometric need, leading to the following input below (basis is 1 kg of algae oil processed).

Component	Input (kg)
Hydrogen	0.124
Carbon Monoxide	0.0776
Carbon Dioxide	0.122

The process begins by expanding the simulated gas across a valve from reaction pressure (both 36 bar and 50 bar are simulated) to 20 bar. Next, the gas is cooled to 41 °C. The PSA block splits the gas stream; 83% of the hydrogen goes to the recycle compressor, and all other gases are routed to the tail gas compressor. The hydrogen stream is compressed and heated back to reaction conditions. The tail gas stream is expanded across a valve to simulate decompression and release of impurities from the PSA unit. The tail gas stream is recompressed to 22 bar and heated to 371 °C and sent to the WGS reactors. All compressors are 70% efficient. The process is shown below:

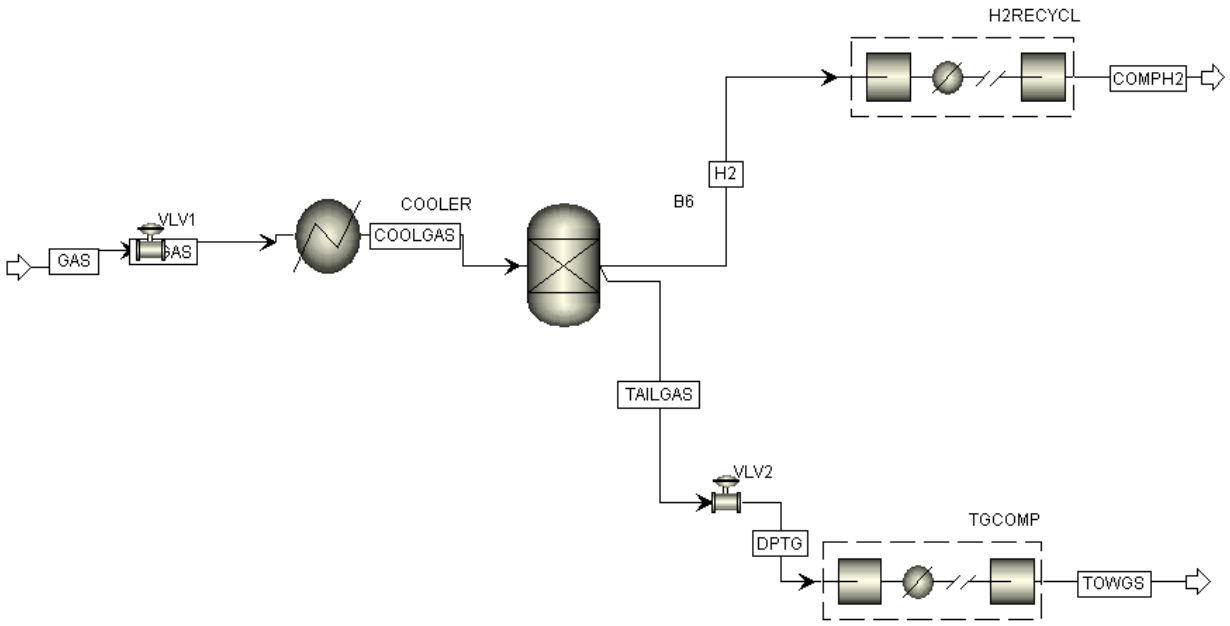

Note that the hydrogen recycle compressors are modeled as multi-stage compressors although both compressors are single stage; this is merely to provide a simultaneous calculation of exit heat duty. The results of this simulation are shown below:

Calculation	36 bar Result	50 bar Result
PSA Inlet Cooling Duty (kJ/kg algae oil)	571	571
Tail Gas Compressor Cooling Duty (kJ/kg algae oil)	73	73
Tail Gas Compressor Electricity (kWh/kg algae oil)	0.0672	0.0672
Hydrogen Recycle Compressor Electricity (kWh/kg algae oil)	0.0343	0.0563
Hydrogen Recycle Heater Duty (kJ/kg algae oil)	302	224

An Aspen simulation consisting of a single compressor and heater was used to determine the electrical and heating duties for make-up hydrogen processing per kg of make-up hydrogen. The results of this simulation are shown below:

Calculation	36 bar Result	50 bar Result
Make-Up Hydrogen Compression Duty (kWh/kg hydrogen)	0.332	0.545
Make-Up Hydrogen Heating Duty (MJ/kg hydrogen)	2.95	2.19

As mentioned in the results section, a sensitivity analysis was performed to test the effects of changing amounts of hydrodeoxygenation. The table below gives the adjusted inputs to the simulation.

Parameter	0% HDO	50% HDO
H_2 In (kg)	0.090	0.159
CO In (kg)	0.103	0.052
CO_2 In (kg)	0.163	0.081
Reactor Temperature (˚C)	300	450
Reactor Pressure (bar)	36	50

The tables below give the results from the Aspen simulations.

Calculation	0% HDO Results	50% HDO Results
PSA Inlet Cooling Duty (kJ/kg algae oil)	392	1040
Tail Gas Compressor Cooling Duty (kJ/kg algae oil)	55	91
Tail Gas Compressor Electricity (kWh/kg algae oil)	0.0547	0.0805
Hydrogen Recycle Compressor Electricity (kWh/kg algae oil)	0.0249	0.0726
Hydrogen Recycle Heater Duty (kJ/kg algae oil)	192	531

Calculation	0% HDO Results	50% HDO Results
Make-Up Hydrogen Compression Duty (kWh/kg hydrogen)	0.332	0.545
Make-Up Hydrogen Heating Duty (MJ/kg hydrogen)	2.59	4.02

The four tables below give the Aspen stream results for the four trials.

Low Pressure Simulation Results

Substream: MIXED	COMPH2	COOLGAS	DPGAS	DPTG	GAS	H2	TAILGAS	TOWGS
Mole Flow kmol/hr								
CO	0	0.00278468	0.00278468	0.00278468	0.00278468	0	0.00278468	0.00278468
CO2	0	0.0027721	0.0027721	0.0027721	0.0027721	0	0.0027721	0.0027721
H2	0.05105462	0.06151159	0.06151159	0.01045697	0.06151159	0.05105462	0.01045697	0.01045697
Total Flow kmol/hr	0.05105462	0.06706838	0.06706838	0.01601376	0.06706838	0.05105462	0.01601376	0.01601376
Total Flow kg/hr	0.10292	0.324	0.324	0.22108	0.324	0.10292	0.22108	0.22108
Total Flow l/min	1.19893638	1.47401321	2.79986266	4.95868139	1.56110524	1.1224639	0.35023045	0.66472688
Temperature K	598.15	314.15	598.883135	312.745703	598.15	314.15	314.15	644.15
Pressure atm	35.1890078	19.7384653	19.7384653	1.38169257	35.5292376	19.7384653	19.7384653	21.372082
Vapor Frac	1	1	1	1	1	1	1	1
Liquid Frac	0	0	0	0	0	0	0	0
Solid Frac	0	0	0	0	0	0	0	0
Enthalpy cal/mol	2104.31093	-4866.8931	-2834.7184	-20755.661	-2834.7184	114.668117	-20755.661	-18228.272
Enthalpy cal/gm	1043.86716	-1007.4527	-586.7901	-1503.4205	-586.7901	56.8824121	-1503.4205	-1320.351
Enthalpy cal/sec	29.8430024	-90.670743	-52.811109	-92.326723	-52.811109	1.62620497	-92.326723	-81.084222
Entropy cal/mol-K	-2.219918	-3.9746535	0.62471157	5.28895263	-0.5522005	-5.5686491	-0.0004104	5.32097647
Entropy cal/gm-K	-1.1012153	-0.822758	0.12931604	0.38310126	-0.1143062	-2.7623912	-2.97E-05	0.38542088
Density mol/cc	0.00070972	0.00075834	0.00039923	5.38E-05	0.00071603	0.00075807	0.00076205	0.00040151
Density gm/cc	0.00143071	0.00366346	0.00192866	0.00074307	0.00345908	0.00152818	0.01052069	0.00554312
Average MW	2.01588	4.83088995	4.83088995	13.8056259	4.83088995	2.01588	13.8056259	13.8056259
Liq Vol 60F l/min	0.04557289	0.05986725	0.05986725	0.01429436	0.05986725	0.04557289	0.01429436	0.01429436

High Pressure Simulation Results

Substream: MIXED	COMPH2	COOLGAS	DPGAS	DPTG	GAS	H2	TAILGAS	TOWGS
Mole Flow kmol/hr								
CO	0	0.00278468	0.00278468	0.00278468	0.00278468	0	0.00278468	0.00278468
CO2	0	0.0027721	0.0027721	0.0027721	0.0027721	0	0.0027721	0.0027721
H2	0.05105462	0.06151159	0.06151159	0.01045697	0.06151159	0.05105462	0.01045697	0.01045697
Total Flow kmol/hr	0.05105462	0.06706838	0.06706838	0.01601376	0.06706838	0.05105462	0.01601376	0.01601376
Total Flow kg/hr	0.10292	0.324	0.324	0.22108	0.324	0.10292	0.22108	0.22108
Total Flow l/min	0.86431062	1.47401321	2.80285086	4.95868139	1.12873586	1.1224639	0.35023045	0.66472688
Temperature K	598.15	314.15	599.525844	312.745703	598.15	314.15	314.15	644.15
Pressure atm	49.0059335	19.7384653	19.7384653	1.38169257	49.3461633	19.7384653	19.7384653	21.372082
Vapor Frac	1	1	1	1	1	1	1	1
Liquid Frac	0	0	0	0	0	0	0	0
Solid Frac	0	0	0	0	0	0	0	0
Enthalpy cal/mol	2108.92726	-4866.8931	-2830.0939	-20755.661	-2830.0939	114.668117	-20755.661	-18228.272
Enthalpy cal/gm	1046.15714	-1007.4527	-585.83282	-1503.4205	-585.83282	56.8824121	-1503.4205	-1320.351
Enthalpy cal/sec	29.9084706	-90.670743	-52.724954	-92.326723	-52.724954	1.62620497	-92.326723	-81.084222
Entropy cal/mol-K	-2.8778644	-3.9746535	0.63242933	5.28895263	-1.2052862	-5.5686491	-0.0004104	5.32097647
Entropy cal/gm-K	-1.4275971	-0.822758	0.13091363	0.38310126	-0.2494957	-2.7623912	-2.97E-05	0.38542088
Density mol/cc	0.00098449	0.00075834	0.00039881	5.38E-05	0.00099031	0.00075807	0.00076205	0.00040151
Density gm/cc	0.00198462	0.00366346	0.0019266	0.00074307	0.00478411	0.00152818	0.01052069	0.00554312
Average MW	2.01588	4.83088995	4.83088995	13.8056259	4.83088995	2.01588	13.8056259	13.8056259
Liq Vol 60F l/min	0.04557289	0.05986725	0.05986725	0.01429436	0.05986725	0.04557289	0.01429436	0.01429436

0% HDO Simulation Results

Substream: MIXED	COMPH2	COOLGAS	DPGAS	DPTG	GAS	H2	TAILGAS	TOWGS
Mole Flow kmol/hr								
CO	0	0.00278468	0.00278468	0.00278468	0.00278468	0	0.00278468	0.00278468
CO2	0	0.0027721	0.0027721	0.0027721	0.0027721	0	0.0027721	0.0027721
H2	0.03705577	0.04464551	0.04464551	0.00758973	0.04464551	0.03705577	0.00758973	0.00758973
Total Flow kmol/hr	0.03705577	0.0502023	0.0502023	0.01314652	0.0502023	0.03705577	0.01314652	0.01314652
Total Flow kg/hr	0.0747	0.29	0.29	0.2153	0.29	0.0747	0.2153	0.2153
Total Flow l/min	0.83418046	1.10306455	2.00886112	4.06085074	1.12037787	0.81469154	0.2868117	0.54579052
Temperature K	573.15	314.15	573.852571	312.037033	573.15	314.15	314.15	644.15
Pressure atm	35.1890078	19.7384653	19.7384653	1.38169257	35.5292376	19.7384653	19.7384653	21.372082
Vapor Frac	1	1	1	1	1	1	1	1
Liquid Frac	0	0	0	0	0	0	0	0
Solid Frac	0	0	0	0	0	0	0	0
Enthalpy cal/mol	1929.1473	-6540.7336	-4675.6909	-25309.809	-4675.6909	114.668117	-25309.809	-22732.789
Enthalpy cal/gm	956.975264	-1132.2755	-809.41537	-1545.4533	-809.41537	56.8824121	-1545.4533	-1388.0967
Enthalpy cal/sec	19.8572369	-91.211084	-65.202906	-92.426695	-65.202906	1.18031006	-92.426695	-83.015897
Entropy cal/mol-K	-2.519056	-3.5065265	0.81495578	6.28478834	-0.3625065	-5.5686491	1.00019647	6.42656835
Entropy cal/gm-K	-1.2496061	-0.6070197	0.14107813	0.38375821	-0.062754	-2.7623912	0.06107343	0.3924155
Density mol/cc	0.00074036	0.00075852	0.0004165	5.40E-05	0.0007468	0.00075807	0.00076394	0.00040145
Density gm/cc	0.00149248	0.00438173	0.002406	0.00088364	0.00431402	0.00152818	0.01251111	0.00657456
Average MW	2.01588	5.77662725	5.77662725	16.3769484	5.77662725	2.01588	16.3769484	16.3769484
Liq Vol 60F l/min	0.03307709	0.04481208	0.04481208	0.01173498	0.04481208	0.03307709	0.01173498	0.01173498

50% HDO Results

Substream: MIXED	COMPH2	COOLGAS	DPGAS	DPTG	GAS	H2	TAILGAS	TOWGS
Mole Flow kmol/hr								
CO	0	0.00278468	0.00278468	0.00278468	0.00278468	0	0.00278468	0.00278468
CO2	0	0.0027721	0.0027721	0.0027721	0.0027721	0	0.0027721	0.0027721
H2	0.06587693	0.0793698	0.0793698	0.01349286	0.0793698	0.06587693	0.01349286	0.01349286
Total Flow kmol/hr	0.06587693	0.08492659	0.08492659	0.01904965	0.08492659	0.06587693	0.01904965	0.01904965
Total Flow kg/hr	0.1328	0.36	0.36	0.2272	0.36	0.1328	0.2272	0.2272
Total Flow l/min	1.34509541	1.86672237	4.2850729	5.9080696	1.72344331	1.44834052	0.41725349	0.79063608
Temperature K	723.15	314.15	724.598366	313.204271	723.15	314.15	314.15	644.15
Pressure atm	49.0059335	19.7384653	19.7384653	1.38169257	49.3461633	19.7384653	19.7384653	21.372082
Vapor Frac	1	1	1	1	1	1	1	1
Liquid Frac	0	0	0	0	0	0	0	0
Solid Frac	0	0	0	0	0	0	0	0
Enthalpy cal/mol	2985.85985	-3819.297	-893.89496	-17428.424	-893.89496	114.668117	-17428.424	-14936.921
Enthalpy cal/gm	1481.16944	-900.99968	-210.87626	-1461.2917	-210.87626	56.8824121	-1461.2917	-1252.3909
Enthalpy cal/sec	54.6386953	-90.099968	-21.087626	-92.223745	-21.087626	2.09832899	-92.223745	-79.039783
Entropy cal/mol-K	-1.5465677	-4.2778023	1.66913183	4.527971	-0.1654228	-5.5686491	-0.7642827	4.48131668
Entropy cal/gm-K	-0.7671923	-1.0091644	0.39376022	0.37964917	-0.0390244	-2.7623912	-0.0640815	0.37573743
Density mol/cc	0.00081626	0.00075825	0.00033031	5.37E-05	0.00082128	0.00075807	0.00076091	0.00040156
Density gm/cc	0.00164548	0.00321418	0.0014002	0.00064093	0.0034814	0.00152818	0.00907521	0.00478939
Average MW	2.01588	4.2389549	4.2389549	11.9267243	4.2389549	2.01588	11.9267243	11.9267243
Liq Vol 60F l/min	0.05880373	0.07580802	0.07580802	0.01700429	0.07580802	0.05880373	0.01700429	0.01700429

8.8 **Appendix G**

To calculate combustion emissions from FAME, a saturated C-16 fatty acid methyl ether is used as a model for molecular weight:

$$\frac{1\text{ kg FAME}}{38\text{ MJ}} \left| \frac{1\text{ kg-mol FAME}}{270.44\text{ kg FAME}} \right| \frac{17\text{ kg-mol } CO_2}{1\text{ kg-mol FAME}} \left| \frac{44.01\text{ kg } CO_2}{1\text{ kg-mol } CO_2} \right| = 0.0728\text{ kg } CO_2/MJ$$

Similarly, n-C_{15} is used as a model for molecular weight of green diesel.

$$\frac{1\text{ kg diesel}}{44\text{ MJ}} \left| \frac{1\text{ kg-mol diesel}}{212.4\text{ kg diesel}} \right| \frac{15\text{ kg-mol } CO_2}{1\text{ kg-mol diesel}} \left| \frac{44.01\text{ kg } CO_2}{1\text{ kg-mol } CO_2} \right| = 0.0706\text{ kg } CO_2/MJ$$

Propane is calculated below:

1 kg C_3	1 kg-mol C_3	3 kg-mol CO_2	44.01 kg CO_2	= 0.0599 kg
50 MJ	44.1 kg C_3	1 kg-mol C_3	1 kg-mol CO_2	CO_2/MJ

It is common knowledge that gasoline (45 MJ/kg) releases 0.07 kg CO_2/MJ.

Typically 0.0375 MJ gasoline and 0.0908 MJ propane are created per MJ of diesel, making an average release of 0.0700 kg CO_2/MJ.